Universidade de Aveiro Departamento de Química

Ano 2018

Tiago Alexandre Teixeira de Sousa Conde

Modulação do fosfolipidoma de macrófagos humanos mediada por flavonóides: um estudo por lipidómica de LC-MS

Flavonoid-mediated modulation of human macrophages phospholipidome: an LC-MS lipidomics study

Universidade de Aveiro Departamento de Química

Ano 2018

Tiago Alexandre Teixeira de Sousa Conde

Modulação do fosfolipidoma de macrófagos humanos mediada por flavonóides: um estudo por lipidómica de LC-MS

Flavonoid-mediated modulation of human macrophages phospholipidome: an LC-MS lipidomics study

Dissertação apresentada à Universidade de Aveiro para cumprimento dos requisitos necessários à obtenção do grau de Mestre em Bioquímica, com especialização em Bioquímica Clínica, desenvolvida sob a orientação científica de Doutora Iola Melissa Fernandes Duarte, Investigadora Principal, CICECO – Instituto de Materiais de Aveiro, Departamento de Química, Universidade de Aveiro, e de Professora Maria do Rosário Gonçalves dos Reis Marques Domingues, Professora Associada com Agregação, Departamento de Química, Universidade de Aveiro.

Dedico este trabalho ao meu avô

o júri

presidente

Professor Doutor Francisco Manuel Lemos Amado

Professor Associado c/Agregação, Departamento de Química, Universidade de Aveiro

orientador

Doutora Iola Melissa Fernandes Duarte

Investigadora Principal, Departamento de Química, Universidade de Aveiro

arguente

Professor Doutor Bruno Miguel Rodrigues das Neves

Professor Auxiliar, Departamento de Ciências Médicas, Universidade de Aveiro

agradecimentos À minha orientadora, Doutora Iola Duarte, agradeço a orientação científica, a disponibilidade, o apoio e o acompanhamento incansáveis que me proporcionou ao longo deste percurso. Agradeço particularmente a atenção e a motivação.

À minha orientadora, Professora Doutora Maria do Rosário Domingues, agradeço a orientação científica, a disponibilidade, o acompanhamento e motivação proporcionados.

Ao Doutor Vítor Gaspar pela incansável orientação e apoio ao longo do procedimento experimental. Agradeço ainda a simpatia e disponibilidade.

À Doutora Tânia Melo, agradeço os ensinamentos e acompanhamento ao longo da identificação e integração dos dados da lipidómica.

Ao Luís Mendes, agradeço o empenho, a cooperação e a ajuda ao longo de toda a realização deste projecto.

Ao Professor Doutor João Mano, pela disponibilização dos seus laboratórios e material para a realização deste projeto. Agradeço ainda o seu envolvimento neste trabalho.

Aos meus amigos e família por todo o apoio, motivo e motivação que me foram dando ao longo desta etapa.

Ao Rafael Coutinho, à Liliana Costa e ao Nuno Paiva, por todo o apoio, motivação e disponibilidade para ajuda. Por estarem lá nos bons e nos maus momentos.

Um especial agradecimento aos meus avós, em particular ao meu avô, a quem dedico este trabalho, pelo incansável sacrifício, por todo o apoio prestado, e por serem exemplos a seguir.

Palavras-chave inflamação, macrófagos, lípidos, metabolismo, flavonoides, quercetina, naringina, naringenina, lipidómica, LC-MS, fosfolipidoma

Resumo

Os macrófagos são células do sistema imune inato com grande envolvimento na resposta inflamatória. A sinalização inflamatória e o metabolismo lipídico estão fortemente interligados, pelo que a caracterização das alterações lipídicas que acompanham o espetro fenotípico e funcional dos macrófagos é especialmente relevante. Vários flavonoides são conhecidos pela sua atividade anti-inflamatória, no entanto, pouco se sabe acerca do seu efeito na composição e metabolismo lipídicos. Neste trabalho, utilizámos uma abordagem lipidómica baseada na análise por cromatografia líquida acoplada a espetrometria de massa (LC-MS) de extratos celulares lipídicos, para caracterizar as alterações no fosfolipidoma de macrófagos humanos (diferenciados a partir de monócitos THP-1) em resposta a três flavonoides: quercetina (Que), naringina (Nar) e naringenina (Ngn). Para efeitos de comparação, foram ainda analisados macrófagos estimulados com LPS/IFN-γ (M1) e IL-4/IL-13 (M2). Este estudo permitiu a identificação de 147 fosfolípidos pertencentes a 8 classes diferentes: fosfatidilcolinas (PC), fosfatidiletanolaminas (PE), lisofosfatidilcolinas (LPC), lisofosfatidiletanolaminas (LPE), fosfatidilgliceróis (PG), fosfatidilinositóis (PI), fosfatidilserinas (PS) e esfingomielinas (SM). Todos os flavonoides tiveram um impacto pronunciado no fosfolipidoma dos macrófagos, provocando variações de grande magnitude em 47-76% de todas as espécies identificadas. Comparando os efeitos mais proeminentes em macrófagos pré-polarizados para M1, verificou-se que a remodelação lipídica induzida pelos flavonoides incluiu aumentos em espécies de LPC, LPE e PG, e diminuições em espécies de SM e plasmalogénios de colina, ao passo que a modulação das outras classes de PL foi claramente diferente para cada flavonoide. No geral, o maior grau de semelhança nos efeitos produzidos foi visto entre a quercetina e a naringenina. Embora não podendo atribuir variações individuais a funções biológicas específicas, foi possível concluir que os três flavonoides afetaram a composição e propriedades das membranas, a sinalização e comunicação celulares e, possivelmente, a atividade antioxidante. Interessantemente, duas espécies emergiram como potenciais marcadores lipídicos da ação anti-inflamatória mediada por flavonoides: PC(32:0) e PE(O-36:6)/PE(P:36:5), decrescendo ambas em resposta à polarização M2 e a qualquer um dos flavonoides. A sua atividade anti-inflamatória e a sua relevância para aspetos da biologia dos macrófagos (por ex., fluidez membranar, produção de citocinas, capacidade fagocítica) deverão ser investigadas em estudos futuros. Em suma, este trabalho demonstrou que o fosfolipidoma de macrófagos humanos é extremamente sensível ao tratamento com flavonoides, abrindo novas perspetivas de investigação rumo a uma melhor compreensão da interligação entre a modulação lipídica mediada por flavonoides e a resposta inflamatória dos macrófagos.

Keywords inflammation, macrophages, lipids, metabolism, flavonoids, quercetin, naringin, naringenin, lipidomics, LC-MS, phospholipidome

Abstract

Macrophages are innate immune cells deeply involved in inflammation. Inflammatory signalling and macrophage lipid composition are closely related, underlying the relevance of characterising lipid alterations accompanying macrophage phenotypic and functional spectrum. Several flavonoids are recognized for their anti-inflammatory activity, although little is known about their effects towards macrophage lipid composition and metabolism. In this work, we have employed a lipidomics approach based on liquid chromatography-mass spectrometry (LC-MS) analysis of cellular lipid extracts to characterize the alterations in the phospholipidome of human macrophages (differentiated from THP-1 monocytes) in response to three flavonoids: quercetin (Que), naringin (Nar) and naringenin (Ngn). Macrophages stimulated with LPS/IFN-γ (M1) and IL-4/IL-13 (M2) were also profiled for comparison. This study enabled the identification and relative quantification of 147 phospholipids (PL) belonging to 8 different classes: phosphatidylcholines (PC), phosphatidylethanolamines (PE), lysophosphatidylcholines (LPC), lysophosphatidylethanolamines (LPE), phosphatidylglycerols (PG), phosphatidylinositols (PI), phosphatidylserines (PS) and sphingomyelins (SM). All flavonoids were seen to have a pronounced impact on the macrophage phospholipidome, causing large magnitude variations in 47-76% of all identified PL species. By comparing the most prominent effects of the three flavonoids on M1 pre-polarized macrophages, it was found that flavonoid-mediated lipid remodelling was generally characterized by increases in LPC, LPE and PG species, accompanied by decreases in choline plasmalogens and SM species, whereas the modulation of other PL species was clearly flavonoid-dependent. Overall, quercetin and naringenin shared the greatest similarity. Although it was not possible to attribute individual variations to specific biological functions, it could be concluded that flavonoids affected cell membrane composition and properties, cell signalling and communication, and, possibly, antioxidant activity. Interestingly, two species emerged as potential anti-inflammatory lipid markers of flavonoid activity, PC(32:0) and PE(O-36:6)/PE(P-36:5), decreasing in response to either M2 polarization and flavonoid treatment. Their anti-inflammatory activity and relevance to macrophage biology (e.g., membrane fluidity, production of cytokines, phagocytic capacity) should be explored in future studies. Overall, this work has shown that human macrophage phospholipidome is exquisitely sensitive to flavonoid treatment, opening new research perspectives towards a greater understanding of the interplay between flavonoid-induced PL modulation and macrophage inflammatory responses.

Index

Index of figures

Index of tables

Abbreviations & Acronyms

AA – arachidonic acid
AB – assay buffer
ABCA – ATP-binding cassette transporter type A
ACC – acetyl-CoA carboxylase
ACOX1 – acyl-CoA oxidase 1
AICAR - 5-aminoimidazole-4-carboxamide ribonucleotide
AMPK - 5' adenosine monophosphate-activated protein kinase
aP2 – adipocyte fatty-acid-binding protein aP2
ATGL – adipose triglyceride lipase
ATP – adenosine triphosphate at
A2AR – adenosine receptor 2A
BCFA – branched-chain fatty acids
BMDM – bone marrow-derived murine macrophages
CARKL – carbohydrate kinase-like protein
CC – compound C
CCL – chemokine C-C motif ligand
CCR7 – chemokine C-C motif ligand receptor 7
CD – cluster of differentiation
CE – cholesterol ester
CHIL-3 – chitinase-like 3
CL - cardiolipin
COX – cyclooxygenase
cPLA2 – cytosolic phospholipase A2
CPT1A – carnitine palmitoyltransferase 1A
CrAT – carnitine O-acyltransferase
CXCL – chemokine C-X-C motif ligand
CYP51A1 – lanosterol 14a demethylase
C75 - 4-methylene-2-octyl-5-oxotetra- hydrofuran-3-carboxylic acid
DAPI - 4′,6-diamidino-2-phenylindole
DAMP – damage-associated molecular patterns
DC-SIGN – dendritic cell-specific intercellular adhesion molecule-3-grabbing non-integrin
DESI - desorption electrospray ionization
dPGJ2 – deoxy-prostaglandin J2
DRM – detergent-resistant microdomains
EHHADH - enoil-CoA hydratase/3-hidroxiacyl-CoA dehydrogenase
ELOVL6 - elongation of very long chain fatty acid protein 6
FA – fatty acids
FABP1 – fatty acid binding-protein 1
FAO – fatty acid oxidation
FASN – fatty acid synthase
FATP1 – fatty acid transporter protein 1
FBS – fetal bovine serum

FFA – free fatty acids
FGF2 – fibroblast growth factor 2LC
GL – glycerophospholipid
FIZZ – resistin-like α
HESI – heated electrospray ionization
HILC-LC - hydrophilic interaction liquid chromatography
HLA-DR - human leukocyte antigen – antigen D related
HPLC - high performance-liquid chromatography
HSL – hormone-sensitive lipase
IFN-γ – interferon-γ
IL-1β – interleukin 1β
iNOS – inducible nitric oxide synthase
IRF – interferon regulatory factors
JAK-STAT – Janus kinase-signal transducer activator of transcription
JNK - c-Jun N-terminal kinase
KLA – Kdo_2 lipid A
LAL – lysosomal lipase
LC-MS – liquid chromatography mass spectrometry
LDL – low-density lipoprotein
LOX-1 - lectin-like oxidized low-density lipoprotein receptor-1
LPC – lysophosphatidylcholine
LPE – lysophosphatidylethanolamine
LPG – lysophosphatidylglycerol
LPL – lipoprotein lipase
LPS – lipopolysaccharide
LT – leukotrienes
LyPS – lysophosphatidylserine
MALDI - matrix assisted laser desorption ionization
MARCO – macrophage receptor with collagenous structure
MCP-1 - monocyte chemoattractant protein 1
MRC-1 – mannose receptor C-type 1
MUFA – monounsaturated fatty acids
NF-κB – nuclear factor kappa B
NLR – nod-like receptor
NLRP3 – nod-like receptor family pyrin domain containing 3
NO – nitric oxide
oxLDL – oxidized-low-density lipoprotein
OXPHOS – oxidative phosphorylation
oxPS – oxidized-phosphatidylserine
PA – phosphatidic acid
PAMP – pathogen-associated molecular patterns
PBS - phosphate-buffered saline solution
PC – phosphatidylcholine
PCA – principal component analysis
PE – phosphatidylethanolamine

PG – phosphatidylglycerol
PGE2 – prostaglandin E2
PLS-DA – partial-least squares discriminant analysis
PMA - phorbol 12-myristate 13-acetate
PTG – prostaglandin
PGC-1β – peroxisome proliferator-activated receptor-gamma coactivator 1β
PKC – protein kinase C
PPARα – peroxisome proliferator-activated receptor
PPP – pentose phosphate pathway
PS – phosphatidylserine
PUFA - polyunsaturated fatty acids
PyE – phycoerythricin
RIC - reconstructed-ion chromatogram
ROS – reactive oxygen species
RPMI - Roswell Park Memorial Institute
SA-PyE - streptavidin-phycoerythrin
SCD – stearoyl-CoA dehydrogenase
sPLA2 – secretory phospholipase A2
SREBP1a – sterol regulatory element-binding protein 1a
SR-A1 – scavenger receptor type A1
STAT6 – signal transducer and activator of transcription 6
TCA – tricarboxylic acid cycle
TG – triglycerides
TGF-β – tumour growth factor β
TIC – total ion chromatogram
TLR- toll-like receptor
TNF-α – tumour necrosis factor α
TX – thromboxane
UCP-2 – uncoupling protein 2
VEGF – vascular endothelial growth factor
VLCFA – very long-chain fatty acids
VLDL – very low-density lipoprotein
WB – wash buffer
XIC – extracted ion chromatogram
12-HETE - 12-eicosatetraenoic acid

I. Introduction

I.1. Macrophage polarization in inflammation

Inflammation is a complex physiological response to potentially harmful stimuli, such as pathogens, external injuries (e.g. incisions, foreign bodies), toxicants or irritants, playing a protective role to promote the return to homeostasis [1]. The initial phase in inflammation involves plasma proteins and multiple cells, such as circulating leucocytes and tissue phagocytes, which recognize damage-associated molecular patterns (DAMP) and pathogen-associated molecular patterns (PAMP), and become activated, releasing a panoply of inflammatory mediators. After the rapid initial onset, the acute inflammatory response typically lasts from hours to a few days, being closely intertwined with repair of damaged tissue. However, inflammation can also be prolonged in time, resulting in a chronic state with harmful consequences. Indeed, it is currently recognized that chronic inflammation is implicated in the pathogenesis of multiple diseases, such as cancer, atherosclerosis and neurodegenerative diseases [2]. Unresolved inflammatory response is also involved in the rejection of transplant organs and medical implants, compromising their successful integration and function [3]. Therefore, finding novel approaches to promote appropriate control and resolution of inflammation is of utmost importance.

Macrophages are myeloid cells of the innate immune system, which reside in most tissues and are part of the mononuclear phagocyte system [4,5]. They first appear in the yolk sac and seed several tissues during embryonic development [6], maintaining their population through self-renewal [7]. Macrophages may also arise from differentiation of blood monocytes [5]. Monocytes are a type of leucocytes, produced in the bone marrow and released into the circulatory system, where they can remain for one to three days. During inflammation, monocytes from the bloodstream are recruited to the inflamed tissue site by different stimuli, such as C-C motif chemokine ligand 1 (CCL1) or CCL5, through a process called chemotaxis [8]. Upon this stimulation, when monocytes reach the tissue, they differentiate into macrophages, a process which involves a set of changes in their morphology, such as: reduction of the nucleocytoplasmatic ratio, due to an increase of the cytoplasmatic volume [9]; enhancement of granularity [10]; and accumulation of lysosomes and mitochondria [11].

Macrophages are heavily involved in all stages of inflammation, mainly through three main functions: phagocytosis, which allows clearance of pathogens and foreign invaders perceived as threats; antigen presenting activity, linking innate to adaptive immunity; and production of inflammatory mediators (such as cytokines and growth factors), which are critical for both the onset and resolution of an inflammatory reaction [1,12]. Due to their different functions, distribution and response to stimuli, macrophages display high heterogeneity and plasticity, which are crucial for their protective role and the outcome of the inflammatory response. When in contact with different microenvironmental stimuli, macrophages acquire different phenotypes through a process called activation or polarization [13]. In simplified terms, the extremes of the phenotypic spectrum can be designated as pro-inflammatory or classically activated (M1) macrophages, and as anti-inflammatory or alternatively activated (M2) macrophages. M2 macrophages are usually further subdivided into M2a, M2b, M2c and M2d subsets, depending on the main stimuli present (**Figure 1**) [14]. Macrophages subsets display distinct gene expression profiles which translate into different functional attributes. In general, M1 macrophages are characterized by increased phagocytic activity and pro-inflammatory cytokines production, while M2 macrophages are responsible for tissue repair, inflammation resolution and production of anti-inflammatory cytokines. Inadequate balance of these populations during the inflammatory response may lead to prolonged and harmful inflammation. Therefore, timely and adequate modulation of macrophage polarization is considered to be an attractive goal in various medical contexts, including treatment of diseases [15] and regenerative medicine [3,16].

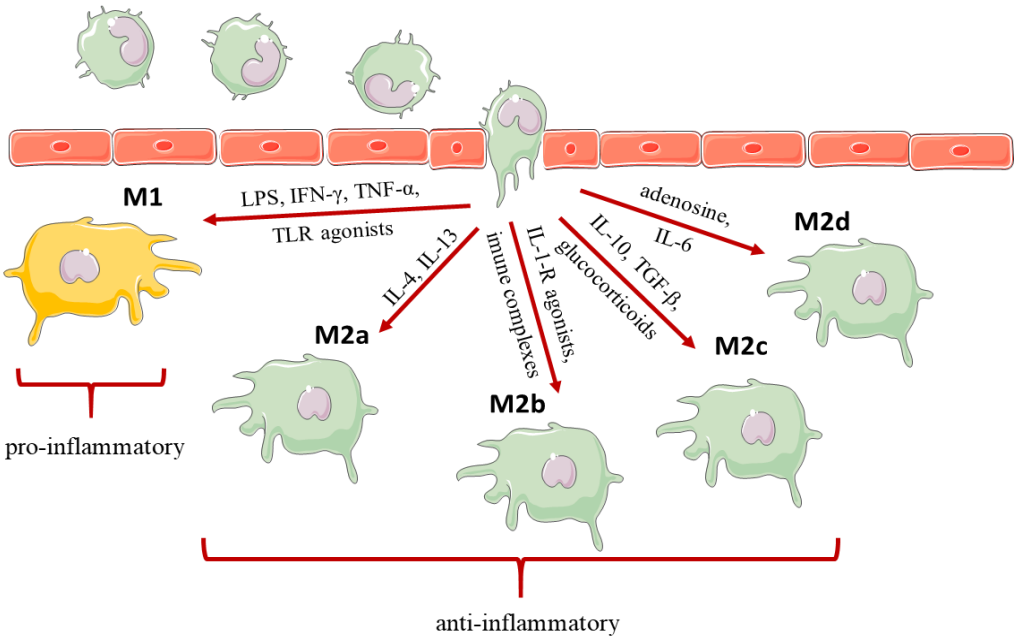

Figure 1 – Activation (or polarization) of macrophages. Blood circulating monocytes are recruited to inflammation site, and penetrate tissue. Monocytes differentiate into steady state macrophages (M0). When in contact with different stimuli macrophages acquire different phenotypes (M1, M2a, M2b, M2c or M2d). Legend: LPS – lipopolysaccharide; IFN-γ – interferon-γ; TNF-α – tumor necrosis factor α; TLR – Toll-like receptors; IL-4 – interleukin 4; IL-13 - interleukin 13; IL-1-R – interleukin 1 receptor; IL-10 – interleukin 10; TGF-β – tumor growth factor β; IL-6 – interleukin 6. Adapted from Weagel *et al* [14].

I.1.1. Classically activated macrophages (M1)

M1-like macrophages are responsible for phagocytosing foreign invaders and display antigen presenting activity. These macrophages are associated with Th1-mediated pathologies, and tend to promote inflammation. Additionally, M1-like macrophages display a protective role against cancer, through clearance of tumor cells [17].

Steady state, or resting, macrophages (M0) may polarize into M1-like macrophages when in contact with i) molecular patterns associated with microbial infection, such as lipopolysaccharides (LPS), or other agonists of Toll-like receptors (TLR), such as free fatty acids, oxidized lipoproteins and high-mobility group protein 1, or ii) pro-inflammatory cytokines, such as tumor-necrosis factor-α (TNF-α), interferon-γ (IFN-γ), among others [18]. Such stimulation leads to induction of several pathways that culminate in the activation of different transcription factors, such as nuclear factor kappa B (NF-κB) or interferon regulatory

factors (IRF). Another important factor that enhances pro-inflammatory expression in M1-like macrophages is the activation of inflammasomes, more precisely, NLRP3 (nucleotide-binding oligomerization domain-like receptor protein-3) inflammasome. Inflammasomes are intracellular multi-protein signalling complexes involved in the activation of inflammatory caspases. When macrophages are M1-stimulated, they increase their ROS (reactive oxygen species) production, which promotes NLRP3 inflammasome activation [19–21]. Activation of NLRP3 inflammasome stimulates caspase-1 which will further cleave the precursor of interleukin-1β (pro-IL-1β), boosting the production of pro-inflammatory IL-1β [22,23].

Several molecules have been highlighted as markers of M1-like polarization including cell surface receptors, cytokines and chemokines, which are small signalling proteins involved in the immune response, in addition to other factors like enzymes and small molecules (**Table 1**) [24–26]. Some of the surface receptors typically expressed in M1-like macrophages are: cluster of differentiation 80 (CD80), adenosine receptor 2A (A2AR), A2BR, CD64, and human leukocyte antigen – antigen D related (HLA-DR), as well as different recognition patterns, such as TLR and Nod-like receptors (NLR) [18,24–26]. M1-like macrophages are also characterized by their increased production of pro-inflammatory cytokines, such as IL-6, IL-12, IL-1β, TNF-α and others. Additionally, M1-like macrophages secrete high levels of some chemokines, such as CXCL8 (chemokine C-X-C motif ligand 8), CXCL11 and CCL5 (chemokine C-C motif ligand 5) [27]. Other molecules reported to be upregulated in M1 macrophages include nitric oxide (NO) synthase (iNOS), cyclooxygenase-2 (COX-2), vascular endothelial factor (VEGF), fibroblast growth factor 2 (FGF2), as well as some oxidative metabolites, such as NO and ROS [18,24–26].

It should be noted that some of these markers are dependent on the species considered. For instance, iNOS, VEGF, FGF2 and HLA-DR are only upregulated in murine M1-like macrophages, not in human M1-like macrophages [12], as indicated in **Table 1**.

I.1.2. Alternatively activated macrophages (M2)

M2-like macrophages participate in tissue repair and remodelling, as well as in resolution of inflammation [14]. Additionally, these macrophages are responsible for

maintaining homeostasis in adipose tissue and mediate the immune response to helminth parasites.

Depending on the polarization stimuli, several M2-like polarization phenotypes have been identified, namely M2a, M2b, M2c and M2d phenotypes [28–30]. M2a macrophages arise from interaction with IL-4, IL-13, and fungal or helminth infections, and are involved with Th2 immune response, type 2 inflammation and clearance of parasites [14]. The M2b subtype is elicited by IL-1 receptor agonists and immune complexes, and is involved in metastasis control and Th1 immune response, being capable of supressing tumour growth [14]. The M2c-like phenotype is acquired through stimulation with IL-10, TGF-β and glucocorticoids [28,29], and is associated with tissue repair and remodelling, matrix deposition and immunoregulation [14]. These three subtypes often display an anti-inflammatory cytokine profile characterized by low production of IL-12 and high production of IL-10 [29]. The fourth M2 subtype described is M2d, which seems to be elicited by IL-6 and adenosine, and displays features of tumour-associated macrophages, promoting angiogenesis [14,30]. However, along this thesis, we will be mostly referring to M2 macrophages in general without distinguishing M2 subtypes.

Different pathways are involved in M2-like polarization, mainly, Janus kinase–signal transducer and activator transporter (JAK-STAT) pathways that activate STAT6. This transcription factor promotes the expression of several genes involved in M2-like macrophage functions [31], often recognized as M2 markers (listed in **Table 1**). Some of them are surface receptors, and mediate interactions with environment, such as mannose receptor C-type 1 (MRC-1), dectin-1, dendritic cell-specific intercellular adhesion molecule-3-grabbing non-integrin (DC-SIGN), CD36, macrophage receptor with collagenous structure (MARCO), CD163, scavenger receptor A1 (SR-A1), SR-B1, lectin-like oxidized low-density lipoprotein (LDL) receptor-1 (LOX-1), A1R, and A3R [18,24–26]. M2-like macrophages also display an increased set of cytokines with an anti-inflammatory role, such as IL-4, IL-10 and resistin-like α (FIZZ1 or RETNL-α). Additionally, some chemokines are increased in M2-like macrophages (CCL16, CCL17, CCL22), as well as some other molecules, like arginase-1, fibronectin, spermine and chitinase-like 3 (Ym1 or CHIL-3). Similar to M1-like macrophages,

murine and human M2-like macrophages display some important differences in gene and protein expression; for example, CHIL-3, FIZZ1 and arginase-1 seem to have no human homologous [32], and are often disregarded as polarization markers for human M2-like macrophages.

Table 1 - Common macrophage polarization markers.

Class type	Markers	Macrophage Phenotype	References
Surface Receptors	CCR7, CD80, A2AR, A2BR, CD64, HLA-DR	M1	[24–26]
	CCR2, CXCR1, CXCR2, MRC-1, dectin-1, DC-SIGN (or CD209), CD36, MARCO, CD206, CD163, SR-B1, SR-A1, LOX1*, A1R, A3R	M2	[24–26]
Cytokines	IL-1, IL-6, IL-12, IL-18, IL-23, IL-1β, TNF-α	M1	[12,24,33]
	IL-4, FIZZ1*, IL-10, IL-1RA, sIL-1R	M2	[24,31]
Chemokines	CXCL8, CXCL9, CXCL10, CXCL11, CXCL16, CCL2, CCL3, CCL4, CCL5	M1	[25]
	CCL1, CCL16, CCL17, CCL18, CCL22, CCL24	M2	[25]
Others	Spermine, NO, O_2^-, iNOS*, COX-2, VEGF*, FGF2*	M1	[24–26]
	CHIL3*, PGC-1β, arginase-1*	M2	[24–26]

Note: Expressed markers vary with polarization stimuli and macrophage's species.

*only found in murine macrophages.

I.2. Lipid composition and metabolism in M1/M2 polarized macrophages

Lipids are a diverse group of biological macromolecules which have many key biological functions, such as acting as structural components, serving as energy storages, and being involved in signalling pathways [34]. Lipids are also crucially important in inflammation [35]. Some lipid species are described to have a pro-inflammatory role, e.g. by

acting as precursors of pro-inflammatory mediators (e.g. prostaglandins), while other display anti-inflammatory activity contributing for resolution of inflammation.

In the context of macrophage polarization, there has been growing interest in assessing how macrophages change their lipid composition and metabolism in response to different stimuli. Most data reported so far focused on the changes induced by canonical M1 and M2 stimuli, as an attempt to deepen current understanding of the molecular biology underlying macrophage plasticity. These data are summarized along the next sections, considering some major lipid classes: fatty acids (FA), acylglycerols, glycerophospholipids, sphingolipids, eicosanoids and sterols [34].

I.2.1. Fatty acids

Fatty acids (FA) are carboxylic acids with long aliphatic chains that can either be saturated or unsaturated [34]. They can arise from endogenous synthesis, where they are formed through elongation of an acetyl-CoA primer with malonyl-CoA, or they can be obtained from diet [36]. These free fatty acids (FFA) are often incorporated in reserve lipids, such as triglycerides, where they are stored as an energy source. When this source of energy is required, FA are released and degraded through β-oxidation (FAO). FA can also be incorporated in structural lipids, such as phospholipids (PL), where they display an important function in maintaining membrane's structure and fluidity. Additionally, FA can be used as precursors for the biosynthesis of signalling molecules, such as prostaglandins (PTG). Due to their different roles in energy storage, structure and fluidity of membrane and cell signalling, FA are considered a fundamental class of lipids for homeostasis of all cells, including macrophages.

When macrophages acquire a M1-like phenotype, they typically display increased FA synthesis [37]. This upregulation results from increased expression and activity of several enzymes, as well as an increased substrate availability, both being essential for the expression of the pro-inflammatory profile [37–43]. The increase in substrate availability arises from downregulation of isocitrate dehydrogenase in M1-like macrophages, resulting in citrate accumulation that can be diverted for anabolic purposes [43]. Export of citrate from the mitochondria is driven by increased expression of mitochondrial citrate carrier in M1-like

macrophages [44]. Once in the cytoplasm, ATP-citrate lyase converts citrate back to oxaloacetate and acetyl-CoA, allowing the latter to be used for FA synthesis [45]. Another substrate involved in FA synthesis is NADPH, generated through the pentose phosphate pathway (PPP), which is upregulated in M1 macrophages. Activation of this pathway is mediated by an increase in glucose uptake and downregulation of carbohydrate kinase-like protein (CARKL) [42]. Increase in both citrate and NADPH support the increase in FA synthesis observed in M1-like macrophages. This FA synthesis is mediated, mainly, by two enzymes, acetyl-CoA carboxylase (ACC) and FA synthase (FASN), which are upregulated in M1-like macrophages [37,38]. In particular, murine bone marrow-derived macrophages (BMDM) stimulated with LPS, a M1-prototypical stimulus, have been reported to display higher expression (and activity) of both ACC and FASN, which has been correlated with increased FA synthesis [37,38]. Moreover, FASN activation was reported to be important for pro-inflammatory activity of M1-like macrophages through activation of caspase-1 mediated by NLRP3 inflammasome [37]. Specifically, uncoupling protein 2 (UCP-2) expression was tightly correlated with FASN expression. Inhibition of UCP-2 in M1 macrophages resulted in downregulation of FASN, associated with a reduced TG synthesis and reduced NLRP3-mediated caspase-1 activation. On the other hand, a more recent study has shown FASN upregulation in LPS-stimulated murine BMDM to be associated with an increase in phosphorylation of c-Jun N-terminal kinase (JNK), suggesting that M1-like polarization induces upregulation of FASN through this pathway [38]. Moreover, inhibition of FASN resulted in changes in labile detergent-resistant microdomains (DRM) content, suggesting that newly synthesized lipids are channelled to DRM, in M1 macrophages. FASN is also a target of hypoxia-inducible factor 1α, which has been described as a major transcriptional modulator of M1-like polarization [46].

Most newly synthesized FA species require additional steps of elongation and desaturation giving rise to monounsaturated FA (MUFA) [47]. Desaturation of FA is catalysed by stearoyl-CoA desaturases (SCD), such as SCD1 and SCD2, while specific FA elongases are responsible for FA elongation. SCD1 was found to be upregulated in M1-polarized peritoneal macrophages and J774 cells, a commercial cell line [48,49]. Moreover, upregulation

of SCD1 in these macrophages resulted in inhibition of ATP-binding cassette transporter protein A1 (ABCA1) [48,49], a cholesterol efflux protein responsible for regulating cholesterol levels, typical of M2-like macrophages [50]. This inhibition of ABCA1 led to accumulation of cholesterol in these macrophages [48,49]. M1 murine BMDM also displayed an increase in elongation of very long chain FA protein 6 (ELOVL6) [51,52]. ELOVL6 is responsible for elongation of C16 and C18 FA. Inhibition of ELOVL6 in murine macrophages seems to be associated with alterations in FA profile of cholesterol esters, as well as cholesterol accumulation [51].

In addition to *de novo* synthesis, FA can arise from exogenous sources [53]. Uptake of FA is regulated by FA transport proteins residing in the cytoplasmic membrane. It was reported that M1 murine primary macrophages displayed upregulation of adipocyte-fatty acid-binding protein aP2 (aP2) [39]. aP2 is involved in fatty acid uptake and is highly expressed by adipocytes. Blocking aP2 resulted in reduction of TNF-α secretion, a cytokine highly produced by M1-like macrophages. This suggests the importance of aP2 as a pro-inflammatory mediator in these cells. Inhibition of aP2 additionally decreased total cholesterol and cholesterol ester, while increasing cellular triglycerides (TG) and FFA contents.

On the other hand, M2-like polarization has been proposed to be characterized by an increase in FAO [54]. In this process, fatty acids are broken down into acetyl-CoA, which can be further used to produce energy through the tricarboxylic acid (TCA) cycle and oxidative phosphorylation (OXPHOS) [36]. In eukaryotic cells, FAO takes place mainly in the mitochondria, and requires FA transport through the mitochondrial membrane, which occurs via conjugation with carnitine. Carnitine palmitoyltransferase 1A (CPT1A), CPT2 and carnitine acetyltransferase (CrAT) are responsible for carnitine conjugated FA transport, and seem to play a role in M2-like macrophages. Indeed, these proteins were found to be upregulated in macrophages stimulated with IL-4, a prototypical M2 polarization stimulus [31,55–57]. Upregulation of CPT1A was reported to occur through activation of peroxisome-proliferator activator receptor α (PPARα) and PPARδ, upon M2- polarization. Additionally, several enzymes involved in FAO were found upregulated in M2-like macrophages [31,54,58]. Vats et al detected an increase in mRNA from enzymes involved in FAO, namely,

acyl-CoA dehydrogenase, enoyl-CoA hydratase and CPT1 [31] in macrophage exposed to IL-4, which was associated with an increase in PGC-1β activity. Upregulation of enzymes involved in FAO has been proposed to result from activation of the STAT6 pathway [59]. Upon M2-like polarization, STAT6 is activated and enhances PPARγ and PPARγ-coactivator-1β (PGC-1β), which further promotes transcription of FAO-related proteins.

However, some recent works have questioned the requirement for FAO in M2 polarization, especially in human macrophages [57,60,61]. Indeed, FAO inhibition with etomoxir had no effect on gene expression of IL-4-stimulated macrophages, showing that this pathway was not essential for M2 activation. Hence, the association between FAO and the M2 phenotype might be more complex that initially thought.

Oxidation of fatty acids can also occur in peroxisomes, namely to degrade very-long-chain FA (VLCFA), branched-chain FA (BCFA) and polyunsaturated FA (PUFA) [62]. BMDM and peritoneal M2-like macrophages have been reported to display increased expression of acyl-CoA oxidase 1 (ACOX1), an enzyme involved in peroxisomal β-oxidation [63]. On the other hand, compared to unstimulated (M0) macrophages, the levels of enoil-CoA hydratase/3-hidroxiacyl-CoA dehydrogenase (EHHCAD) in M2 macrophages were neither increased nor reduced. However, there was a strong downregulation of these enzymes in LPS-stimulated macrophages, suggesting its possible pro-resolving role.

FA can either arise from exogenous sources, with uptake from membrane transporters [58,64], or they can be released from endogenous storage [54,65]. M2-polarized BMDM were reported to display an upregulation in fatty acid transporter protein 1 (FATP1) [58], a membrane protein involved in the uptake of long-chain fatty acids, suggesting upregulated FA uptake from exogenous sources. Additionally, mRNA levels of FATP4 were also upregulated in M2 macrophages. On the other hand, when macrophages acquired the M1-like phenotype, FATP1 was downregulated, compared to basal levels, whereas FATP1 overexpression resulted in attenuation of inflammation. This supports the importance of FA uptake to the anti-inflammatory activity of M2-like macrophages, although this could be species-dependent.

I.2.2. Acylglycerols

Acylglycerols (or glycerolipids) are a class of lipid species composed of mono-, di-, or tri-substituted glycerols [66]. TG are the most well-known acylglycerols, acting as an energy storage. Through lipolysis, the esterified FA are released and can be used. Adipose triglyceride lipase (ATGL) and hormone-sensitive lipase (HSL) have been reported to be upregulated in murine M1-polarized BMDM, compared to M2-polarized macrophages [40]. Both lipases are responsible for the release of FA from TG, making FA available to be used by cells. ATGL inhibition resulted in reduction of the pro-inflammatory cytokine IL-6, reflecting the role of ATGL as a pro-inflammatory mediator in M1-like macrophages.

In another study of LPS-stimulated BMDM, transcriptomic data revealed the upregulation of some enzymes involved in TG synthesis, including aldehyde dehydrogenase 1 family member B1, 1-acyl-glycerol 3-phosphate *O*-acyltransferase 4 and diacylglycerol *O*-acyltransferase 1 and 2 [67]. Additionally, this study explored lipidomic changes in TG species upon M1-like polarization, having found increases in several TG, such as TG (50:1), TG (53:2), TG(54:4), TG(54:6), TG(56:4) and TG(58:6). Another study also found the TG content to be increased upon M1 polarization, compared to unstimulated (M0) and M2-polarized macrophages [54]. Some of the TG species, detected through mass spectrometry, found to be increased in M1 macrophages were: TG(50:1), TG(52:2), TG(54:1) and TG(54:2).

Increased lipolysis (i.e. the breakdown of TG into FFA and glycerol) has also been suggested to characterize M2-like macrophages [54]. In particular, BMDM and M2 murine peritoneal macrophages stimulated with IL-4 and exposed to very-low density lipoproteins (VLDL) displayed enhanced lipolysis in association with increased expression of lipoprotein lipase (LPL). This enzyme was proposed to regulate FA uptake from exogenous sources by acting as a rate-limiting enzyme in lipolysis of exogenous lipoproteins. Lysosomal lipase (LAL), which is another enzyme involved in the release of FA from exogenous sources, was also highly expressed in IL-4-polarized macrophages [54]. In fact, upregulation of LAL appeared to be important for the role of these macrophages resolving inflammation, as inhibition of LAL resulted in exacerbation of inflammation, as well as in increased lipid body formation [54]. In correlation with this increased lipolysis, extracellular levels of glycerol

were also increased, and so were the levels of some monoacylglycerol species, namely 1-oleoglycerol, 1-stearoylglycerol, 1-palmitoylglycerol, and 2-palmitoylglycerol [54].

I.2.3. Glycerophospholipids

Glycerophospholipids are a class of lipids with a polar head (containing a phosphate group) and two hydrophobic tails (consisting of two fatty acids), which are crucially important for cell homeostasis [68]. Due to their amphiphilic nature, phospholipids can form bilayers, which makes them the major component of cell membranes. These lipids can also be involved in cell signalling, and play an important role in inflammation, namely through release of arachidonic acid (AA) that will be further converted in PTG [69–71]. Due to their involvement in inflammation, specifically regarding PTG production, phospholipids play an important role in macrophages.

The metabolism of phospholipids in differentially polarized macrophages has been explored by some researchers [70–73]. In LPS-stimulated Raw 264.7 macrophages (M1), there was an increase in mRNA levels of several enzymes involved in phospholipid biosynthesis, namely 1-acylglycerol-3-phosphate O-acyltransferase 4, phospholipid phosphatase 1, cytidine 5-diphosphate-diacylglycerol-inositol 3-phosphatidyltransferase, phospholipase D1 and phosphatidylserine decarboxylase [73]. Concomitantly, some phospholipid species were also increased, compared to resting macrophages (M0), namely molecular species belonging to different phospholipid classes: phosphatidylcholine (PC), phosphatidylserine (PS), phosphatidylglycerol (PG) and phosphatidylethanolamine (PE); however, the exact identities of such species were not detailed in this study. Additionally, some diacyl-glycerol and phosphatidic acid (PA) species (32:0, 34:0, 34:1, 36:0 and 36:1) were increased as well.

Changes in phospholipase A2 enzymes, responsible for the release of AA (used to produce PTG), have also been reported in association with macrophage polarization [70–72]. These enzymes can be classified as cytosolic phospholipase (cPLA2) and secreted phospholipase (sPLA2). cPLA2, also referred to as Group IV phospholipase A2, has been found upregulated in M1-polarized macrophages [70]. Induction of cPLA2 seems to occur in a TLR-dependent manner, as a result of LPS-induced polarization stimulus [71]. Increase in

cPLA2 levels was accompanied by an increase in the release of AA [70]. On the other hand, M2-like polarization has been associated with an increase in sPLA2 levels, also referred as Group V phospholipase A2 [72]. Such upregulation was not observed in M1-like macrophages. Additionally, sPLA2 displayed a preference for hydrolysis of PE species, which was detected by an increase in LPE species.

I.2.4. Sphingolipids

Sphingolipids are a class of lipid species with a sphingoid base as their backbone, and are involved in cell signalling and recognition [74]. Based on their structure, sphingolipids can be classified as simple (e.g. ceramides), or complex (e.g. cerebrosides). Some studies have suggested an integral role for sphingolipids in inflammation [75]. In particular, some species, like ceramide, ceramide-1-phosphate and sphingosine-1-phosphate, were found to promote activation of pro-inflammatory factors and induction of COX-2, further resulting in pro-inflammatory PTG production.

Raw 264.7 macrophages have been reported to increase their *de novo* synthesis of sphingolipids, upon activation with Kdo2-Lipid A (KLA) [76]. Furthermore, mRNA levels of several enzymes involved in sphingolipids biosynthesis were increased, namely, serine palmitoyltransferase (Sptl1 and Sptc2), ceramide synthase 4, sphingosine kinase 1, sphingosine kinase 2, sphingosine-1-phosphate lyase, and sphingolipid-1 Δ-4-desaturase [73]. Despite the increase in mRNA levels, evaluation of protein levels or activity of these enzymes has not been explored yet.

I.2.5. Eicosanoids

Eicosanoids are 20-carbon lipid species derived from AA, which are heavily involved in the regulation of inflammation [77]. When AA is released from phospholipids it can enter different pathways - cyclooxygenase, lipoxygenase, and cytochrome P450 - that will result in the synthesis of different subtypes of eicosanoids, such as PTG, thromboxanes (TX), or leukotrienes (LT). Some enzymes are responsible for synthesis of these eicosanoids, namely, COX1, COX-2 and several lipoxygenases. Therefore, changes in the expression and/or activity

of these enzymes in M1 and M2 macrophages give interesting insights into the role of eicosanoid metabolism in macrophage polarization.

Up-regulation of COX-2 has been identified as a crucial hallmark of LPS/IFN-γ (M1) macrophage polarization [78]. Up-regulation of COX-2 in M1 macrophages was accompanied by an increased activity, resulting in increased PGE2 production [69]. Additionally, TXB2 production was also increased. Such increase in these eicosanoid species in M1-polarized macrophages, compared to M2-polarized macrophages, might suggest a different pattern of eicosanoid synthesis. Some lipidomic studies have unravelled the eicosanoids profile of M1 macrophages [58,67]. Through liquid chromatography-mass spectrometry (LC-MS), Johnson and colleagues found an increase in PGD2, PGE2 and TXB2, in M1 macrophages stimulated with LPS [58]. In a different study, other eicosanoids were found to be increased in M1 macrophages: PGD2, PGE2, PGF2a, PGJ2, dPGD2, dPGJ2 (15-deoxy PGJ2), TXB2, 12-eicosatetraenoic acid (12-HETE), 17-HETE, 18-HETE, and 19-HETE. On the other hand, M2-like macrophages were reported to display an upregulation in COX-1 activity [79]. However, PGE2 and TXB2 were not increased in M2-like macrophages. Interestingly, there was an increase in dPGJ2, in these macrophages.

I.2.6. Sterols

Sterols are a group of amphipathic lipid molecules, with cholesterol being the most well-known sterol. Cholesterol has well known functions as a mediator to maintain membrane fluidity, and as a precursor for the synthesis of hormones [80]. Macrophages control their cholesterol levels through surface receptors that are capable of taking up cholesterol (in the form of lipoproteins), as well as through efflux proteins and of cholesterol biosynthesis [26,50,54,58,67].

Upon M1 polarization of BMDM macrophages, some enzymes involved in cholesterol biosynthesis have been reported to be downregulated, including lanosterol synthase, lanosterol 14a demethylase (CYP51A1) and hydroxysteroid 17-β-dehydrogenase 7 [67]. On the other hand, 3-hydroxy-3-methylglutaryl-coenzyme A reductase was upregulated in M1-like macrophages, and so were the levels of desmosterol [67]. These results are in line with

another study, which evaluated mRNA levels of enzymes involved in sterol biosynthesis, using Raw 264.7 M1-polarized macrophages [73], where mRNA levels of these enzymes were also decreased. Furthermore, cholesterol 25-hydroxylase mRNA levels were increased. Still, along with desmosterol, lanosterol was reported to be increased in M1-like macrophages [58,67]. There was also an increase in several products of the cholesterol biosynthesis pathway.

M2 macrophages display an upregulation in surface scavenger receptors, and are often identified by some of those receptors, such as CD36, LOX1 and SR-A1 [26]. These receptors are involved in the uptake of oxidized circulating LDL (oxLDL). An increase in these receptors would suggest an increase in the uptake of oxLDL, related with foam cell formation [81,82]. This would suggest the involvement of M2-like macrophages in foam cell formation. However, when M2-like macrophages acquire their phenotype, there is an increase cholesterol efflux proteins, such as ABCA1 [50], which is responsible for the efflux of oxLDL, avoiding oxLDL accumulation, and ABCG1, SR-B1 and 27-hydroxylase (responsible for cholesterol efflux) [26]. Furthermore, cholesterol esters were found decreased in M2-like macrophages [54,64], with some species being notably decreased: CE16:0, CE16:1, CE18:1 and CE18:2 [54].

Summarizing, M1-like macrophages seem to rely on lipid biosynthesis, specifically though increase in FA synthesis, sphingolipid biosynthesis and production of eicosanoids with pro-inflammatory properties. On the other hand, M2-like macrophages are characterized by increased FAO and synthesis of anti-inflammatory eicosanoids. Additionally, polarization seems to induce changes in membrane composition and glycerophospholipid content, that differ between M1-like and M2-like phenotypes. A few of these glycerophospholipid species were described as possible activation state biomarkers for human macrophages.

I.3. Anti-inflammatory potential of modulating macrophage lipid metabolism

The modulation of macrophage lipid composition and metabolism upon activation raises the question as to whether targeting enzymes or regulators of lipid metabolism could alter macrophage phenotype and inflammatory activity. This principle of metabolic immunomodulation has just started to be explored, mainly by hitting targets involved in glucose metabolism [83]. Still, a few studies, reviewed below, have addressed the potential of modulating macrophage lipid metabolism to attenuate inflammation.

One study explored the contribution of FASN to the pro-inflammatory activity of M1 murine peritoneal and Raw 264.7 macrophages [38]. M1-polarized macrophages with FASN knock-out displayed decreased levels in JNK phosphorylation, essential for activation of M1 mediators, and production of pro-inflammatory cytokines, such as TNFα, IL-1β, monocyte chemoattractant protein 1 (MCP-1) and IL-12p40 (**Figure 2A** and **B**). Additionally, cholesterol levels were decreased and DRM's lipid content from cell membrane was found to be altered. Furthermore, Wei and colleagues used cerulenin and C75 (4-methylene-2-octyl-5-oxotetra- hydrofuran-3-carboxylic acid), which are drugs with FASN inhibitory action [38], to further explore the effects of FASN inhibition on M1 expression pattern. The results showed decreased M1-induced phosphorylation of JNK (**Figure 2C**), suggesting a possible attenuation of pro-inflammatory mediators. Another study explored the pro-resolving effect of FASN inhibition, through knocking-out FASN in murine macrophages, in the context of atherosclerosis [84]. The results revealed reduced atherosclerosis development, as well as decreased cholesterol accumulation in these macrophages. Thus, FASN inhibition in macrophages produced some interesting pro-resolving effects that could suggest its use as a therapeutic target to help regulating inflammation.

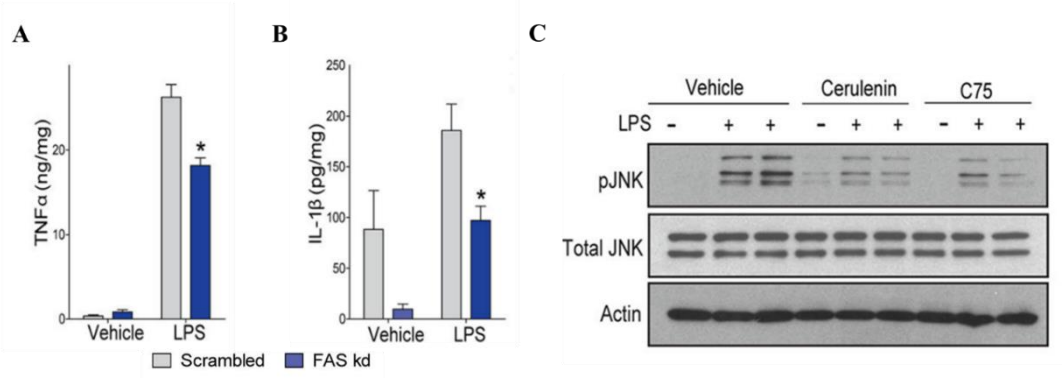

Figure 2 – Results showing the impact of FASN inhibition on M1 macrophages. Raw264.7 macrophages FASN$^{+/+}$ and FASN$^{-/-}$ were stimulated with LPS to acquire M1 phenotype. FASN knock-down resulted in attenuation of LPS-induced pro-inflammatory cytokines, TNF-α (**A**) and IL-1β (**B**) (*p<0,05). Additionally, Raw264.7 were treated with FASN inhibitory drugs (cerulenin and C75), and p-JNK levels were evaluated. Cerulenin and C75 promoted decrease in p-JNK (**C**). Adapted from Wei *et al* [43].

Makowski and colleagues explored the contribution of aP2, a membrane protein involved in the uptake of FA, to the pro-inflammatory activity of murine primary macrophages. Macrophages from aP2$^{-/-}$ mice reduced cholesterol and cholesterol esters accumulation, which was associated with an increase in cholesterol efflux proteins, typical of M2-like macrophages [39]. Moreover, pro-inflammatory cytokines IL-1α, IL-1β, IL-6, IL-12p40, and TNFα levels were also reduced in these aP2-deficient macrophages (**Figure 3A** and **3B**). Additionally, aP2$^{-/-}$ macrophages treated with LPS were deficient in MCP-1, COX-2 and iNOS expression, commonly highly expressed in M1-like macrophages. This attenuation in the expression of pro-inflammatory mediators suggests aP2 as a possible pro-resolving target.

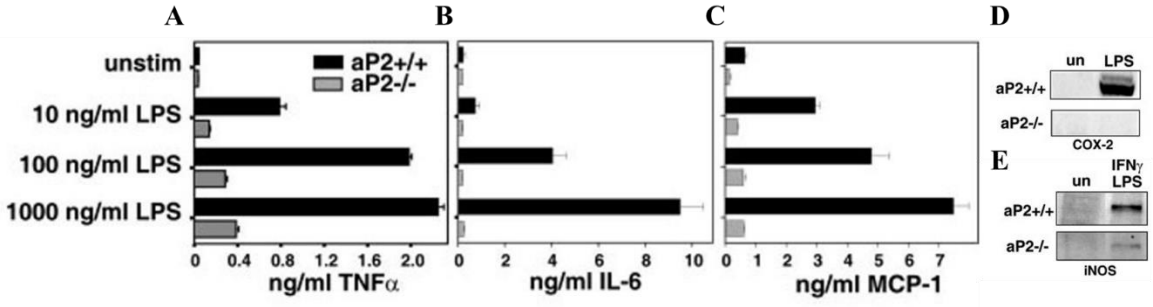

Figure 3 – Impairment of aP2 attenuates M1-like pro-inflammatory phenotype. aP2$^{-/-}$ macrophages treated with LPS (M1 stimulus) display a downregulation in pro-inflammatory cytokines (**A**) TNF-α and (**B**) Il-6, and (**C**) MCP-1. M1-like typical enzymes, (**D**) COX-2 and (**E**) iNOS were also downregulated in M1 aP2-deficient macrophages. Adapted from Makowski *et al* [44].

Another study involved knocking-out sterol receptor element-binding protein 1a (SREBP1a), a transcription factor activated during M1-like polarization, which promotes transcription of enzymes involved in lipid metabolism [85]. Compared to the control group, BMDM murine macrophages deficient in SREBP1a decreased their levels of pro-inflammatory cytokine IL-1β. This decrease was associated with reduced expression of *Nlrp1a* gene, involved in activation of caspase-1 which promotes cleavage of pro-IL-1β. Decrease in IL-1β, a pro-inflammatory cytokine, suggests a possible pro-resolving role for targeting SREBP1a and downstream associated pathways, including lipid metabolism.

AMP-activated protein kinase (AMPK) is a crucial enzyme for cellular energy homeostasis, which is implicated in the regulation of mitochondrial oxidative phosphorylation, and lipid metabolism (through inhibition of FA synthesis and activation of FAO) [86]. Moreover, AMPK is capable of phosphorylating ACC and SREBP1c, inhibiting synthesis of FA, cholesterol and TG, and activating FA uptake and FAO. In macrophages, M1 stimulation decreases activation of AMPK, while M2 stimulation seems to induce AMPK activation [87,88], and upregulation of FAO mediators [89]. Therefore, activating AMPK might be an interesting approach in the context of macrophage polarization towards M2-like pro-resolving phenotypes. Indeed, murine M1 BMDM treated with AMPKβ1-specific activator, A769662, displayed a significant increase in FAO and reduced JNK activation [90]. Metformin is a well-known drug, commonly used for the treatment of type 2 diabetes, that promotes activation of AMPK [91]. Recently, metformin has been explored as a pro-resolving drug in order to attenuate the pro-inflammatory phenotype [92,93]. Kim et al reported that metformin downregulated LPS-induced production of pro-inflammatory cytokines, TNF-α and IL-6 [93], and increased phosphorylation of acetyl-CoA carboxylase (ACC). Attenuation of these pro-inflammatory cytokines was a result of AMPK activation, as corroborated by the similar results obtained through treatment with AICAR (5-aminoimidazole-4-carboxamide ribonucleotide), a direct AMPK activator. Additionally, treatment of M1-like macrophages with Compound C (CC), an AMPK inhibitor, impaired this attenuation.

Activation of AMPK was also implicated in the anti-inflammatory action of palmitoleate and associated changes in lipid metabolism [94]. Palmitoleate (C16:1) was co-

incubated with BMDM treated with palmitate, an M1-polarization stimulus. M1 BMDM treated with palmitoleate displayed reduced levels of *Nos2*, *Cxcl1* and *Il6* expression (**Figure 4A, 4B** and **4C**), reduced levels of CXCL1 and IL-6 secretion, and decreased NO production (**Figure 4D, 4E** and **4F**). Some M2 typical genes were increased (*Tgfb1*, *Il10* and *Mgl2)*, and so was FAO activity. The authors suggested that the pro-resolving effect of palmitoleate involved activation of AMPK, as the use of CC impaired the observed changes. However, the mechanism through which palmitoleate activates AMPK remains unclear.

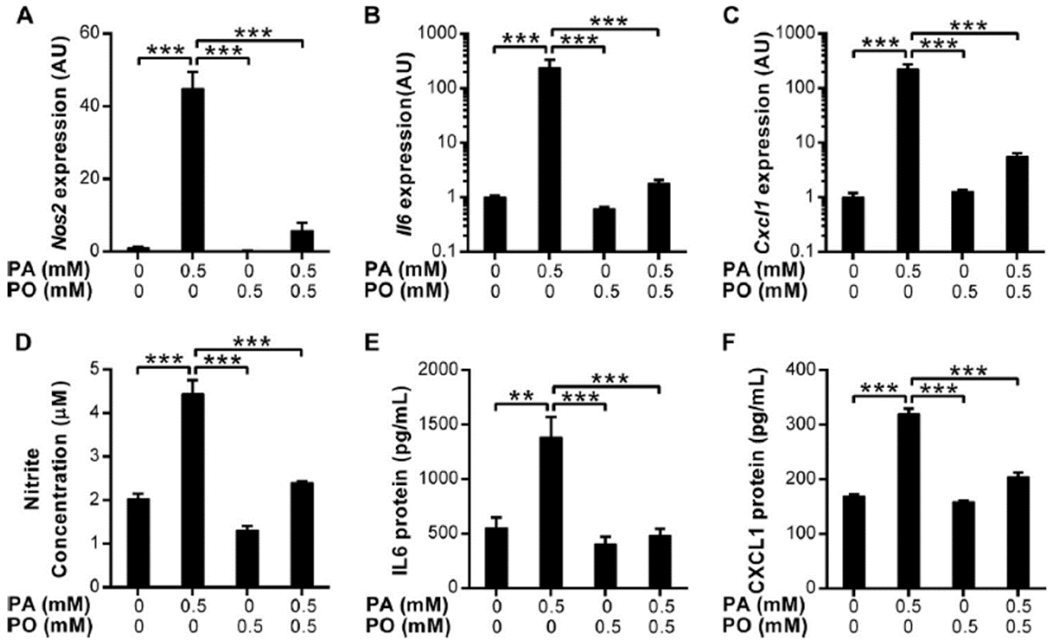

Figure 4 – Palmitoleate attenuated pro-inflammatory phenotype profile of M1 macrophages. BMDM treated with palmitate (M1 stimulus) were co-incubated with palmitoleate. Palmitoleate treated M1 macrophages displayed an attenuation in (**A**) *Nos2*, (**B**) *Il6* and (**C**) *Cxcl1* expression. Attenuation expression was accompanied with (**D**) decreased NO production, and decreased protein levels of (**E**) IL-6 and (**F**) CXCL1. Adapted from Chan *et al* [110].

Results from these studies suggest several lipid related mediators as potential targets for attenuating macrophage pro-inflammatory activity. However, the implications in terms of promoting M2-like pro-resolving activity remain poorly studied. Future studies should include evaluation of M2 markers in order to explore the possible M1 to M2 transition, and not only

M1 attenuation, as the ability to promote M2-like anti-inflammatory activity is critical for a balanced response and the resolution of inflammation.

I.4. Immunomodulatory activity of flavonoids

Bioflavonoids are a class of natural compounds with a polyphenolic structure, which are widely found in fruits, vegetables, plants and tea leaves [95], fulfilling several functions. For instance, some flavonoids are important flower pigments, while others are used in UV filtration or act as secondary messengers and physiological regulators. According to their structure, flavonoids can be subdivided in different groups (**Figure 5**): flavones and flavonols (which can be included in a single group called anthoxanthins), flavonones, flavanonols, flavans and anthocyanidins.

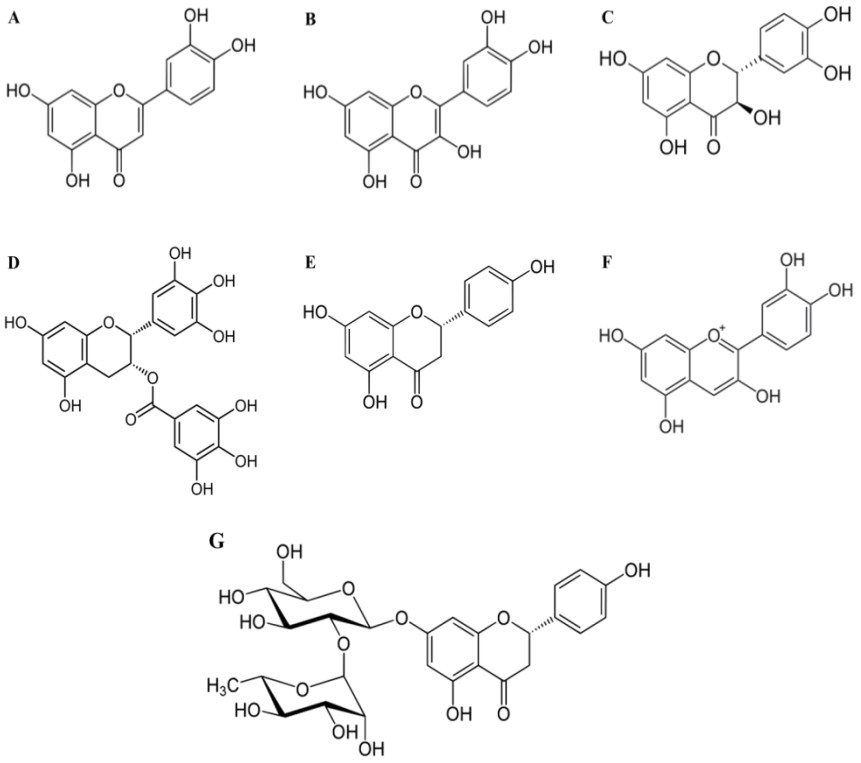

Figure 5 – Representative structure of each subclass of flavonoids. **A** is the structure for luteolin, an example of a flavone. **B** is the structure for quercetin, an example of a flavonol. **C** is the structure of taxifolin, an example of a flavanonol. **D** is the structure of epigallocatechin 3-gallate (EGCG), an example of a flavan. **E** is the structure of naringenin, an example of a flavanone. **F** is the structure of cyanidin, an example of an anthocyanidin. **G** is the structure of naringin, an example of a glycosided flavanone.

These compounds display a wide range of health-promoting properties that have been thoroughly explored in the past decade [96]. In particular, flavonoids have been shown to have anti-oxidant, anti-inflammatory and anti-cancer properties, to help preventing cardiovascular diseases, to display anti-fungal and anti-bacterial properties, as well as favourable properties against different diseases, such as, diabetes, Alzheimer's, atherosclerosis, and others. Flavonoids have also been studied for their immunomodulatory activity. The following sections will address how flavonoids modulate macrophage activation and lipid metabolism.

I.4.1. Flavonoids and macrophage polarization

The use of flavonoids to modulate macrophage polarization has been widely explored [97]. In terms of inflammation control, some studies have focused on downregulating pro-inflammatory features, such as NO production, pro-inflammatory cytokines, and pathways related with their genetic activation. Interestingly, others have employed flavonoids to promote a shift from M1 macrophages to M2-like macrophages, i.e. towards a pro-resolving phenotype.

The use of naringenin (**Figure 5E**) to modulate macrophage polarization has been explored in several studies. In Raw 264.7 macrophages, 25-200 μM of naringenin markedly promoted a decrease in LPS-induced (5 μg/mL) NO production and iNOS expression, as well as a decrease in TNF-α and MCP-1 [98]. In LPS-stimulated U937 macrophages, pre-incubation with 5-50 μg/mL of naringenin reduced LPS-induced (1 μg/mL) increase in TNF-α, IL-1β, IL-6 and IL-8 [99], as shown in **Figure 6**. Chao et al, observed a decrease in iNOS, COX-2 expression and NO production, in Raw264.7 macrophages incubated with 30-200 μM of naringenin and 0.1-100 μg/mL of LPS [100]. Additionally, another study observed inhibition of PGE2 LPS-induced production, in J774 macrophages incubated with 1-100 μM of naringenin [101]. In the same cell line infected with *C. Trachomatis*, 48h treatment with 0.01-10 μg/mL naringenin attenuated the increase of pro-inflammatory cytokines, such as IL-6, TNF, IL-12p70, IL-1α, IL-1β and GM-CSF, and pro-inflammatory chemokines, such as

CCL4, CXCL10, CXCL5, CCL5 and CXCL1 [102]. More recently, Pinho-Ribeiro et al pre-incubated LPS-induced (1µg/mL) Raw 264.7 macrophages with 30-1000 nM of naringenin and observed a decrease in NF-κB activity, essential for activation of several pro-inflammatory genes, as well as a decrease in cytokines and O_2^- production [103]. Concordantly, Jin et al observed an inhibition in LPS-induced increase in TNF-α and IL-6 [104], after incubation with 100 µM of naringenin.

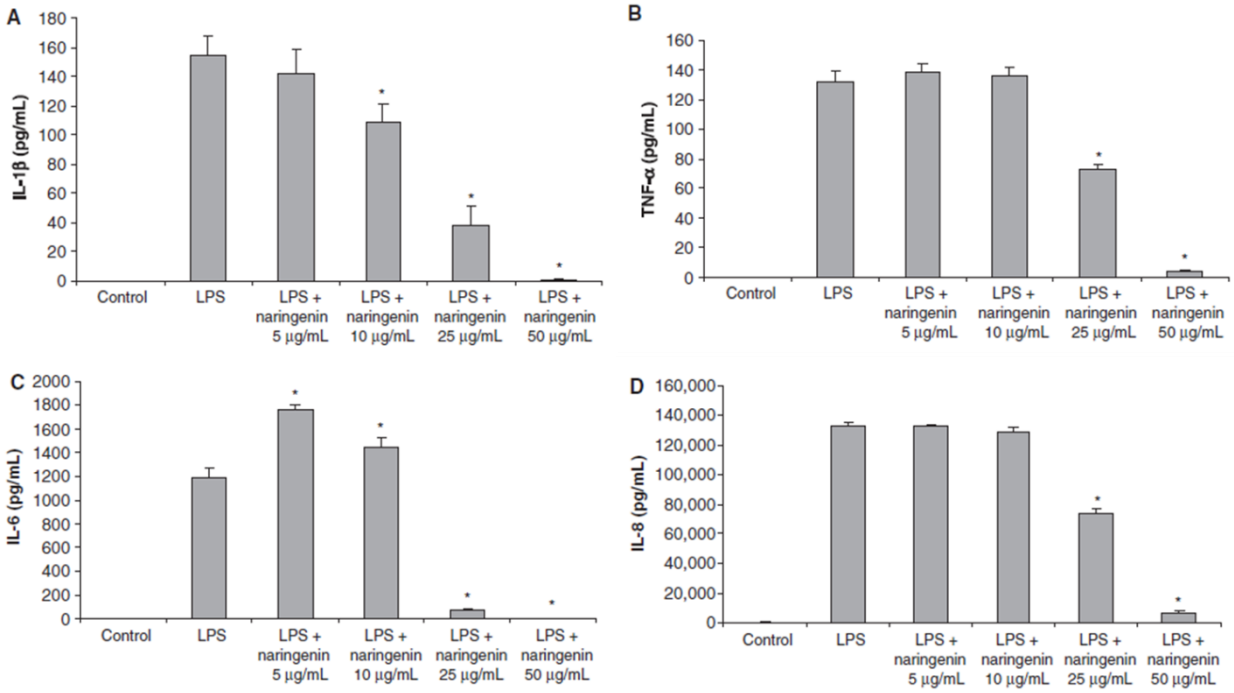

Figure 6 – Naringenin attenuated pro-inflammatory cytokines from LPS-induced U937 macrophages. U937 macrophages were pre-incubated with naringenin concentrations ranging from 5-50 µg/mL, for 2 hours, and then incubated with 1 µg/mL of LPS (from *Aggregatibacter actinomycetemcomitans*). IL-1β (**A**), TNF-α (**B**), IL-6 (**C**) and IL-8 (**D**) LPS-induced levels were reduced with pre-treatment with naringenin at 25 and 50 µg/mL. *p<0.05 compared to control. Adapted from Bodet *et al* (108).

Quercetin (**Figure 5B**) is another abundant bioflavonoid that has been shown to display interesting anti-inflammatory and macrophage modulating properties [105–107]. In Raw 264.7 macrophages, pre-treatment with 2.5-20 µM of quercetin and post-incubation with

100 ng/mL of LPS promoted a decrease in iNOS and COX-2 expression, accompanied by a decrease in NO and PGE_2 production [105]. Endale et al also observed a decrease in pro-inflammatory cytokines, such as TNF-α, IL-1β, IL-6 and GM-CSF, as shown in **Figure 7**. Guzman and colleagues also observed a decrease in pro-inflammatory cytokines (TNF-α, IL-1β, IL-12 and MCP-1) in BMDM pre-treated with 20 μM of quercetin and stimulated with 10μg/mL of LPS [107]. Moreover, the pro-inflammatory activity and IL-1β production induced by cholesterol crystals were attenuated in quercetin treated macrophages. Another study involving treatment with this flavonoid reported a reduction in base levels of several pro-inflammatory mediators (IL-6, IL-8, IL-1β, TNF-α, IFN-γ and COX-2) [106],as well as in NF-κB and JNK pathways. More recently, quercetin was reported to ameliorate kidney injury, liver inflammation and fibrosis, through modulation of macrophage polarization [108,109]. Lu et al, observed that quercetin inhibited infiltration of CD68+ macrophages in renal interstitium [108], which was associated with a decrease in iNOS and IL-12. Moreover, quercetin-treated macrophages displayed a decrease in M1-like activation, found to be associated with decreased expression of Notch1, both *in vivo* and *ex vivo* [109]. Altogether, these results suggest an immunomodulatory effect for quercetin and its potential therapeutic use in inflammatory diseases.

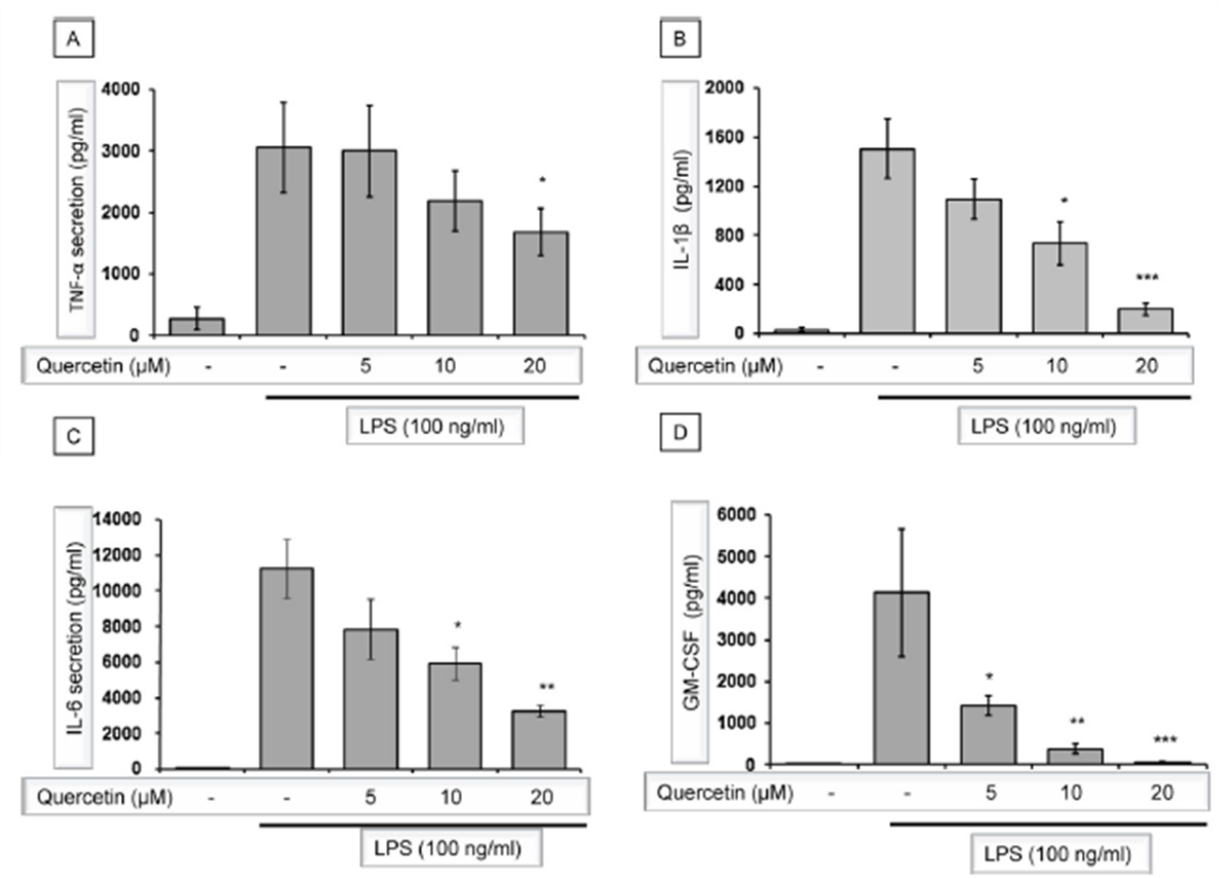

Figure 7 – Quercetin attenuates TNF-α (**A**), IL-1β (**B**), IL-6 (**C**) and GM-CSF (**D**) LPS-induced levels. Pre-incubation with 5-20 μM of quercetin markedly reduced LPS-induction of pro-inflammatory cytokines. *p<0.05, **p<0.01, ***p<0.001, compared to only LPS treated group. Adapted from Endale *et al* (114).

Naringin (**Figure 5G**) was also explored as a natural modulator of macrophage polarization. In Raw 264.7 cells, naringin (50 μM – 1 mM) attenuated LPS-induced levels of several pro-inflammatory mediators [110,111]. This attenuation was associated with suppression of NF-κB activation, through inhibition of IκBα degradation and translocation of p65. Naringin also attenuated activation of MAPK by inhibiting phosphorylation of ERK1/2, JNK and p38 MAPK. More recently, Gil et al observed that incubation of in Raw264.7 macrophages with ≤200 μM of naringin promoted a decrease in M1 markers, such as TNF-α and HMGB1 (**Figure 8**), and inhibition of AMPK [112].

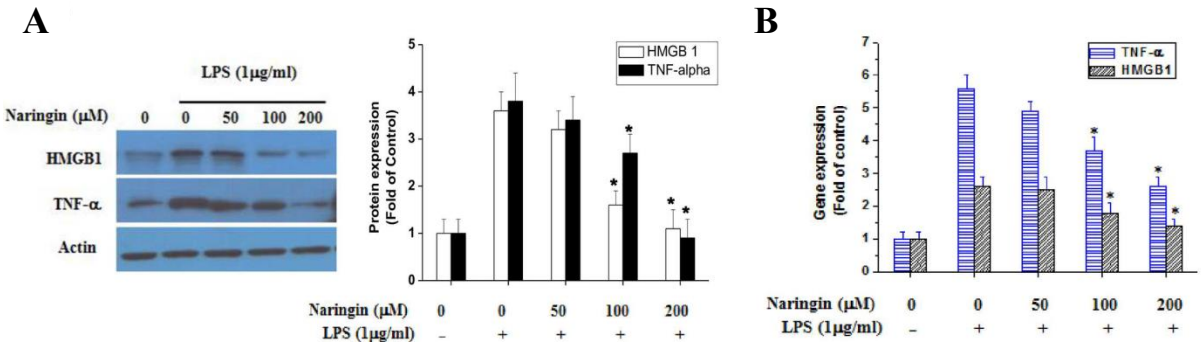

Figure 8 – Effect of naringin on LPS-induced expression of TNF-α and HMGB1 in Raw264.7 macrophages. Cells were pre-treated with concentrations of naringin varying from 0 to 200 µM for 1h, and then stimulated with LPS (1 µg/mL) for 24h. Cells were harvested, lysed and subjected to Western Blott (**A**) and RT-PCR (**B**) to determine TNF-α and HMGB1 expression levels. *p<0.05. Adapted from Gil et al [112].

Other flavonoids have been reported to have some interesting effects on macrophage polarization. For instance, epigallocatechin-3-gallate (EGCG), an abundant flavonol from green tea with anti-inflammatory properties [113], has been shown to reduce pro-inflammatory mediators, such as NO and PGE_2, through downregulation of iNOS and COX-2 expression, in LPS-stimulated macrophages [114]. The use of procyanidin dimer B2, from cocoa, which belongs to the flavonoid subclass of procyanidins, was shown to reduce COX-2 expression in THP-1 macrophages stimulated with LPS [115]. This reduction was associated with a decrease in the activity of pathways important for COX-2 expression and pro-inflammatory activity, JNK, ERK and p38 MAPK, while NF-κB was supressed. In Raw 264.7 cells, the use of proanthocyanidins extracts from green tea also displayed a decrease in COX-2 expression [116]. LPS-stimulated (40 ng/mL) macrophages were pre-incubated with the proanthocyanidins (0-50 µM), and revealed decreased levels of PGE_2 compared to control groups. This decrease in COX-2 expression was also associated with a suppression of JNK, ERK, p38 MAPK and NF-κB pathways. Another flavonoid studied for its immunomodulatory activity was curcumin, a yellow pigment from the plant *Curcuma longa* [117]. Pre-treatment with curcumin (0.5-10 µM) of LPS-stimulated human PBMC and alveolar macrophages resulted in inhibition of several pro-inflammatory cytokines (IL-8, MIP-1α, MCP-1, IL-1β, and TNF-α). In Raw 264.7 macrophages, curcumin was found to inhibit of LPS-induced TNF-α and IL-1β gene expression [118], as well as the production of the pro-inflammatory cytokine IL-8 [119].

Hence, there is already a convincing amount of evidence showing that bioflavonoids are able to attenuate macrophage-mediated inflammation and possibly promote pro-resolving phenotypes. Still, the information on the underlying biological mechanisms remains scarce.

I.4.2. Flavonoids and macrophages lipid metabolism

Assessing how flavonoids modulate macrophage lipid metabolism might provide relevant insights into the role of these important cell constituents on macrophage plasticity and effector functions. However, to our knowledge, only a few works have addressed this issue, as reviewed below.

Naringin was found to inactivate ACC (likely downregulating FA synthesis) in Raw 264.7 macrophages via activation of AMPK signaling [112]. AMPK was also implicated in the action of naringenin towards THP-1 derived macrophages, where it caused increased expression of the Liver X Receptor LXR-α (a key regulator of transcriptional programs involved in lipid homeostasis and inflammation), and of proteins controlling cholesterol efflux (ABCA1 and ABCG1) [120]. Reverse cholesterol transport was increased and cell migration was inhibited, leading the authors to suggest that this polyphenol could be useful in preventing atherosclerosis and foam cell progression. The proteins LXR-α, ABCA1 and/or ABCG1 were also found to be modulated by quercetin [121], cyanidin [122] and chrysin [123], promoting increased cholesterol efflux in both human and murine macrophages. Additionally, in M1-like macrophages, quercetin was reported to inhibit ACC and to up-regulate CPT1a, a crucial mediator of FAO, while decreasing several pro-inflammatory mediators (**Figure 9**) [124].

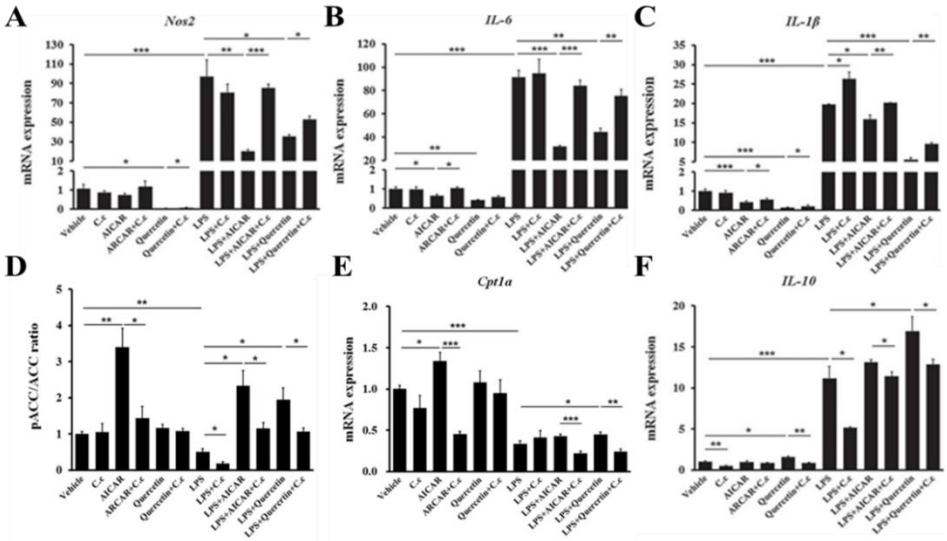

Figure 9 - Modulation of M1-like phenotype profile by quercetin. Murine BMDM were pre-treated with quercetin, followed by treatment with LPS, compound C (CC) and/or AICAR, an inhibitor and an inducer of AMPK, respectively. Quercetin pretreatment resulted in attenuation of M1-like genes, such as (**A**) Nos2, and pro-inflammatory cytokines (**B**) *Il-6* and (**C**) *Il-1β*. Additionally, (**D**) ACC was inhibited, as depicted by increased ACC phosphorylation. Pre-treatment with quercetin also promoted expression of M2-like typical genes, (**E**) *Cpt1a* and (**F**) *Il-10*. *p<0.05, **p<0.01, ***p<0.001. Adapted from Dong et al [108].

The few works described above attest the implication of lipid-related pathways in the attenuation of macrophage inflammatory activity, promoted by flavonoids. However, there is still very little knowledge on how macrophage lipids change upon flavonoid treatment or about the role of different lipid species in macrophage responses to these natural compounds. The lipidomics approach employed in this thesis, and briefly presented in the following section, constitutes a powerful tool to address this problem.

I.5. Macrophage lipidomics

I.5.1. The Lipidomics approach

The whole set of lipid species comprised within a cell, tissue or organism is known as the lipidome, and is considered to be a subset of the metabolome [125]. Lipidomics addresses the large-scale characterization of the lipidome, aiming at simultaneously detecting and/or quantifying a large number of different lipid molecules, as well as their variations in response to exogenous stimuli, diseases or any biological/biomedical condition under study.

The central analytical platform in lipidomics is mass spectrometry (MS), which can be employed based on direct infusion (shotgun lipidomics) or after chromatographic separation of lipids, e.g. through liquid chromatography (LC) [126]. The general workflow for LC-MS lipidomics, performed in this work, is show in **Figure 10**. The first step involves extracting lipids from the biological matrix, typically through Folch or Bligh Dyer methods [127,128], which use chloroform and methanol as extracting solvents. After extraction, the lipid mixture is injected into an HPLC column to perform separation of lipid species before MS-based detection. To be detected, molecular lipid ions must be generated, using an ionization method, such as electrospray ionization (ESI), matrix assisted laser desorption ionization (MALDI) or desorption electrospray ionization (DESI). As a soft ionization technique with minimal ion-source fragmentation, ESI is predominantly employed in lipidomics. Full MS and/or MS/MS data (to provide fragment ion information) are then acquired, so that the resulting data consist of ion chromatograms and MS spectra. Finally, data analysis typically entails peak identification and integration, together with multivariate analysis to identify consistent variation patterns and the varying lipid species.

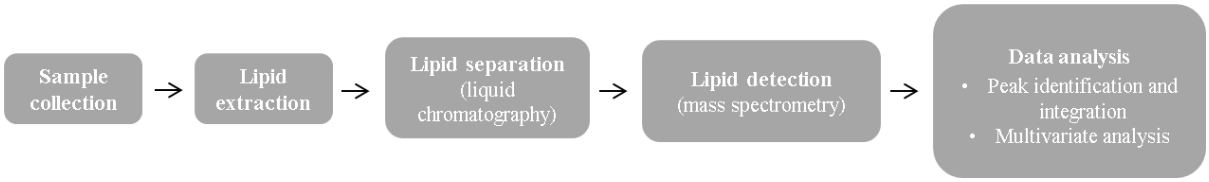

Figure 10 - Workflow of lipidomics. Lipids from biological samples are extracted in organic solvents. Extracted lipids are then separated through chromatography or they are directly infused (shotgun lipidomics) in the mass spectrometer. Peak identification and integration allows characterizing changes in lipids.

I.5.2. Lipidomics studies of macrophages

The utility of MS-based lipidomics for unravelling the lipidome of macrophages has been demonstrated by several recent works. **Table 2** provides a compilation of some representative studies addressing the lipidomic changes of murine or human macrophages in response to different stimuli.

In an early work, Dennis and coauthors have described the lipidomic response of murine RAW 264.7 cells to Kdo2-lipid A (KLA), an active component of LPS [73]. Several changes were identified in the cells fatty acids profile, which, together with transcriptomics data, suggested increased eicosanoid synthesis. Remodelling of glycerolipids, glycerophospholipids, and prenols was also observed, reflecting alterations in most lipid classes during the inflammatory response. The impact of KLA on the RAW macrophage lipidome has also been studied at the subcellular level [129]. It was found that while some changes were common to all organelles (e.g., increases in the levels of ceramides and cholesterol precursors), others were organelle-specific. For example, oxidized sterols increased and unsaturated cardiolipins decreased in mitochondria, whereas unsaturated ether-linked phosphatidylethanolamines decreased in the endoplasmic reticulum. KLA-primed mouse bone marrow-derived macrophages were also examined for lipidomic changes upon exposure to ATP (interpreted as ‘a danger signal’) [67]. The results suggested that STATs were synergistically activated, with STAT1 and STAT3 regulating triacylglycerols and eicosanoids metabolism, respectively. In a more recent study, LC-MS based lipidomics was used to profile different lipid classes in Raw 264.7 macrophages treated with various LPS concentrations [130]. Triglycerides, diacylglycerol, cholesterol, phosphatidylethanolamine (PE), phosphatidylserine (PS), phosphatidylinositol (PI), phosphatidic acid (PA), lyso-phosphatidylcholine (LPC), lyso-phosphatidylethanolamine (LPE), ceramides (Cer), and dihydroceramides (dCer) were increased, whereas cholesterol, PC and lysophosphatidic acid (LPA) were decreased in a concentration-dependent manner. Moreover, treatment of activated macrophages with an anti-inflammatory compound, rosiglitazone, recovered the levels of several lipid species.

Table 2 - MS-based lipidomics studies of macrophages exposed to different stimuli.

Cells	Stimuli	Analytical technique	Main lipidomic findings	Reference
M1/M2 canonical stimuli				
Primary human macrophages	IFN-γ+LPS (M1) IL-4 (M2a) IL-10 (M2c)	SFC-IM-MS	Different levels of AA mobilization; Thromboxane A2 production; Changes in FA profile.	[131]
Raw 264.7, THP-1 macrophages	LPS (M1) IL-4+IL-13 (M2)	HPLC-ESI-MS	Higher levels of lysophospholipids in M2.	[132]
Incubation with Lipids				
Primary human macrophages	eLDL, oxLDL	ESI-MS/MS	Saturation dependent changes in PC and PE plasmalogens; downregulation of endogenous synthesis of cholesterol and its exogenous uptake.	[133]
Mouse BMDM	Laurate, myristate, palmitate, stearate, oleate	LC-ESI-MS/MS	Altered PL saturation status.	[134]
Mouse BMDM	Palmitic acid, gamma-T3	LC-MS/MS	Gamma-T3 treatment caused: decreases in lysophospholipids, diacylglycerol and free AA; decreased PGE_2 secretion; attenuated ceramide synthesis; rescued ATP production.	[135]
Other Stimuli				
Raw 264.7	Aspirin+KLA, Ibuprofen+KLA	UPLC-Q-TOF-MS	PC(17:1/18:1) and PA(18:0/18:4) identified as inflammatory response targets to aspirin and ibuprofen; Aspirin and ibuprofen inhibited COX, induced FA desaturation and changes of PL components.	[138]
J774A.1	Bisphenol S	LC-MS/MS	BPS modulated, glycerophospholipids and acylglycerols.	[137]
Raw 264.7, BMDM	TiO_2 nanoparticles	GC-MS	Decreased levels of cardiolipins; Increased PGD_2, PGE_2, 15d-PGJ_2, COX-2 metabolites.	[136]

The lipidomic profile of M1- and M2-polarized human macrophages has been investigated in two recent studies. Montenegro-Burke and colleagues obtained primary human macrophages differentiated from blood monocytes and activated them with IFN (M1), IL-4 (M2a) and IL-10 (M2c) [131]. By employing supercritical fluid chromatography-ion mobility mass spectrometry analysis, alterations in several classes of membrane phospholipids and fatty acids were found in differentially polarized cells. Moreover, some biologically relevant eicosanoids were quantified in cells culture media. The results showed different levels of arachidonic acid mobilization as well as other fatty acid changes, reflecting activation of processes related to the cell membrane remodelling and the biosynthesis of lipid signalling molecules. In the other study, Zhang et al. detected 300 lipid molecules in human and murine macrophages and identified changes during their polarization with LPS (M1) and with IL-4/IL-13 (M2) [132]. In general, macrophage activation was accompanied by a striking shift in the composition of glycerophospholipids (GLs) from saturated and monounsaturated to polyunsaturated. Moreover, M2 macrophages showed higher levels of lysophospholipids (lysoGLs) than M1 macrophages. Differences in specific lipid species noted in macrophages differentiated from monocytic THP-1 cells (also used in this thesis), at different polarization states, are summarized in **Table 3**.

Table 3 - Variations in GLs of THP-1 macrophages activated with LPS (M1) or with IL-4 and IL-13 (M2), compared to unstimulated macrophages (M0).

Class	Phenotype	Glycerophospholipids	Variation
PC	M1	PC(34:5), PC(36:4), PC(36:5), PC(38:1), PC(38:2), PC(38:4), PC(38:5), PC(38:6), PC(38:7), PC(40:4), PC(40:5), PC(40:6), PC(40:7), PC(40:8)	↑
	M2	PC(34:5), PC(36:5), PC(38:1), PC(38:2), PC(38:4), PC(38:7), PC(40:5), PC(40:6); PC(40:7), PC(40:8)	↑
PI	M1	PI(32:2), PI(34:4), PI(36:4), PI(36:5), PI(36:6), PI(38:4), PI(38:5), PI(38:6), PI(40:7)	↑
		PI(30:0), PI(30:2), PI(34:0), PI(34:1), PI(36:0), PI(36:1), PI(36:2), PI(38:1), PI(38:2), PI(40:5)	↓
	M2	PI(32:2), PI(34:4), PI(36:4), PI(36:5), PI(38:4), PI(38:5), PI(38:6), PI(40:7)	↑
		PI(30:0), PI(32:1), PI(34:1), PI(36:0), PI(36:1), PI(36:2), PI(38:1), PI(38:2), PI(40:5)	↓
PS	M1	PS(36:3), PS(36:5), PS(38:3), PS(38:4), PS(38:5), PS(38:6), PS(40:4), PS(40:5), PS(40:6)	↑
		PS(32:1), PS(32:2), PS(34:1), PS(34:2), PS(38:1)	↓
	M2	PS(36:3), PS(36:5), PS(38:3), PS(38:5), PS(38:6), PS(40:5), PS(40:6)	↑
		PS(32:1), PS(34:1), PS(38:1)	↓
LPC	M1	LPC(20:3), LPC(20:4), LPC(20:5), LPC(22:4), LPC(22:6)	↑
	M2	LPC(20:4), LPC(20:5), LPC(22:4)	↑
LPE	M1	LPE(20:1), LPE(20:4), LPE(20:5), LPE(22:6)	↑
	M2	LPE(20:1), LPE(20:4), LPE(20:5), LPE(22:6)	↑
		LPI(18:0), LPI(18:2), LPI(20:4)	↓
LPG	M1	LPG(14:0), LPG(16:1), LPG(18:1)	↓
LyPS	M1	LyPS(18:2), LyPS(20:3), LyPS(20:4), LyPS(20:5), LyPS(22:4), LyPS(22:5)	↑
		LyPS(16:0), LyPS(16:1), LyPS(18:0), LyPS(22:0)	↓
	M2	LyPS(16:0), LyPS(16:1), LyPS(18:0), LyPS(22:0)	↓

Legend: PC – phosphatidylcholine; PE – phosphatidylethanolamine; PI – phosphatidylinositol; PS – phosphatidylserine; LPC – lysophosphatidylcholine; LPE – lysophosphatidylethanolamine; LPG – lysophosphatidylglycerol; LyPS – lysophosphatidylserine; ↑ - increase; ↓ - decrease.

A few studies have addressed lipidomic changes upon macrophage loading with lipids, which represents a pro-inflammatory stimulus particularly relevant in the context of atherosclerosis, obesity and other metabolic diseases. Exposure of primary human macrophages to enzymatically modified and oxidatively modified lipoproteins (eLDL and oxLDL, respectively) led to a transient, strong elevation of LysoPC [133]. Analysis of individual lipid species showed LDL-dependent effects for LysoPC, choline plasmalogens (PC-P) and ethanolamine plasmalogens (PE-P) species. On the other hand, changes related to downregulation of endogenous lipid synthesis were common to all stimuli. In another work, primary murine macrophages were treated with saturated and unsaturated fatty acids (FA) [134]. All FA produced strong changes in numerous lipid species within all classes assessed, being especially pronounced for phosphatodylcholine and ether-phosphatidylcholine lipid species. Kim et al. have also stimulated LPS-primed bone marrow derived macrophages with saturated FA along with gamma-tocotrienol (gamma-T3), an unsaturated vitamin E that has been shown to attenuate the NLRP3 inflammasome [135]. The SFA-mediated inflammasome activation induced robust changes in species of glycerolipids, glycerophospholipids, and sphingolipids in BMDM, while the gamma-T3 treatment caused substantial decreases of lysophospholipids, diacylglycerol, and free arachidonic acid (AA, C20:4), indicating its limited availability for the synthesis of eicosanoids. In addition, gamma-T3 attenuated ceramide synthesis by transcriptional downregulation of key *de novo* synthesis enzymes.

Additionally, the MS-based lipidomics approach has also been employed to assess macrophage responses to titanium nanoparticles [136], the chemical Bisphenol S [137] and anti-inflammatory drugs [138], as summarized in **Table 3**.

The studies mentioned above demonstrate that MS-based lipidomics is an exquisitely valuable approach to characterize changes in macrophage lipid composition and metabolism in response to various stimuli. However, to the best of our knowledge, the effects of flavonoids on macrophage lipidome haven't been previously studied. In this work, LC-MS lipidomics is employed for the first time to evaluate how three flavonoids (Quercetin, Naringin and Naringenin), with reported anti-inflammatory activity, modulate different lipid classes in human macrophages.

I.6. Objectives of this work

This work aims at characterizing the changes in the phospholipidome of human macrophages in response to three flavonoids with well-known anti-inflammatory activity: quercetin, naringin and naringenin. In particular, specific objectives are:

- To reveal the main variations in PL species upon flavonoid treatment of resting (M0) and M1 pre-polarized macrophages;

- To identify PL variations in flavonoid-treated macrophages that may potentially be related to their anti-inflammatory activity;

- To compare the effects induced by the three flavonoids;

- To highlight features that may advance current understanding of flavonoids mode of action, particularly regarding the remodeling of cellular lipids.

II. Materials and methods

II.1. Differentiation and polarization of THP-1 cells

Human monocytic THP-1 cells (ATCC, Virginia, USA) were cultured in Roswell Park Memorial Institute medium (RPMI 1640, Gibco, #51800-035) culture medium containing 10% of heat-inactivated fetal bovine serum (FBS), 1% of penicillin/streptomycin and supplemented with 2.0 g/l sodium bicarbonate (Sigma Aldrich, #55761-500G). Cells were maintained in culture at 37ºC and 5% of CO_2.

THP-1 monocytes were differentiated into macrophages (M0) by 24-hour incubation with 50 ng/mL of phorbol 12-myristate 13-acetate (PMA, Sigma Aldrich, #P8139-1MG) in RPMI medium, which was followed by a 24h rest in new medium. M1 macrophage polarization was carried out by 24-hour incubation with 20 ng/mL of interferon-γ (IFN-γ, Biolegend, #570206) and 100 ng/mL of lipopolysaccharides (LPS, Sigma Aldrich, L4391-1MG). To obtain M2 macrophages, M0 cells were incubated with 20 ng/mL of interleukin-4 (IL-4, Biolegend, #574004) and 20 ng/mL of interleukin-13 (IL-13, Biolegend, #571104), for 48h. All experiments were performed with cells at passage 10 to 17.

II.2. Fluorescence microscopy

THP-1 monocytes were seeded at 30.000 cells/well in µ-slide 8 well adherent plates (ibidi, Germany), differentiated into macrophages, and subsequently polarized to M1 and M2, as described above.

After medium removal and phosphate-buffered saline solution (PBS) washing, cells were fixated with Formaline 4%, washed once with PBS, blocked with a 5% BSA solution for 30 mins and washed again for three times with PBS. Fixated macrophages were incubated with respective antibody panels for the M1 phenotype (Alexa Fluor 488 anti-human CD 80 [Biolegend, clone #305214 2D10] and PyE [phycoerythricin] anti-human CD64 [Biolegend, #305008 clone 10.1]) and the M2 phenotype (FITC anti-human CD36 [Biolegend, #336206 clone 5-771] and PyE anti-human CD209 [Biolegend, #330104 clone 9E9A8]) for a 1-hour period. This was followed by a 15-min incubation with a 2:1000 solution of DAPI (4′,6-diamidino-2-phenylindole). Cells were washed 5 times with PBS and stored in PBS at 4ºC

until observation. Mounting medium was added to each well and observation proceeded in a fluorescence microscope (ZEISS AxioImager M2, equipped with a 10x/0.25 objective – Carl Zeiss, Germany).

II.3. Cell Viability Assay

To assess the toxicity of flavonoids in THP-1-derived macrophages and select the concentrations to be used in subsequent experiments, the Alamar Blue reduction assay was performed. THP-1 monocytes were seeded at 30.000 cells/well in 96-well, differentiated, and treated with quercetin (Alfa Aesar, #A15807), naringin (Sigma Aldrich, #71162-25G), or naringenin (Sigma Aldrich, #BCBT8724) at concentrations ranging from 0 to 200 µM, during 24h incubation period. The medium was then discarded and cells were incubated with a 10% solution of alamar BlueTM Cell Viability Reagent (Invitrogen, #DAL1025, alamar Blue/RPMI 1640 medium) for 24 h. Each well's solution was then transferred into a black flat bottom 96-well plate, and fluorescence was measured at 540/600 with BioTek Synergy HTX Multi-mode Reader, using Gen5 Microplate Reader and Imager Software Version 2.09 (BioTek Software, Wisconsin, VT, USA).

Statistical analysis was performed using GraphPad Prism version 6.01 (GraphPad Software, San Diego, CA). All data were analysed by one-way ANOVA, with a Newman-Keuls multiple comparison test, to evaluate statistical significance of intergroup differences in all the tested variables. p-values <0.05 were considered statistically significant.

II.4. Quantification of cytokines (LEGENDplex assay)

To assess the production of pro- and anti-inflammatory cytokines by macrophages exposed to M1 and M2 canonical stimuli, as well as to the three flavonoids, cell medium supernatants were analysed by bead-based LEGENDplex assay (#740509, Human M1/M2 Macrophage Panel 10-plex with V-bottom plate, BioLegend, London). The M1 panel was composed of IL-12p70, TNF-α, IL-6, IL-1β, IL-12p40, IL-23 and CXCL10, whilst the M2 panel was composed of IL-6, IL-10, CCL17 and IL-1RA. Standards were initially prepared

from a cocktail of cytokines. Standards and samples were added to a V-bottom plate, together, with 25 µL of Assay Buffer (AB). A solution of fluorescence-encoding beads was then added to both standards and samples. The plate was sealed, covered from light, and placed in a plate shaker at 750 rpm for 2h, at room temperature. After shaking, the plate was centrifuged for 5 min at 250x*g*, the supernatant discarded, the plate was washed with 1X Wash Buffer (WB) and submitted to a second centrifugation for 5 min at 250x*g*. Then after discarding the supernatant, detection antibodies were added to each well. The plate was sealed and shook for 1 hour at 750 rpm, at room temperature, after which, 25 µL of streptavidin-phycoerythrin (SA-PyE) were added to each well. The plate was again sealed and shook for 30 min at 750 rpm, supernatant discarded and a final centrifugation/washing step was performed. Finally, beads were ressuspended in 150 µL of WB.

Standards and samples were read on a flow cytometer BD Accuri™ C6 (BD Biosciences). The minimum detection limits of the LEGENDplex assay for the analysed cytokines were: IL-12p70 (1.0 pg/mL), TNF-α (1.4 pg/mL), IL-6 (1.1 pg/mL), IL-1β (1.3 pg/mL), IL-12p40 (9.9 pg/mL), IL-23 (1.7 pg/mL), CXCL10 (1.4 pg/mL), IL-10 (1.0 pg/mL), CCL17 (2.1 pg/mL), IL-1RA (48.7 pg/mL). The maximum measurable was 10 ng/mL for all cytokines.

To analyse cytokine measurements, the LEGENDplex v8.0 software was used. Statistical analysis was performed using GraphPad Prism version 6.01 (GraphPad Software, San Diego, CA).

II.5. Sample preparation for lipidomics

II.5.1. Flavonoid treatments

THP-1 monocytes at cell passage 15-17 were seeded at $1x10^6$ cells/mL in cell culture dishes and differentiated as described in **II.1**. After 24-hour in fresh medium, macrophages were treated with 60 µM of quercetin (Alfa Aesar, #A15807), 200 µM of naringin (Sigma Aldrich, #71162-25G), or 100 µM of naringenin (Sigma Aldrich, #BCBT8724), for a period of 48h. Pre-polarized M1 macrophages were also subjected to 24h flavonoid exposure (at the

same concentrations). Appropriate controls were used in all cases. **Figure 11** provides a schematic representation of the samples collected for subsequent extraction.

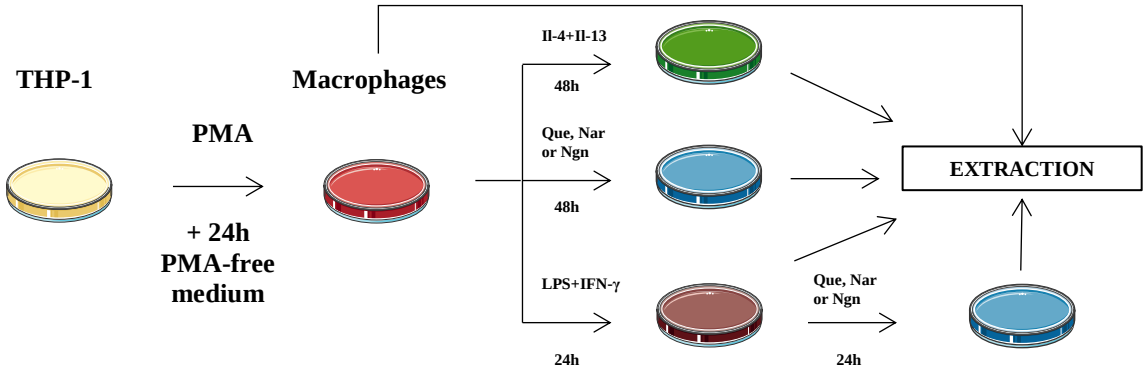

Figure 11 – Schematic representation of cell culture and incubation with flavonoids and other compounds. THP-1 monocytes were differentiated into macrophages using 50 ng/mL of PMA for a 24-hour period, followed by a 24-hour resting period in new medium. Macrophages were then stimulated with either 60 µM of quercetin, 200 µM of naringin, 100 µM of naringenin, 100 ng/mL of LPS and 20 ng/mL of IFN-γ, or 20 ng/mL of IL-4 and 20 ng/mL of IL-13. Additionally, some dishes with cells treated with 100 ng/mL of LPS and 20 ng/mL of IFN-γ were also treated with 60 µM of quercetin, 200 µM of naringin and 100 µM of naringenin.

II.5.2. Cell extraction

Lipids were extracted from macrophages according to the extraction protocol established by Bligh and Dyer [128]. This method partitions lipids into an organic phase by using a 1:2 chloroform:methanol ratio.

Firstly, the medium was removed and the cells were washed four times with PBS. Then, 1 mL methanol 80% (v/v) (Sigma Aldrich, HPLC grade) was added to the dish to quench metabolic activity and cells were scrapped off. The cell suspension was transferred into a glass tube containing 0.5 mm glass beads (to aid cell suspension), which was kept on ice until cell samples were quenched.

After 2 min vortexing, 400 µL of cold chloroform (VWR, HPLC grade) were added to each tube followed by vortexing and another addition of 400 µL of chloroform and 360 µL cold milli-Q water. Samples were vortexed again and left to rest on ice for 20 min.

Then, after centrifugation at 3000x*g* for 10 min (Centrifuge 5702, Eppendorf), two phases were separated. The bottom organic phase was transferred into an amber glass vial and the remaining sample was re-extracted with 400 µL of chloroform, to collect the organic phase again and add it to the previous vial.

Removed medium was collected and centrifuged at 1000xg for 10 min. The supernatants were then collected and stored at -80ºC. Aqueous phases were also processed and stored for NMR metabolomics, performed in the scope of another thesis.

II.5.3. Phospholipid quantification

In order to determine the phospholipid (PL) amount in each lipid extract, the phosphorous assay was performed according to Bartlett and Lewis [140]. Phosphate standards from 0.1 to 2 µg of phosphorous (P) were prepared from a monosodium phosphate solution (100 µg/mL, $NaH_2PO_4.2H_2O$).

Dried aliquots of samples and standards were re-suspended in 125µ of perchloric acid. Samples were then heated at 180ºC in a heating block (Stuart, U.K.), for 40-60 min, followed by cooling at room temperature. Thereafter, 825 µL of milli-Q water 125 µL of 2.5% solution of ammonium molybdate (2.5g ammonium molybdate/100 mL milli-Q water) and 125 µL of 10% ascorbic acid (10g ascorbic acid/100 mL milli-Q water) were added to samples and standards, vortexed after each addition and incubated for 10 min at 100ºC in a water bath. After cooling in a cold water bath, the samples and standards absorbance was measured at 797 nm in a microplate reader (Multiscan 90, ThermoScientific). Four independent measurements were performed for each sample type (i.e. exposure condition).

II.5.4. Sample preparation for LC-MS

Dried samples were resuspended in dichloromethane to have a PL concentration of 1 µg/µL (each volume was determined based on phospholipid quantification). From each sample, 5 µL (representing 5 µg of phospholipid) were taken and transferred to an appropriate vial, followed by addition of 91 µL of a solvent system consisting of two mobile phases in a proportion of 60% eluent B (60% acetronitrile, 40% methanol, and 1 mM of amonium acetate), and 40% eluent A (50% of acetonitrile, 25% of methanol, 25% of water, and 1 mM

of amonium acetate, and 4 µL of an internal standards mixture containing PC(14:0/14:0), PE(14:0/14:0), PG(14:0/14:0), PI(14:0/14:0), PS(14:0/14:0), PA(14:0/14:0), LPC(19:0), Cer(18:1/15:0), SM(d18:1/17:0), and CL(14:0/14:0/14:0/14:0).

II.6. Mass Spectrometry

II.6.1. Data acquisition

Phospholipids were separated through hydrophilic interaction liquid chromatography (HILC-LC) using an Ascentis Si HPLC Pore (15 cm x 1.0 mm, 3 µm; Sigma-Aldrich) and a high performance-liquid chromatography (HPLC) system (Ultimate 3000 Dionex, Thermo Fisher Scientific, Bremen, Germany) with an autosampler coupled online to the Q-Extractive® hybrid quadrupole Orbitrap® mass spectrometer (Thermo Fisher Scientific, Bremen, Germany). An aliquot of 5 µL of each sample mixture was injected into the HPLC column, at a flow rate of 40 µL/min and a temperature of 30ºC. Initially, 40 % of mobile phase A was held isocraticallty at 8 min, followed by a linear increase to 60% of mobile phase A for 7 min, a 5-min maintenance period and the return to initial conditions within 5 min. A 10-min interval was given between injections to allow return to equilibrium. The mass spectrometer with a Q-Extractive® orbitrap and a heated electrospray ionization (HESI) operated simultaneously in positive mode (voltage of 3 kV) and negative mode (voltage of -2.7 kV). The sheath gas flow rate was maintained at 15 units and the capillary temperature was 250ºC, while S-lenses RF was of 50 units and probe's temperature was 100ºC. Mass spectral acquisition method was at full scan in a scale of m/z values of 200-1600, with a resolution of 70.000, automatic gain control of $1x10^6$ and 2 microscans. The 10 most abundant ions were selected for ion fragmentation at collision cell HCD. Collision energy varied between 25, 30 and 35 eV. The tandem mass spectra (MS/MS spectra) were obtained at a resolution of 17.500, automatic gain control of $1x10^5$, 1 microscan, and an isolating window of 1 *m/z*. Ion selection was limited to $2x10^4$ countings. Maximum accumulated ions were established at 100 ms for MS spectra and 50 ms for MS/MS spectra. Dynamic exclusion was defined as 60 s.

II.6.2. Peak assignment and integration

To identify phospholipid classes in each experimental condition, the acquired spectra were analysed using the data acquisition software Xcalibur v3.3 (Thermo Fisher Scientific, USA). Identification was performed based on 5 ppm of the lipid exact mass measurements and MS/MS spectra interpretation. After identification, quantification of molecular species was performed through integration of chromatographic peaks. Mass spectra were processed and integrated using the software MZmine v2.32. The software allows for filtering and smoothing, peak detection, peak processing, and assignment against in-house database [141]. During the processing of raw data acquired in full MS mode, all the peaks with raw intensity lower than $1x10^5$ were excluded.

Relative quantification was performed by exporting peak areas values into a computer spreadsheet (Excel, Microsoft, Redmond, WA). For normalizing the data, peak areas of the extracted-ion chromatograms (XIC) of each lipid molecular species were divided by the sum of total XIC areas of the identified PL species.

II.6.3. Multivariate and univariate statistics

Multivariate analysis of data matrices (normalized peak areas of lipid species in the different samples) was performed using Metaboanalyst [142]. The data was log-transformed and scaled to unit variance (auto-scaling) before Principal Component Analysis (PCA) and Partial-least Squares Discriminant Analysis (PLS-DA). The results were visualized in scores scatter plots and VIP plots showing the top variables contributing for sample discrimination. Univariate data analysis was performed using Excel (Microsoft, Redmond, WA), to produce Volcano Plots, and R software (R i386 version 3.2.3), to obtain Boxplots and Heatmaps. For assessing statistical significance using multiple comparisons, ANOVA with Sidak correction was performed on GraphPad Prism version 6.01 (GraphPad Software, San Diego, CA).

III. Results and Discussion

III.1. Characterization of M1 and M2 macrophages

III.1.1. Phenotypic markers

To confirm that M1 and M2 macrophages were obtained through the canonical stimuli employed (LPS/IFN-γ and IL-4/IL-13, respectively), the expression levels of surface receptors typically increased in each phenotype were evaluated through immunostaining and fluorescence microscopy. The surface proteins CD64 and CD80 were used as M1 markers, while CD209 and CD36 were used as M2 markers [143]. **Figure 12A** displays the expression of CD64 in LPS/IFN-γ stimulated macrophages, stained in orange. Expression of CD80 was not detected. **Figure 12B** represents the expression of CD209 (stained in green) and CD36 (stained in orange) in IL-4/IL-13-stimulated macrophages. Both receptors were markedly detected.

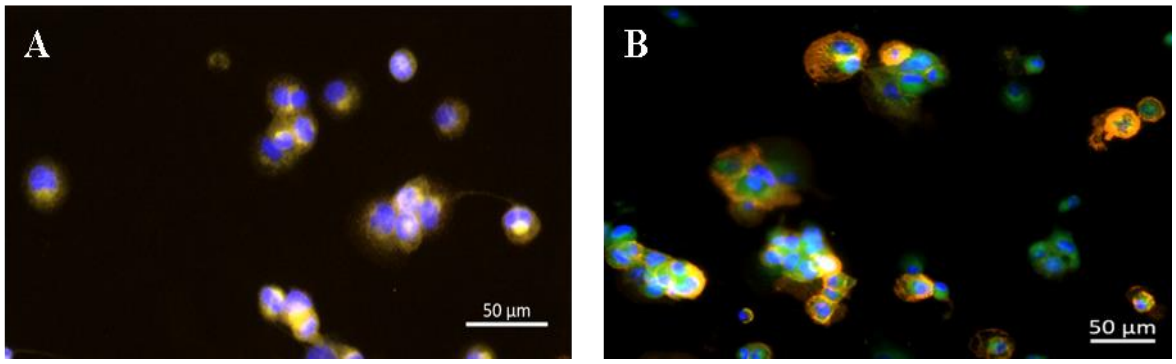

Figure 12 – Expression of surface receptors in THP-1 macrophages activated to M1 (LPS+IFN-γ, 24h) and M2 (IL-4+IL-13, 48h) phenotypes. (**A**) M1 activated macrophages expressing CD64. (**B**) M2 activated macrophages expressing CD209 and CD36. CD64 and CD36 are stained in orange, while CD209 is stained in green. Cell nuclei are stained in blue.

To further assess macrophage phenotypic features, we measured the levels of different cytokines in the cells medium supernatant. LPS/IFN-γ produced an up-regulation of some pro-inflammatory cytokines (**Figure 13A**). In particular, TNF-α, IL-6, IL-1β and CXCL10 were significantly increased compared to control M0 macrophages ($p<0.0001$). On the other hand, when macrophages were activated with 20 ng/mL of IL-4 and 20 ng/mL of IL-13, we observed an up-regulation of the levels of CCL17 and IL-1RA, two anti-inflammatory cytokines (**Figure 13B**). CCL17 is a small cytokine belonging to the chemokine class that

attracts dendritic cells and monocytes. CCL17 has been previously found up-regulated in M2-like macrophages [27]. IL-1RA is a natural inhibitor of the pro-inflammatory effect of IL-1β and has also been identified to characterize M2-like phenotype [144]. Curiously, the levels of another well-known anti-inflammatory cytokine (IL-10) did not increase significantly in IL-4/IL-13 polarized macrophages.

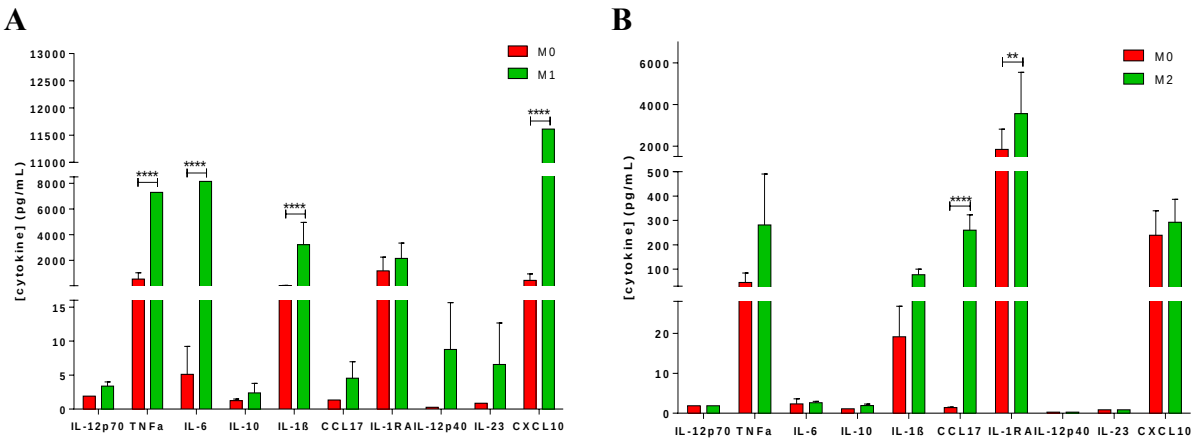

Figure 13 – Changes in the expression of pro- and anti-inflammatory cytokines of M1-like and M2-like polarized macrophages. IL-12p70, TNFαa, IL-6, IL-1β, IL-12p40, IL-23 and CXCL10 are pro-inflammatory cytokines. IL-10, CCL17 and IL-1RA are anti-inflammatory cytokines. **, **** statistical significance ($p<0.01$, $p<0.0001$, respectively). Error bars represented as mean±SD. (n=3)

Still, based on the data described above, comprising surface markers and cytokine production, we may conclude that the polarization stimuli employed generated pro-inflammatory and anti-inflammatory macrophages. For the sake of simplicity, these macrophages will be designated as M1 and M2 cells along this thesis.

III.1.2. Lipid composition

III.1.2.1. Description of macrophage phospholipidome

Interpretation of mass spectrometry data collected for macrophage lipid extracts allowed identification and quantification of phospholipid (PL) species. Each PL class typically displays a characteristic retention time (RT) range. The chromatogram in **Figure 14** shows a time-dependent representation of the relative abundance of PL species from a sample, often referred to as total ion chromatogram (TIC), in negative ion mode. The reconstructed-ion chromatogram (RIC) is a mass-dependent representation of the relative abundance of PL species. **Figures 15-21 A** display a representative MS spectrum of each class identified. Identification of individual PL species was achievable through MS and MS/MS data interpretation. We identified 147 PL species belonging to 8 different classes: phosphatidylcholines (PC; with both diacyl and alkyl-acyl species), phosphatidylethanolamines (PE; with both diacyl and alkyl-acyl species), lyso-phosphatidylcholines (LPC), lyso- phosphatidylethanolamines (LPE), phosphatidylglycerols (PG), phosphatidylinositols (PI), phosphatidylserines (PS), and sphingomyelins (SM). These PL species can be found on **Table 5**.

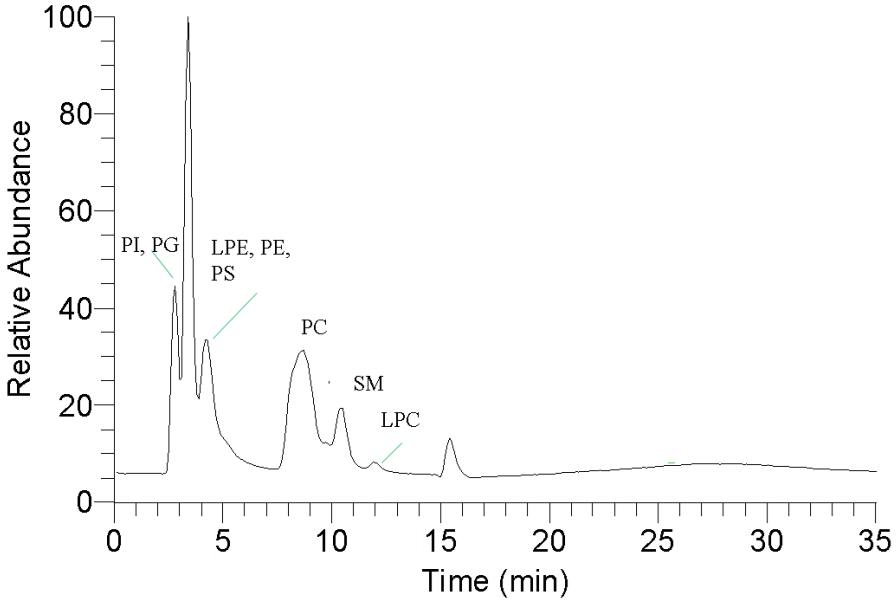

Figure 14 - Representative TIC from THP-1 macrophages.

Identification of each PL species was based on the retention time of its class and exact mass of the species, together with characteristic fragment ions or neutral losses for each class found in MS/MS spectra, in both negative and positive ion mode. Additionally, fatty acyl-chains were identified through interpretation of MS/MS spectra of each species, in negative ion mode, by the identification of carboxylate anions, $RCOO^-$ ions. The identification of the most abundant species from each class is explained in detail along the following paragraphs.

Phosphatidylcholines (PC) were identified in positive ion mode, as $[M+H]^+$ ions. The most abundant PC molecular species was identified at *m/z* 760.5848 [PC(34:1)]. The MS/MS spectrum showed the abundant ion at *m/z* 184.0730, which corresponds to the phosphocholine polar head group. PC were also identified in negative ion mode, as $[M+CH3COO]^-$ ions, which corresponds to a mass shift of plus 58.0055 Da in comparison with the $[M+H]^+$ ions. The most abundant PC molecular species was found at *m/z* 818.5908 [PC(34:1)]. The MS/MS spectrum showed product ions at *m/z* 168.0421, corresponding to the demethylated phosphocholine polar head group. The presence of these two types of product ions in both positive and negative ion mode MS/MS allowed to confirm the presence of PC molecular species. It was also possible to observe the carboxylate anions of fatty acyl chains 16:0 (R_1COO^-) at *m/z* 255.2324 and 18:1 (R_2COO^-) at *m/z* 281.2482. Therefore, this PC species could be identified as PC(34:1) [PC(16:0/18:1)].

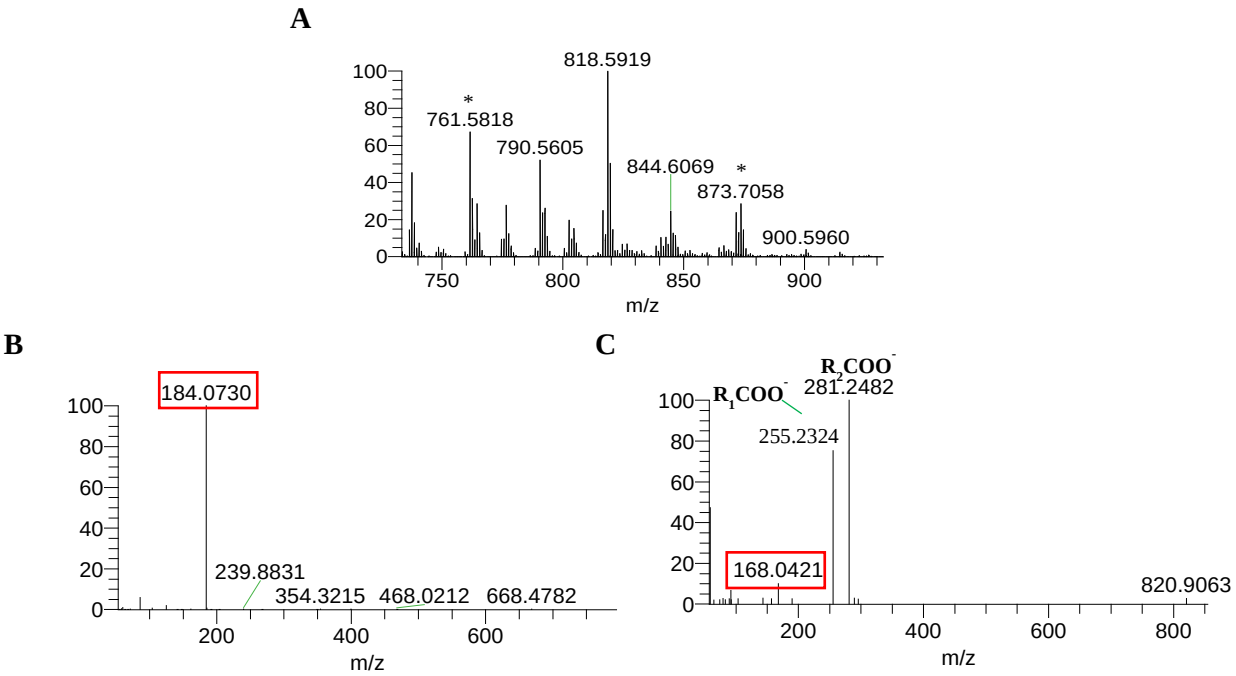

Figure 15 - Identification of phosphatidylcholine (PC). (**A**) MS spectrum of PC region. (**B**) ESI-MS/MS spectrum (HCD fragmentation) of the $[M+H]^+$ ion of PC(34:1) (*m/z* 760.5848). (**C**) ESI-MS/MS spectrum (HCD) fragmentation of the $[M+CH_3COO]^-$ ion of PC(34:1) (*m/z* 818.5908). Fragment ions characteristic for the PC class were highlighted in a red box. *background

Phosphatidylethanolamines (PE) were identified in positive ion mode, as $[M+H]^+$ ions. The most abundant PE molecular species were identified at *m/z* 768.5531 [PE(38:4)]. The MS/MS spectrum showed product ions at *m/z* 627.5308, formed due to neutral loss of 141.0191, which corresponds to the phosphoethanolamine polar head group. PE were also identified in negative ion mode, as $[M-H]^-$ ions. The most abundant PE molecular species was found at *m/z* 766.5367 [PE(38:4)]. The MS/MS spectrum showed the abundant ion at *m/z* 140.0108 corresponding to the phosphoethanolamine polar head group. The presence of these two types of product ions allowed to confirm the presence of PE molecular species. It was also possible to observe the carboxylate anions of fatty acyl chains 18:0 (R_1COO^-) at *m/z* 283.2644 and 20:4 (R_2COO^-) at *m/z* 303.2330. Therefore, this PE species could be defined as PE(38:4) [PE(18:0/20:4)].

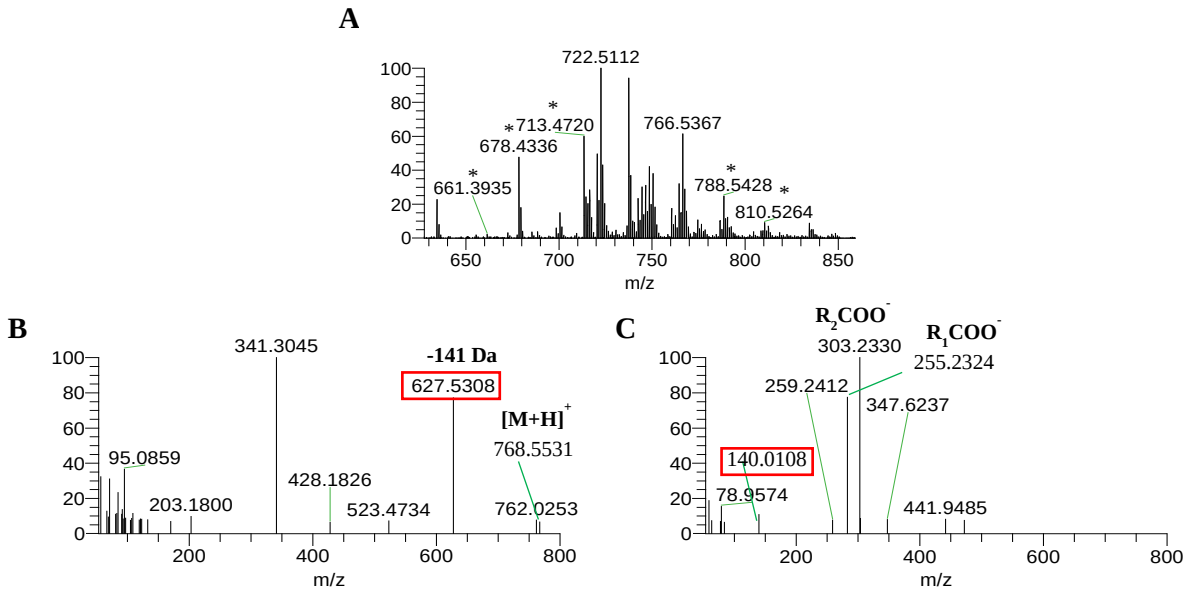

Figure 15 - Identification of phosphatidylethanolamine (PE). (**A**) MS spectrum of PE region. (**B**) ESI-MS/MS spectrum (HCD fragmentation) of the $[M+H]^+$ ion of PE(38:4) (*m/z* 768.5531). (**C**) ESI-MS/MS spectrum (HCD) fragmentation of the $[M-H]^-$ ion of PE(38:4) (*m/z* 766.5367). Fragment ions characteristic for the PE class were highlighted in a red box. *background

Phosphatidylglycerols (PG) were identified in negative ion mode, as $[M-H]^-$ ions. The most abundant PG molecular species was found at *m/z* 747.5174 [PG(34:1)]. The MS/MS spectrum showed the abundant ion at *m/z* 153.9944 and 171.0061, corresponding to the phosphoglycerol group. The presence of these product ions allowed to confirm the presence of PG molecular species. It was also possible to observe the carboxylate anions of fatty acyl chains 16:0 (R_1COO^-) at *m/z* 255.2326 and 18:1 (R_2COO^-) at *m/z* 281.2482. Therefore, this PG species was identified as PG(34:1) [PG(16:0/18:1)].

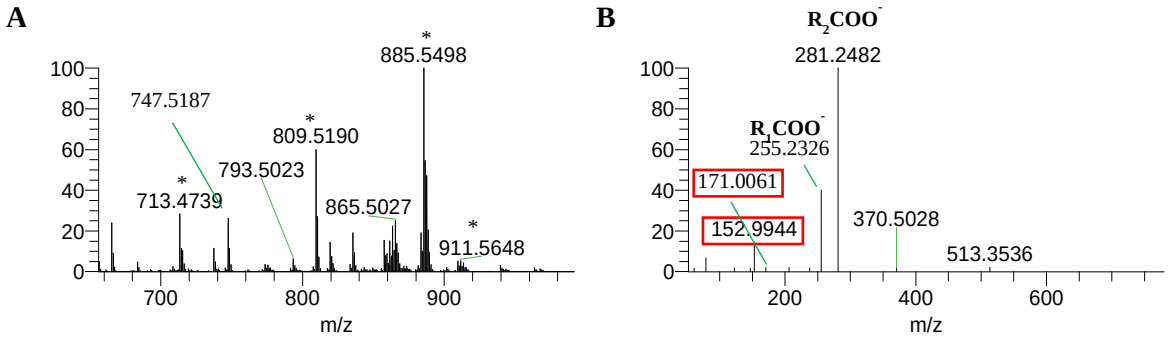

Figure 17 - Identification of phosphatidylglycerol (PG). (**A**) MS spectrum of PG region. (**B**) ESI-MS/MS spectrum (HCD) fragmentation of the $[M-H]^-$ ion of PG(34:1) (*m/z* 747.5174). Fragment ions characteristic for the PG class were highlighted in a red box. *background

Phosphatidylinositols (PI) were identified in negative ion mode, as $[M-H]^-$ ions. The most abundant PI molecular species was found at *m/z* 885.5488 [PI(38:4)]. The MS/MS spectrum showed the characteristic ion at *m/z* 241.0111 corresponding to the phosphatidylinositol polar head group. Additionally, the MS/MS spectrum showed the abundant ion at *m/z* 153.9947. The presence of these product ions allowed to confirm the presence of PI molecular species. It was also possible to observe the carboxylate anions of fatty acyl chains 18:0 (R_1COO^-) at *m/z* 283.2647 and 20:4 (R_2COO^-) at *m/z* 303.2334. Therefore, this PI species could be defined as PI(38:4) [PI(18:0/20:4)].

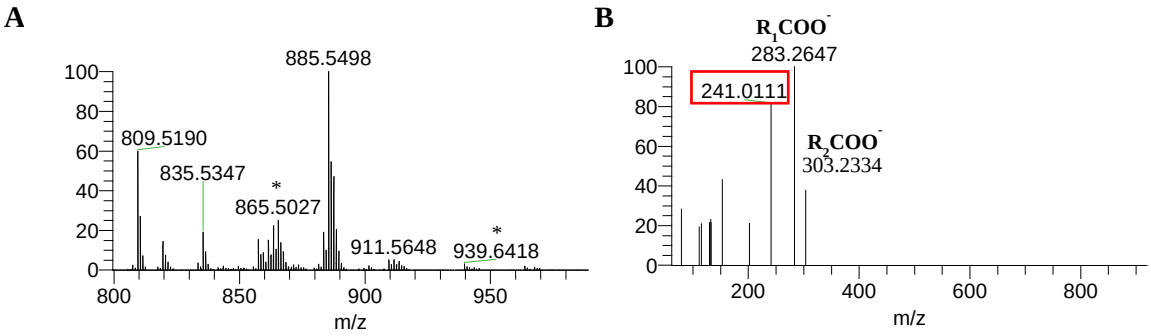

Figure 18 - Identification of phosphatidylinositol (PI). (**A**) MS spectrum of PI region. (**B**) ESI-MS/MS spectrum (HCD) fragmentation of the $[M-H]^-$ ion of PI(38:4) (*m/z* 885.5488). Fragment ions characteristic for the PI class were highlighted in a red box. *background

Phosphatidylserines (PS) were identified in negative ion mode, as $[M-H]^-$ ions. The most abundant PS molecular species was found at *m/z* 810.5278 [PS(38:4)]. The MS/MS spectrum showed the abundant ion at *m/z* 152.9945. MS/MS did not show product ions formed due to loss of 87.0320, corresponding to serine from polar head group. The presence of these product ions, retention time at which these species were identified, and comparison to exact mass measurements allowed to confirm the presence of PS molecular species. It was also possible to observe the carboxylate anion of fatty acyl chain 18:0 (R_1COO^-) at *m/z* 283.2633. Therefore, this PS species was identified as PS(38:4) [PG(18:0/20:4)].

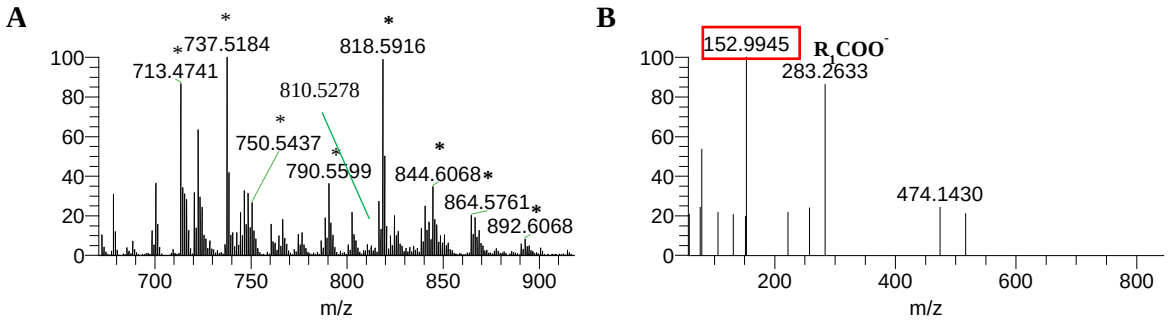

Figure 19 - Identification of phosphatidylserine (PS). (**A**) MS spectrum of PS region. (**B**) ESI-MS/MS spectrum (HCD fragmentation) of the $[M-H]^-$ ion of PS(38:4) (*m/z* 810.5278). Fragment ions characteristic for the PS class were highlighted in a red box. *background

Sphingomyelins (SM) were identified in positive ion mode, as $[M+H]^+$ ions. The most abundant SM molecular species was identified at *m/z* 703.5750 [SM(d34:1)]. The MS/MS spectrum showed the abundant ion at *m/z* 184.0730, which corresponds to the phosphocholine polar head group. SMs were also identified in negative ion mode, as $[M+CH_3COO]^-$ ions, which corresponds to a mass shift of plus 58.0055 Da in comparison with the $[M+H]^+$ ions. The most abundant SM molecular species was found at *m/z* 761.5814. The MS/MS spectrum showed product ions at *m/z* 687.5455, formed due to neutral loss of 74.03678 Da (CH_3COOCH_3), and ions at *m/z* 168.0420, corresponding to the demethylated phosphocholine polar head group. The presence of these two types of product ions allowed to confirm the presence of SM molecular species. This SM species was identified as SM(d34:1).

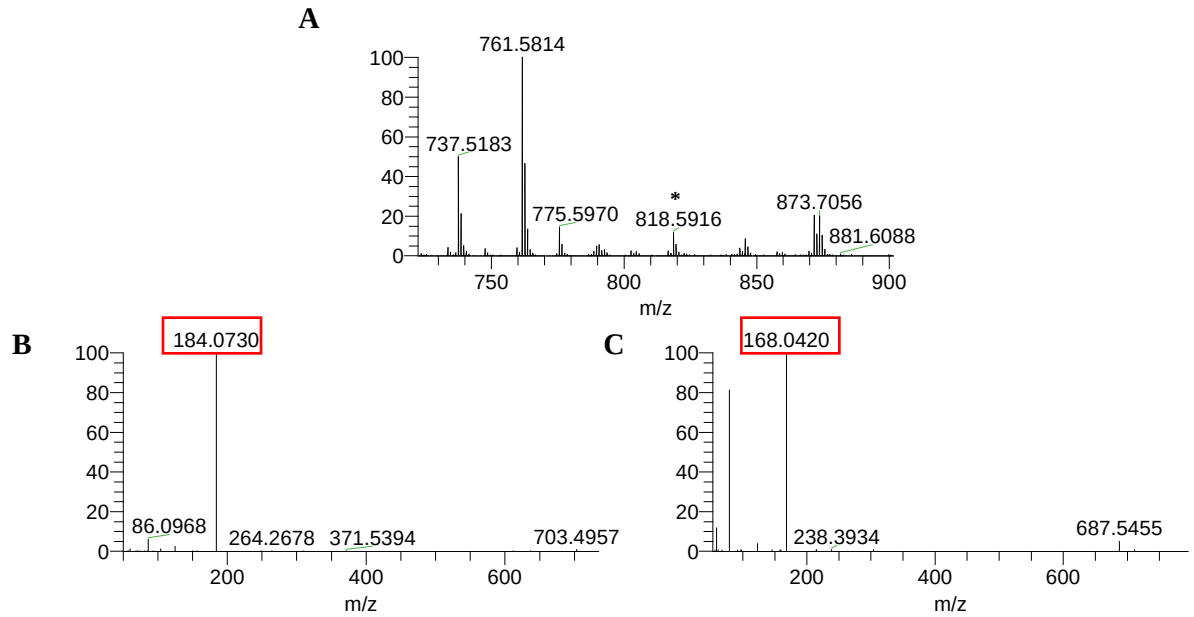

Figure 20 - Identification of sphingomyelin (SM). (**A**) MS spectrum of SM region. (**B**) ESI-MS/MS spectrum (HCD fragmentation) of the $[M+H]^+$ ion of SM(d34:1) (*m/z* 703.5750). (**C**) ESI-MS/MS spectrum (HCD) fragmentation of the $[M+CH_3COO]^-$ ion of SM(d34:1) (*m/z* 761.5814). Fragment ions characteristic for the SM class were highlighted in a red box. *background

Lyso-phosphatidylcholines (LPC) were identified in positive ion mode, as $[M+H]^+$ ions. The most abundant LPC molecular species was identified at *m/z* 496.3398 [LPC(16:0)]. The MS/MS spectrum showed the abundant ion at *m/z* 184.0727, which corresponds to the phosphocholine polar head group. LPC were also identified in negative ion mode, as $[M+CH_3COO]^-$ ions, which corresponds to a mass shift of plus 58.0055 Da in comparison with the $[M+H]^+$ ions. The most abundant LPC molecular species was found at *m/z* 554.3460. The MS/MS spectrum showed product ions at *m/z* 687.5455, formed due to neutral loss of 74.03678 Da (CH_3COOCH_3). The presence of these two types of product ions allowed to confirm the presence of LPC molecular species. It was also possible to observe the carboxylate anion of fatty acyl chain 16:0 ($RCOO^-$) at *m/z* 255.2324. Therefore, this LPC species could be defined as LPC(16:0).

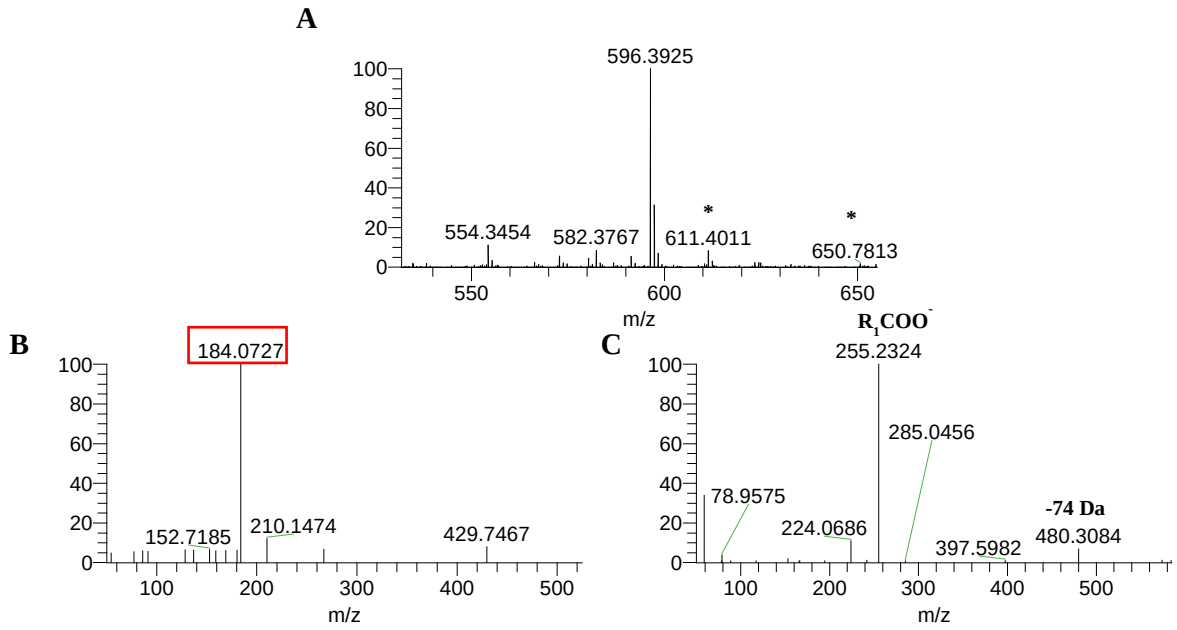

Figure 21 – Identification of lyso-phosphatidylcholine (LPC). (**A**) MS spectrum of LPC region. (**B**) ESI-MS/MS spectrum (HCD fragmentation) of the $[M+H]^+$ ion of LPC(16:0) (*m/z* 496.3398). (**C**) ESI-MS/MS spectrum (HCD) fragmentation of the $[M+CH_3COO]^-$ ion of LPC(16:0) (*m/z* 554.3460). Fragment ions characteristic for the LPC class were highlighted in a red box. *background

Table 4 – Phospholipid molecular species identified in THP-1 macrophages.

Lipid species (C:N)	Calculated *m/z*	Observed *m/z*	Error (ppm)	Fatty acyl chains (C:N)	Formula
LPC identified as [M+CH3COO]$^-$					
LPC(16:0)	554,3455	554,3458	**0,4755**	**16:0**	C26H53NO9P
LPC(18:0)	582,3770	582,3771	**0,1904**	**18:0**	C28H57NO9P
LPC(18:1)	580,3614	580,3614	**0,0639**	**18:1**	C28H55NO9P
LPE identified as [M-H]-					
LPE(16:0)	452,2779	452,2777	**-0,5021**	**16:0**	C21H43NO7P
LPE(18:0)	480,3093	480,3090	**-0,5484**	**18:0**	C23H47NO7P
LPE(18:1)	478,2931	478,2934	**0,6425**	**18:1**	C23H45NO7P
LPE(18:2)	476,2774	476,2777	**0,6402**	**18:2**	C23H43NO7P
LPE(20:3)	502,2939	502,2934	**-1,1113**	**20:3**	C25H45NO7P
LPE(20:4)	500,2778	500,2777	**-0,0800**	**20:4**	C25H43NO7P
LPE(20:5)	498,2619	498,2621	**0,3767**	**20:5**	C25H41NO7P
LPE(22:5)	526,2933	526,2934	**0,0517**	**22:5**	C27H45NO7P
LPE(22:6)	524,2774	524,2777	**0,5377**	**22:6**	C27H43NO7P
PC identified as [M+CH3COO]$^-$					
PC(30:0)	764,5442	764,5447	**0,6631**	**14:0/16:0**	C40H79NO10P
PC(30:1)	762,5285	762,5287	**0,2465**	**14:0/16:1 and 14:1/16:0**	C40H77NO10P
PC(32:0)	792,5755	792,5753	**-0,2333**	**16:0/16:0**	C42H83NO10P
PC(32:1)	790,5598	790,5584	**-1,7588**	**14:0/18:1 and 16:0/16:1**	C42H81NO10P
PC(32:2)	788,5442	788,5434	**-0,9330**	**16:0/16:2 and 14:0/18:2**	C42H79NO10P
PC(34:1)	818,5911	818,5888	**-2,8451**	**16:0/18:1**	C44H85NO10P
PC(34:2)	816,5755	816,5755	**0,0696**	**16:0/18:2 and 16:1/18:1**	C44H83NO10P
PC(34:3)	814,5598	814,5601	**0,3822**	**16:0/18:3 and 16:1/18:2**	C44H81NO10P
PC(34:4)	812,5442	812,5418	**-2,9035**	******	C44H79NO10P
PC(36:1)	846,6224	846,6196	**-3,2861**	**18:0/18:1**	C46H89NO10P
PC(36:2)	844,6068	844,6063	**-0,4993**	**18:1/18:1**	C46H87NO10P
PC(36:3)	842,5911	842,5909	**-0,2680**	**16:0/20:3 and 18:1/18:2**	C46H85NO10P
PC(36:4)	840,5755	840,5728	**-3,1724**	**16:0/20:4 and 16:1/20:3**	C46H83NO10P
PC(36:5)	838,5598	838,5590	**-0,9799**	**16:0/20:5 and 16:1/20:4**	C46H81NO10P
PC(36:6)	836,5442	836,5422	**-2,2891**	**16:1/20:5**	C46H79NO10P
PC(38:3)	870,6224	870,6213	**-1,2845**	**16:0/22:3, 18:0/20:3, 18:1/20:2 and 18:2/20:1**	C48H89NO10P
PC(38:4)	868,6068	868,6041	**-3,0474**	**18:0/20:4**	C48H87NO10P
PC(38:5)	866,5911	866,5913	**0,1832**	**18:1/20:4**	C48H85NO10P
PC(38:6)	864,5755	864,5745	**-1,0878**	**16:0/22:6**	C48H83NO10P
PC(38:7)	862,5598	862,5587	**-1,3147**	**18:0/22:7**	C48H81NO10P
PC(40:4)	896,6381	896,6349	**-3,4845**	**18:1/22:3 and 18:2/22:2**	C50H91NO10P
PC(40:5)	894,6224	894,6224	**-0,0355**	******	C50H89NO10P
PC(40:6)	892,6068	892,6043	**-2,7152**	**18:1/22:5**	C50H87NO10P

Table 4 (Cont.)

Lipid species (C:N)	Calculated *m/z*	Observed *m/z*	Error (ppm)	Fatty acyl chains (C:N)	Formula
PC(40:7)	890,5911	890,5897	**-1,5679**	**18:1/22:6**	C50H85NO10P
PC(O-28:0)	722,5336	722,5335	**-0,1785**	**	C38H77NO9P
PC(O-30:0)	750,5649	750,5634	**-1,9413**	**14:0/16:0 and 16:0/14:0**	C40H81NO9P
PC(O-30:1)/PC(P-30:0)	748,5492	748,5483	**-1,2073**	**14:0/16:1 and 16:0/14:1**	C40H79NO9P
PC(O-32:0)	778,5962	778,5947	**-1,9795**	**	C42H85NO9P
PC(O-32:1)/PC(P-32:0)	776,5805	776,5792	**-1,7513**	**16:0/16:1 and 16:1/16:0**	C42H83NO9P
PC(O-34:1)/PC(P-34:0)	804,6118	804,6093	**-3,1557**	**16:0/18:1 and 18:1/16:0**	C44H87NO9P
PC(O-34:2)/PC(P-34:1)	802,5962	802,5944	**-2,2724**	**16:0/18:2, 16:1/18:1, 18:1/16:1 and 18:2/16:0**	C44H85NO9P
PC(O-34:3)/PC(P-34:2)	800,5805	800,5808	**0,3135**	**18:2/16:1**	C44H83NO9P
PC(O-36:1)/ PC(P-36:0)	832,6431	832,6432	**0,0440**	**18:1/18:0**	C46H91NO9P
PC(O-36:2)/PC(P-36:1)	830,6275	830,6252	**-2,7152**	**18:1/18:1**	C46H89NO9P
PC(O-36:3)/PC(P-36:2)	828,6118	828,6107	**-1,3701**	**18:1/18:2, 18:2/18:1 and 20:3/16:0**	C46H87NO9P
PC(O-36:5)/PC(P-36:4)	824,5805	824,5796	**-1,1001**	**20:4/16:1**	C46H83NO9P
PC(O-38:4)/ PC(P-38:3)	854,6275	854,6247	**-3,2888**	**20:4/18:0 and 20:3/18:1**	C48H89NO9P
PC(O-38:5)/PC(P-38:4)	852,6118	852,6102	**-1,9716**	**20:4/18:1**	C48H87NO9P
PC(O-38:6)/PC(P-38:5)	850,5962	850,5943	**-2,1765**	**16:1/22:5, 18:0/20:6 and 22:6/16:0**	C48H85NO9P
PC(O-40:5)/PC(P-40:4)	880,6431	880,6408	**-2,6434**	**20:4/20:1**	C50H91NO9P
PC(O-42:4)/PC(P-42:3)	910,6901	910,6882	**-2,0772**	**20:4/22:0**	C52H97NO9P
PC(O-42:5)/PC(P-42:4)	908,6744	908,6745	**0,0779**	**	C52H95NO9P
PC(P-32:1)	774,5649	774,5634	**-1,9079**	**16:1/16:1**	C42H81NO9P
PC(P-36:5)	822,5649	822,5667	**2,1702**	**20:5/16:1**	C46H81NO9P
PC(P-38:6)	848,5805	848,5795	**-1,1941**	**18:1/20:5 and 18:0/20:6**	C48H83NO9P
PC(P-40:6)	876,6118	876,6099	**-2,2685**	**	C50H87NO9P
PE identified as $[M-H]^-$					
PE(32:0)	690,5050	690,5074	**3,4798**	*	C37H73NO8P
PE(32:1)	688,4911	688,4917	**0,9429**	**16:0/16:1**	C37H71NO8P
PE(34:1)	716,5223	716,5230	**1,0321**	**16:1/18:0 and 16:0/18:1**	C39H75NO8P
PE(34:2)	714,5077	714,5074	**-0,4095**	**16:1/18:1 and 16:0/18:2**	C39H73NO8P
PE(36:1)	744,5542	744,5543	**0,1327**	**18:0/18:1**	C41H79O8NP
PE(36:2)	742,5372	742,5387	**1,9930**	**18:1/18:1 and 18:0/18:2**	C41H77O8NP
PE(36:5)	736,4904	736,4917	**1,8313**	**16:0/20:5 and 16:1/20:4**	C41H71O8NP
PE(38:3)	768,5524	768,5543	**2,5380**	**18:0/20:3**	C43H79NO8P
PE(38:4)	766,5379	766,5367	**-1,5655**	**18:0/20:4**	C43H77O8NP
PE(38:5)	764,5221	764,5230	**1,2435**	**18:1/20:4 and 18:0/20:5**	C43H75NO8P
PE(38:6)	762,5087	762,5074	**-1,6821**	**16:0/22:6 and 18:1/20:5**	C43H73O8NP
PE(40:4)	794,5687	794,5700	**1,6131**	**18:2/22:2**	C45H81NO8P
PE(40:5)	792,5531	792,5543	**1,5114**	**	C45H79O8NP
PE(40:6)	790,5375	790,5387	**1,4475**	**18:0/22:6**	C45H77O8NP
PE(O-32:2)/PEp(32:1)	672,4966	672,4968	**0,3567**	**16:1/16:1**	C37H71O7NP

Table 4 (Cont.)

Lipid species (C:N)	Calculated *m/z*	Observed *m/z*	Error (ppm)	Fatty acyl chains (C:N)	Formula
PE(O-32:3)/PEp(32:2)	670,4818	670,4812	**-0,9665**	**	C37H69O7NP
PE(O-34:2)/PE(P-34:1)	700,5281	700,5281	**0,0531**	**16:1/18:1, 16:0/18:2, 18:1/16:1 and 18:2/16:0**	C39H75NO7P
PE(O-34:3)/PE(P-34:2)	698,5116	698,5125	**1,2949**	**18:2/16:1**	C39H73NO7P
PE(O-34:4)/PE(P-34:3)	696,4978	696,4968	**-1,4398**	**18:3/16:1 and 18:1/16:2**	C39H71NO7P
PE(O-34:5)/PEp(34:4)	694,4799	694,4812	**1,8002**	**20:4/14:1**	C39H69O7NP
PE(O-36:2)/PE(P-36:1)	728,5582	728,5594	**1,7134**	**18:1/18:1**	C41H79NO7P
PE(O-36:3)PE(P-36:2)	726,5433	726,5438	**0,6971**	**18:1/18:2 and 18:2/18:1**	C41H77NO7P
PE(O-36:4)/PE(P-36:3)	724,5275	724,5281	**0,8448**	**	C41H75NO7P
PE(O-36:5)/PE(P-36:4)	722,5118	722,5125	**0,8599**	**20:4/16:0**	C41H73NO7P
PE(O-36:6)/PEp(36:5)	720,4963	720,4968	**0,7853**	**20:5/16:1**	C41H71O7NP
PE(O-38:5)/PE(P-38:4)	750,5425	750,5438	**1,6653**	**20:3/18:2, 20:4/18:1, 20:5/18:0 and 22:4/16:1**	C43H77NO7P
PE(O-38:6)/PE(P-38:5)	748,5264	748,5281	**2,3491**	**20:4/18:2, 20:5/18:1 and 22:4/16:1**	C43H75NO7P
PE(O-38:7)/PEp(38:6)	746,5121	746,5125	**0,4529**	**22:6/16:1**	C43H73O7NP
PE(O-40:4)/PE(P-40:3)	780,5899	780,5907	**1,0527**	**	C45H83NO7P
PE(O-40:5)/PE(P-40:4)	778,5731	778,5751	**2,5602**	**	C45H81NO7P
PE(O-40:6)/PE(P-40:5)	776,5599	776,5594	**-0,5948**	**	C45H79NO7P
PE(O-40:7)/PEp(40:6)	774,5422	774,5438	**2,0109**	**	C45H77O7NP
PE(O-40:8)/PEp(40:7)	772,5262	772,5281	**2,5021**	**22:6/18:2**	C45H75O7NP
PE(O-42:5)/PEp(42:4)	806,6038	806,6064	**3,1809**	**20:3/22:2**	C47H85O7NP
PE(O-42:6)/PEp(42:5)	804,5902	804,5907	**0,6666**	**20:4/22:2**	C47H83O7NP
PE(O-42:7)/PEp(42:6)	802,5742	802,5751	**1,0630**	**20:5/22:4**	C47H81O7NP
PG identified as $[M-H]^-$					
PG(32:1)	719,4850	719,4863	**1,8758**	**16:0/16:1 and 14:0/18:1**	C38H72O10P
PG(34:1)	747,5172	747,5176	**0,5169**	**16:0/18:1**	C40H76O10P
PG(34:2)	745,5005	745,5020	**1,8998**	**16:1/18:1 and 16:0/18:2**	C40H74O10P
PG(36:1)	775,5486	775,5489	**0,3628**	*	C42H80O10P
PG(36:2)	773,5309	773,5333	**3,0111**	**18:1/18:1**	C42H78O10P
PG(36:3)	771,5165	771,5176	**1,3925**	**	C42H76O10P
PG(36:4)	769,4994	769,5020	**3,2777**	**	C42H74O10P
PG(38:4)	797,5318	797,5333	**1,8597**	**18:1/20:3**	C44H78O10P
PG(38:5)	795,5172	795,5176	**0,5386**	*	C44H76O10P
PG(38:6)	793,5003	793,5020	**2,1095**	**16:0/22:6 and 18:0/20:6**	C44H74O10P
PG(38:7)	791,4861	791,4863	**0,2925**	**16:1/22:6**	C44H72O10P
PG(40:7)	819,5161	819,5176	**1,8256**	**18:1/22:6**	C46H76O10P
PG(42:10)	841,5016	841,5020	**0,4182**	**20:4/22:6**	C48H74O10P
PG(44:12)	865,5006	865,5020	**1,5970**	**22:6/22:6**	C50H74O10P
PI identified as $[M-H]^-$					
PI(32:1)	807,5019	807,5024	**0,5280**	**16:0/16:1**	C41H76O13P

Table 4 (Cont.)

Lipid species (C:N)	Calculated *m/z*	Observed *m/z*	Error (ppm)	Fatty acyl chains (C:N)	Formula
PI(34:1)	835,5334	835,5337	**0,3223**	**16:0/18:1 and 16:1/18:0**	C43H80O13P
PI(34:2)	833,5161	833,5180	**2,2643**	**16:0/18:2 and 16:1/18:1**	C43H78O13P
PI(36:1)	863,5630	863,5650	**2,2416**	**18:0/18:1**	C45H84O13P
PI(36:2)	861,5489	861,5493	**0,5287**	**18:1/18:1, 18:0/18:2 and 16:0/20:2**	C45H82O13P
PI(36:3)	859,5336	859,5337	**0,0875**	**	C45H80O13P
PI(36:4)	857,5174	857,5180	**0,6807**	**16:0/20:4**	C45H78O13P
PI(36:5)	855,5005	855,5024	**2,1891**	**16:0/20:5**	C45H76O13P
PI(38:4)	885,5487	885,5493	**0,6412**	**18:0/20:4**	C47H82O13P
PI(38:5)	883,5309	883,5337	**3,1067**	**18:1/20:4 and 18:0/20:5**	C47H80O13P
PI(38:6)	881,5163	881,5180	**1,9126**	**16:0/22:6**	C47H78O13P
PI(40:3)	915,5946	915,5963	**1,8068**	**	C49H88O13P
PI(40:4)	913,5792	913,5806	**1,5046**	**18:0/22:4**	C49H86O13P
PI(40:5)	911,5656	911,5650	**-0,6823**	**18:0/22:5**	C49H84O13P
PI(40:6)	909,5473	909,5493	**2,2401**	**18:0/22:6 and 18:1/22:5**	C49H82O13P
PI(40:7)	907,5320	907,5337	**1,8724**	**18:1/22:6**	C49H80O13P
PS identified as $[M-H]^-$					
PS(32:1)	732,4812	732,4816	**0,5496**	**16:0/16:1**	C38H71NO10P
PS(34:1)	760,5112	760,5129	**2,2047**	**16:0/18:1 and 16:1/18:0**	C40H75NO10P
PS(34:2)	758,4955	758,4972	**2,2935**	**16:0/18:2**	C40H73NO10P
PS(36:1)	788,5433	788,5442	**1,1095**	**18:0/18:1**	C42H79NO10P
PS(36:2)	786,5263	786,5285	**2,8574**	**18:0/18:2**	C42H77NO10P
PS(36:3)	784,5115	784,5129	**1,6923**	**	C42H75NO10P
PS(36:4)	782,4969	782,4972	**0,4135**	**	C42H73NO10P
PS(38:3)	812,5417	812,5442	**3,0853**	**18:0/20:3**	C44H79NO10P
PS(38:4)	810,5289	810,5285	**-0,5074**	**18:0/20:4**	C44H77NO10P
PS(38:5)	808,5129	808,5129	**-0,0777**	**18:2/20:3**	C44H75NO10P
PS(40:6)	834,5270	834,5285	**1,8138**	**18:0/22:6**	C46H77NO10P
SM identified as $[M+CH3COO]^-$					
SM(d32:1)	733,5496	733,5492	**-0,5039**	-	C39H78N2O8P
SM(d34:1)	761,5809	761,5799	**-1,2386**	-	C41H82N2O8P
SM(d34:2)	759,5652	759,5645	**-0,9840**	-	C41H80N2O8P
SM(d36:1)	789,6122	789,6107	**-1,8237**	-	C43H86N2O8P
SM(d36:2)	787,5965	787,5957	**-1,0015**	-	C43H84N2O8P
SM(d38:1)	817,6435	817,6414	**-2,5599**	-	C45H90N2O8P
SM(d40:1)	845,6748	845,6738	**-1,1689**	-	C47H94N2O8P
SM(d40:2)	843,6591	843,6599	**0,8738**	-	C47H92N2O8P
SM(d42:1)	873,7061	873,7058	**-0,3445**	-	C49H98N2O8P
SM(d42:2)	871,6904	871,6884	**-2,3429**	-	C49H96N2O8P

Table 4 (Cont.)

Lipid species (C:N)	Calculated *m/z*	Observed *m/z*	Error (ppm)	Fatty acyl chains (C:N)	Formula
SM(d42:3)	869,6748	869,6729	**-2,1697**	-	C49H94N2O8P
SM(d44:2)	899,7217	899,7207	**-1,1302**	-	C51H100N2O8P

Legend: C – carbons; N – number of double bonds; *identified based on exact mass measurements; ** no FA acyl-chain fragments observed

III.1.2.2. Changes in macrophage phospholipidome induced by canonical M1 and M2 stimuli

As a first approach to assess the effects of M1 and M2 polarization on the phospholipidome of macrophages, we have compared relative abundances of the eight PL classes identified (**Figure 22A**). M1 macrophages showed an increase in the relative abundance of PC ($p<0.05$), while LPE displayed a non-significant tendency to increase. The relative abundances of LPC, PG and SM were non-significantly lower, in comparison to the control group. As for M2, there was a significant increase in the total relative amount of PC ($p<0.001$) and a significant decrease in the total relative amount of PS ($p<0.01$). PS species are known for their anti-inflammatory properties [145]. In this sense, we would expect PS species to increase upon M2 polarization. However, the adaptation of macrophages to M2 stimuli might involve an increase in consumption of PS species, rather than an increase in their synthesis, not allowing for PS levels to be restituted. Also, we did not identify nor quantify oxidized PS (oxPS) which have been recently highlighted for their anti-inflammatory/pro-resolving properties [146]. Furthermore, despite not being statistically significant, M2 macrophages displayed higher relative abundances of PI and SM classes, compared to the non-stimulated cells, while relative abundances of LPC, LPE, PE and PG class appeared to be lower.

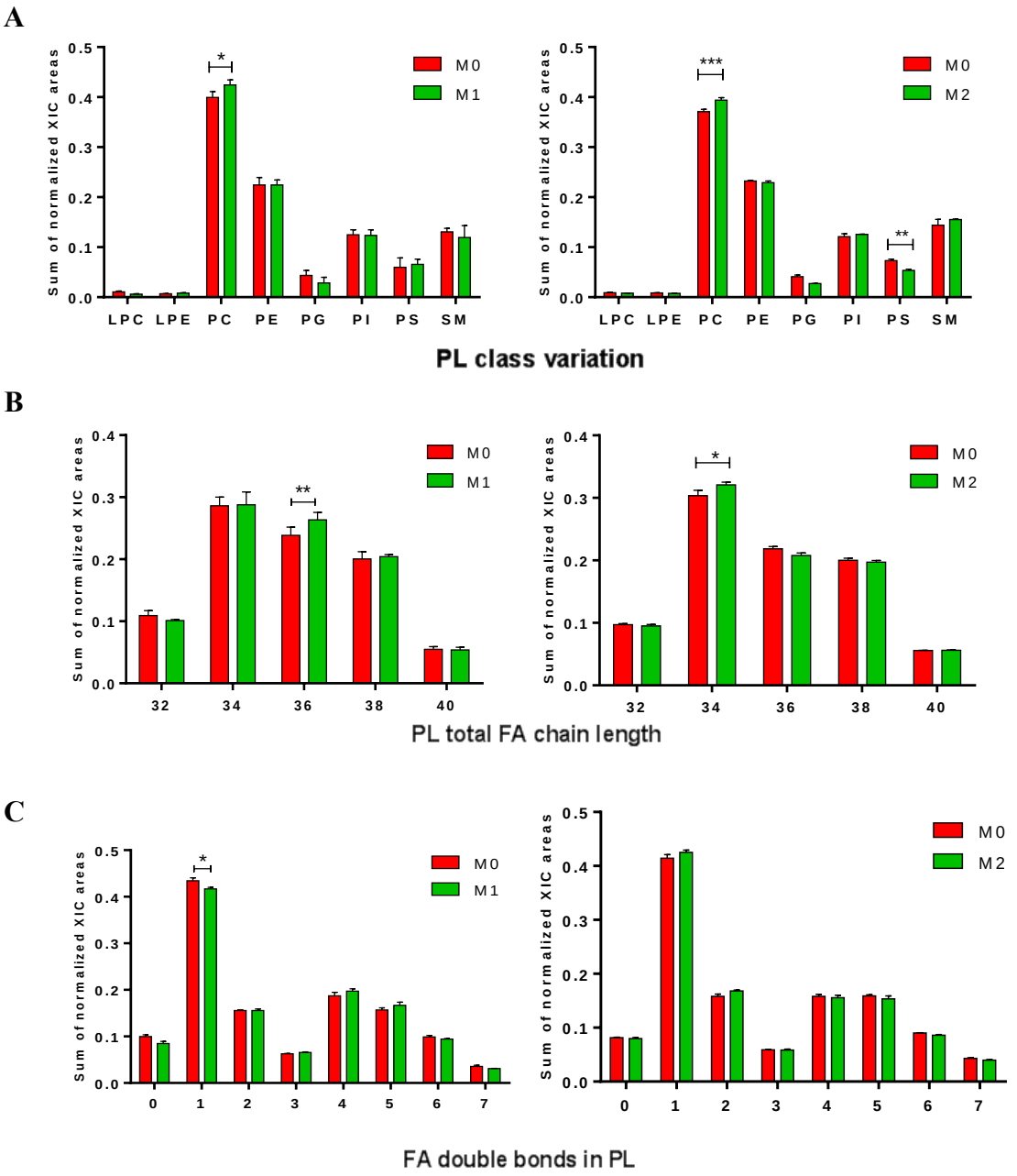

Figure 22 – Changes in PL class and structure observed in M1 (24h, LPS+IFN-γ) and M2 (48h, IL-4/IL-13). The different graphs represent total amounts of (**A**) different PL classes, (**B**) PL-composing FA differing in total number of carbons, (**C**) C18 FA-containing PL species, (**D**) AA-containing PL species, (**E**) PL-composing FA differing in the number of double bonds. *, **, ****, Statistical significance ($p<0.05$, $p<0.01$, $p<0.0001$). Error bars represented as mean±S (n=5).

We have also looked at the chain lengths of FA constituting the different PL (**Figure 22B**). Compared to M0 controls, M1 cells showed a significant increase in species with 36 carbons, accompanied by a decreasing trend for 32 carbon-containing PL. Species containing 36 carbons are mainly composed of two C18 FA, which were indeed found to increase in M1 macrophages (**Figure 23**). ELOVL 6 is an elongase responsible for synthesizing C18 from C16 [51]. In macrophages, ELOVL6 has been found increased in M1-induced BMDM [51,52], and to contribute to foam cell formation and atherosclerosis [51]. Saito et al observed that when macrophages from *ELOVL6*$^{-/-}$ mice were transplanted to an atherosclerotic mice model, aortic atherosclerotic lesion areas and infiltration of macrophages were significantly smaller. This suggests a pro-inflammatory role for ELOVL6 in which could be possibly relating with the C36 increase observed in our work. On the other hand, M2 macrophages showed higher relative abundance of PL containing 34 carbons, whereas a decrease in PL with 36 carbons was suggested.

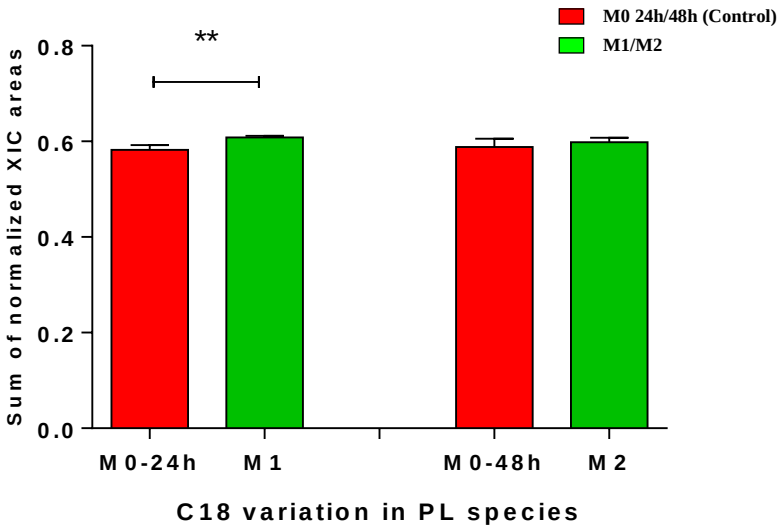

Figure 23 – Changes in C18-containing PL species in M1 and M2 macrophages. **, statistically significance ($p<0.01$).

Regarding FA unsaturation degree (**Figure 22C**) M1 activation decreased the relative amount of PL species containing MUFA (mono-unsaturated fatty acids; $p<0.05$). We also observed a tendency to decrease the relative abundance of PL containing SFA (saturated fatty

acids). The amount of PL containing PUFA in cellular membrane is an effective modulator of membrane fluidity [147]. An increase in PL containing PUFA suggests membranes to be more fluid. Decrease in MUFA and a tendency to increase PUFA are possibly associated with an increased activity from stearoyl-CoA desaturases (SCD). They have been previously reported in M1 macrophages [49]. PUFA are also known inflammatory mediators [148]. Among PUFA species, arachidonic acid (AA) is well known for its involvement in inflammation. For instance, AA acts as precursor for the synthesis of eicosanoids, which can display either pro- or anti-inflammatory activity [77]. In M1 macrophages, we observe an increase in PL species containing AA (**Figure 24**). M1 macrophages are characterized by production of prostaglandins, known members of the eicosanoid family [149]. It is also known that COX-2 is a hallmark of M1 polarization [150]. Therefore, increase in AA might be the result of its extensive use to produce prostaglandins. Future studies should evaluate COX-2 activity, as well as characterize produced prostaglandins and other eicosanoids. In M2 macrophages, there were no statistically significant changes in the number of unsaturations. We observed a tendency to increase the relative amount of PL species containing MUFA or two double bonds in their structure.

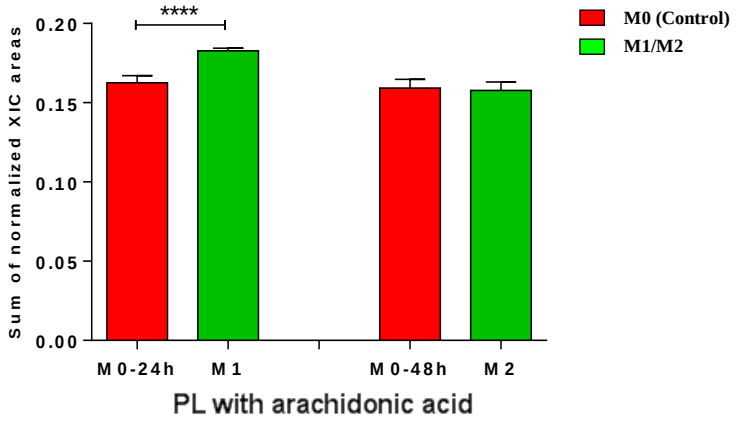

Figure 24 – Changes in AA-containing PL species in M1 and M2 macrophages. **** statistical significance ($p<0.0001$)

To further analyse the data and reveal individual lipid species differing consistently upon M1 and M2 polarization, multivariate analysis was applied. All macrophage subsets tended to cluster away from each other in the PCA scores scatter plots (**Figure 25A,B**), although the separation between M0 and M1 macrophages (**Figure 25A**) was less clear than that of M0 and M2 cells (**Figure 25B**). PLS-DA (**Figure 25C,D**), which maximizes separation between pre-defined classes, showed good discriminant ability in both cases, as indicated by the high Q^2 values obtained. In each case, the top 20 variables with higher VIP values, reflecting the most important lipid species accounting for macrophage phenotypic distinction, are shown in **Figure 25E,F**.

To validate the results of multivariate analysis and assess the magnitude of variations, the relative amounts of individual lipid species were calculated based on chromatographic peak areas, normalized to the total area of all identified species. The variations with an effect size (ES) greater than 0.8 (considered to be large according to Berben et al. [151]) were represented in Volcano plots (**Figure 26A,B)**. In general, there was good agreement with the multivariate analysis results. The levels of the 20 species with higher magnitude of variation (ES) in M1 and in M2 macrophages relative to their respective controls were represented in boxplots. For M1 macrophages, the top 20 variations (**Figure 27**) comprised: i) increases in 9 PCs, 3 LPEs, 1 PE, 1 PE plasmalogen, 1 PI and 1 SM, ii) decreases in 2 LPCs, 1 PE plasmalogen and 1 PG. On the other hand, M2 macrophages displayed as the main 20 top variations (**Figure 28**): i) increases in 3 PCs, 4 PE plasmalogens and 2 PIs, ii) decreases in 1 PE plasmalogen, 7 PGs and 2 PIs.

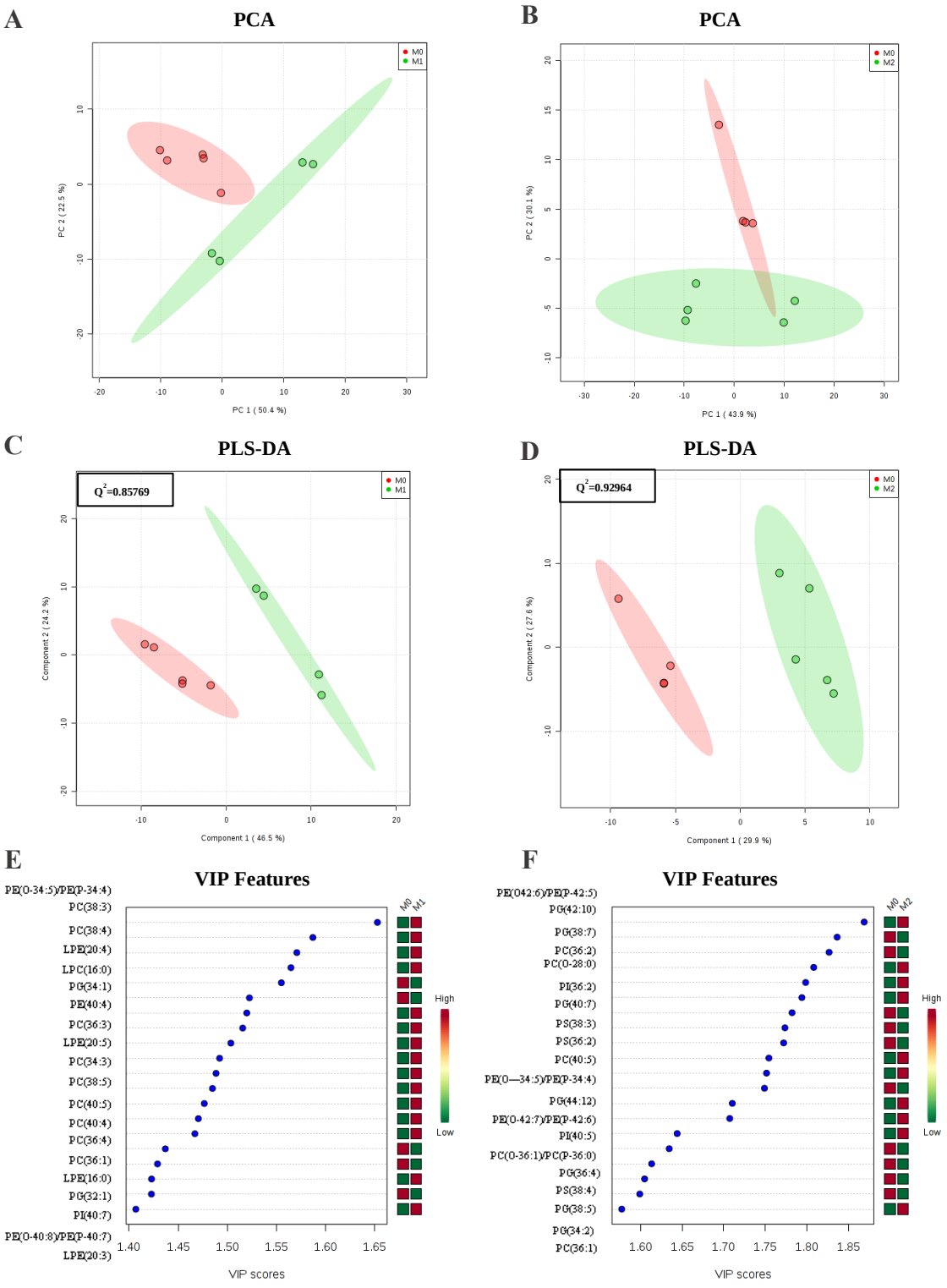

Figure 25 – Multivariate analysis of LC-MS data collected for M1 (LPS/IFN-γ, 24h) and M2 (IL-4/IL-13, 48h) macrophages. (**A**),(**B**) PCA scores scatter plot; (**C**),(**D**) PLS-DA scores scatter plot obtained for pairwise comparisons between M1 and M2 cells and their respective controls; (**E**), (**F**) Twenty PL species with higher VIP values i.e. higher importance to PLS-DA discrimination.

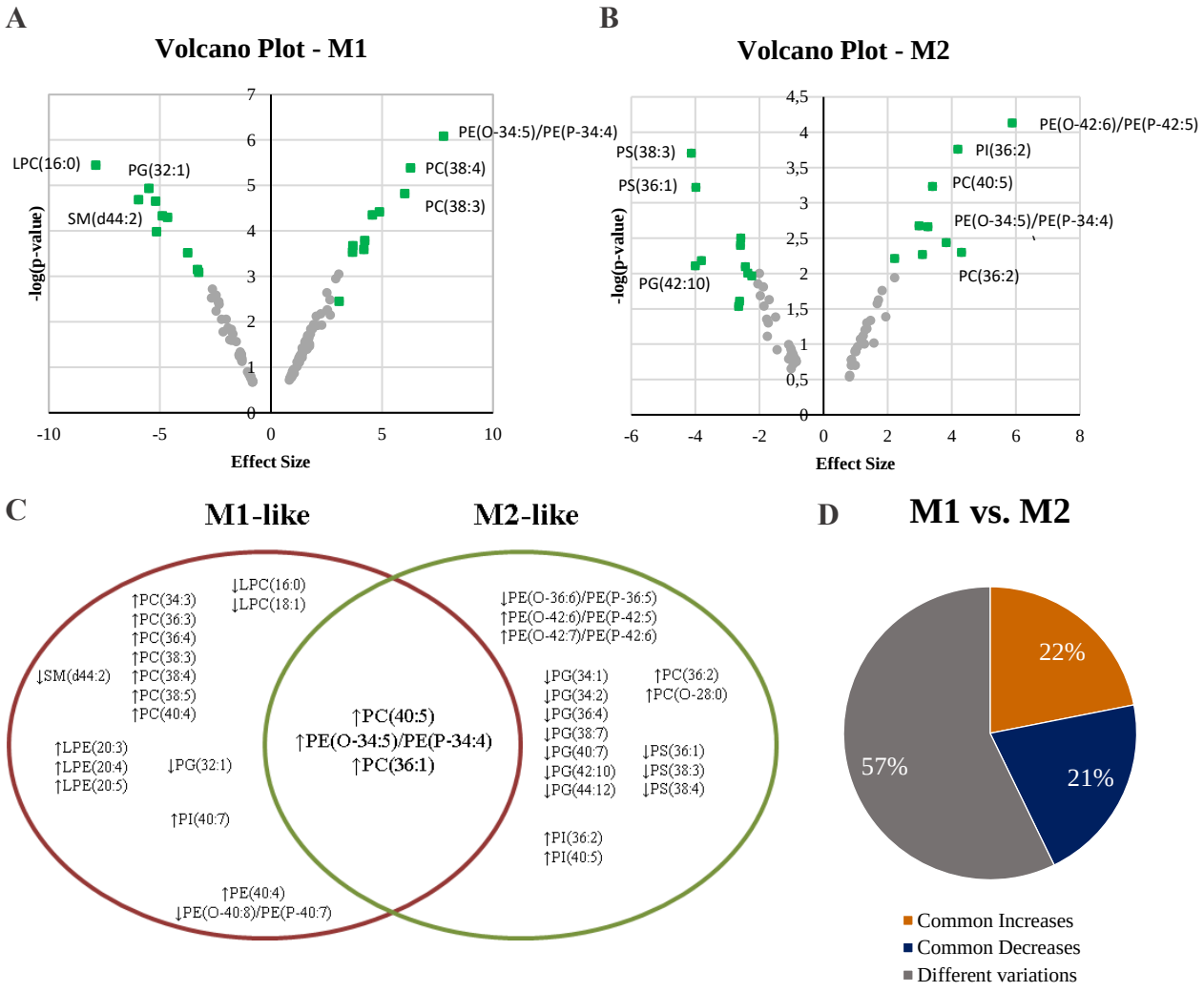

Figure 26 (**A**) and (**B**) Volcano Plots representing the PL species with large magnitude (|ES|>0.8) in M1 (LPS/IFN-γ, 24h) and M2 (IL-4/IL-13, 48h) macrophages, relatively to respective controls. The 20 species with the highest |ES| are highlighted in green squares. (**C**) Schematic representation of similarity between the top-20 varying PL species in M1 and M2 macrophages. (**D**) Pie chart representing the % of common increases, common decreases and discrepant variations between PL data subsets collected for M1 and M2 macrophages

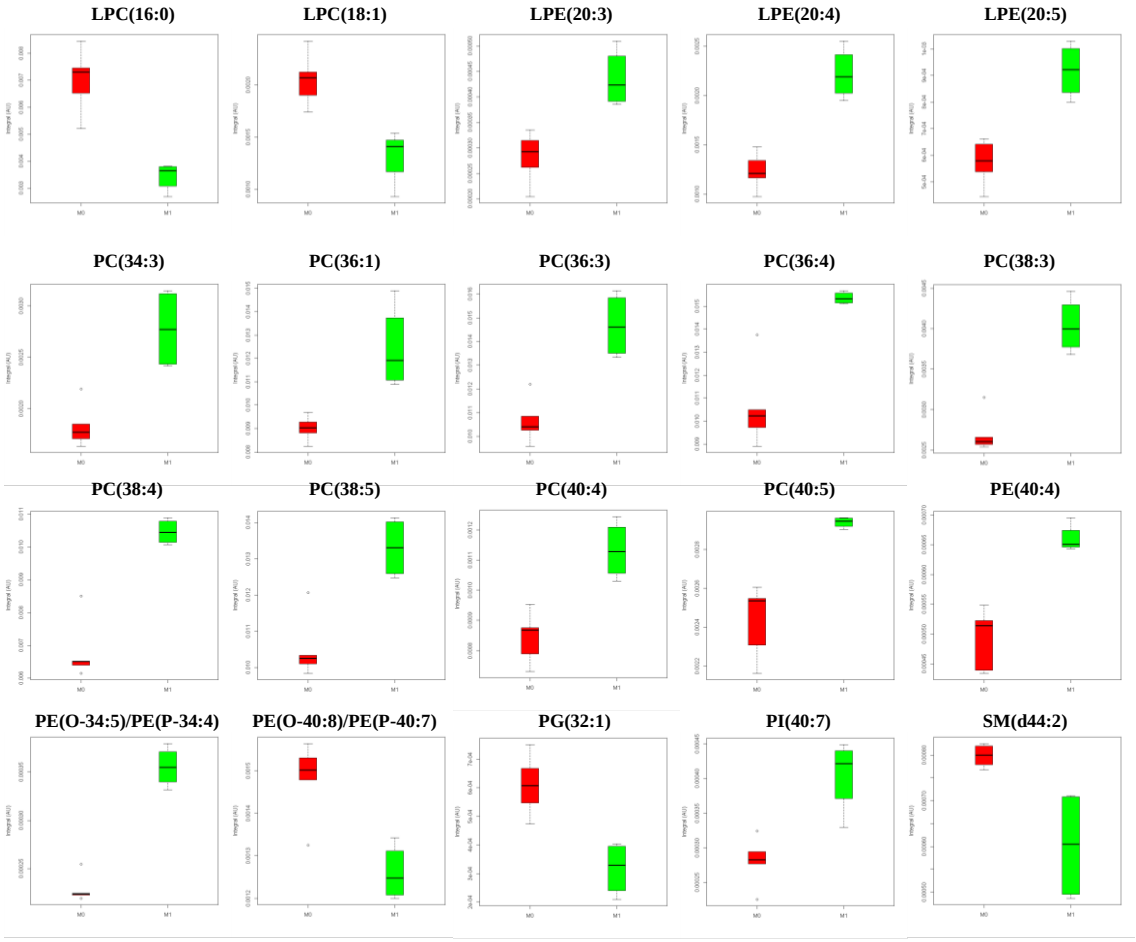

Figure 27 - Boxplots showing the levels of the top-20 varying PL species in M1 macrophages (24h, LPS/IFN-γ). M0; M1.

Several phosphatidylcholine (PC) species varied significantly upon M1 and M2 polarization. PCs are the major class of PL in mammalian cells [152]. They are a key component of cell membranes and seem to help regulate membrane fluidity. When PC/PE ratio is elevated, membranes tend to become more fluid [153]. In this sense, macrophage activation seems to induce changes in membrane fluidity. Interestingly, the increase in PC(34:1) was one of the most important variations during M1 polarization. PC(34:1) is a ligand of PPAR-α [154], which is responsible for the regulation of several inflammation-related genes.

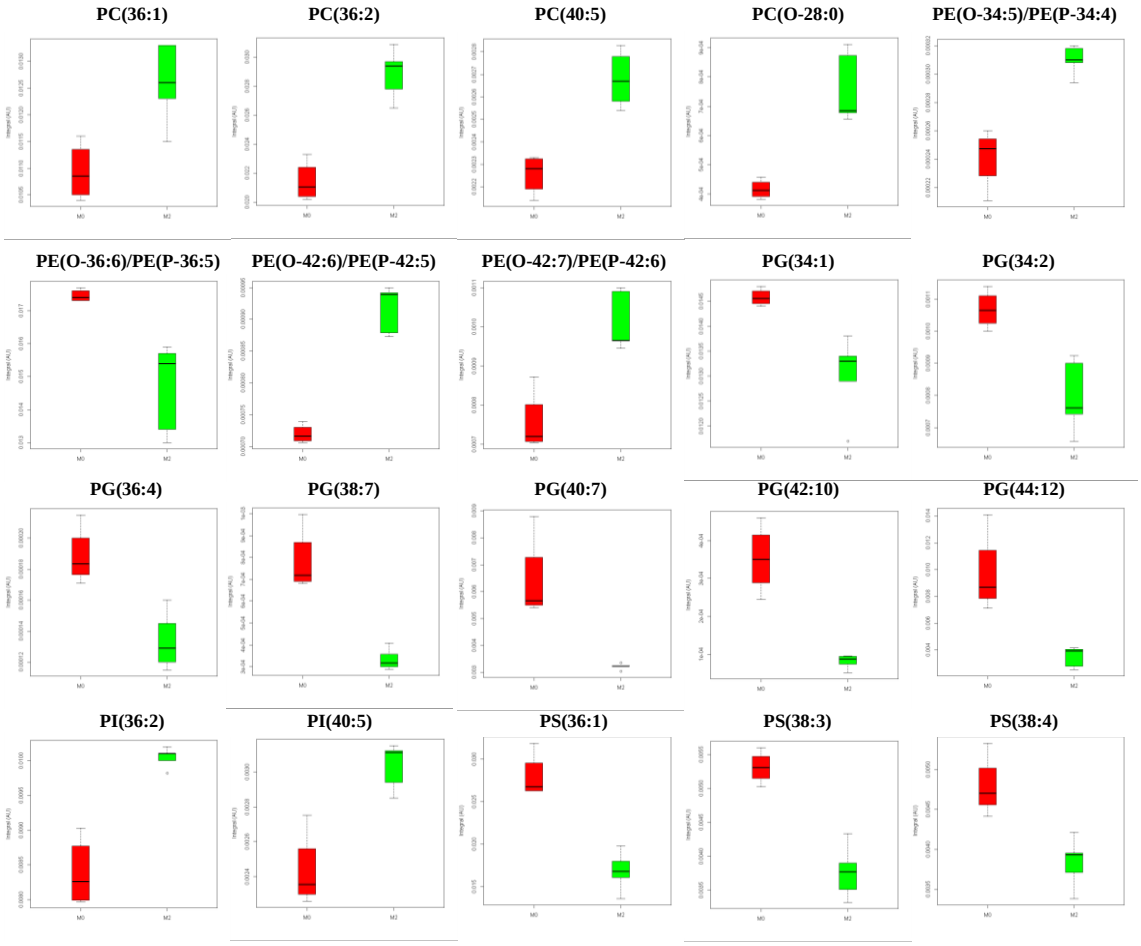

Figure 28 – Boxplots showing the levels of the top-20 varying PL species in M2 macrophages (48h, IL-4/IL-13). M0; M2.

In agreement with previous profiling of THP-1-derived macrophages [132], LPC(18:1) was down-regulated in M1 macrophages, while several LPEs, including LPE(20:4) and LPE(20:5), were up-regulated. This increase in LPE species suggests increased hydrolysis of PE species. PLA_2 is responsible for hydrolysis of PLs, and has previously been reported to be up-regulated in M1-like macrophages [69]. Therefore, increase in these LPE species might be the result of increased PLA_2 activity, an hypothesis which requires further verification.

Although little changes were observed in the PE class, down-regulation of PE(O-32:2)/PE(P-32:1), PE(O-36:2)/PE(P-36:1) and PE(40:8)/PE(P40:7), together with up-regulation of PE(O-34:5)/PE(P-34:4) had significant impact on M1 polarization. M2 macrophages also displayed increased PE(O-34:5)/PE(P-34:4), along with some other

variations in this class of PL, the ethanolamine plasmalogens. These species display a vinyl ether linkage at the *sn-1* position. Ethanolamine plasmalogens are more predominant plasmalogen class in most mammalian cells, representing 50% of PE species in immune cells [155]. The unique biological characteristics of ethanolamine plasmalogens have been associated with their key biophysical properties, such as membrane fluidity, fusion tendency and thickness [156,157]. For instance, the vinyl ether linkage at the *sn-1* position of plasmalogens allows the proximal regions of the *sn-1* and *sn-2* chains to become parallel, diminishing distances between the carbons of these chains. This enhances condensation and ordering of PL in the membrane, decreasing membrane fluidity [158]. They tend to accumulate in lipid raft microdomains and are essential to maintain the stability of these structures [159,160], which suggests a possible role in cell signaling, as microdomains are essential for cell communication. Plasmalogens were also reported to have an antioxidant role [161,162]. However, their signalling effect is far from being fully elucidated.

Several PG species were altered upon macrophage polarization, being down-regulated in M2 macrophages. However, little is known about PG biological activity, and, to the extent of our knowledge, the role of PG in inflammation is yet to be explored. Alterations in PI species were also identified. PIs are often associated with cell signalling [163]. For instance, they act as substrates in the formation of PIP for PI3K pathway [164]. This pathway is involved in the regulation of inflammatory mediators, such as TNF-α. These pro-inflammatory mediators are up-regulated in M1 activated macrophages, underlying a possible link to the levels of certain PIs in activated macrophages.

Notably, out of the top-20 variations only 3 were common to M1 and M2 phenotypes, namely the increases in PC(36:1), PC(40:5) and PE(O-34:5)/PE(P-34:4) (**Figure 26C**). By performing a broader comparison of variations with $|ES| > 0.8$ in M1 or M2 macrophages relative to resting cells, we found that 57% of PL changes were distinct depending on the polarization stimulus (**Figure 26D**). On the other hand, 43% of changes were commonly seen in M1 and M2 macrophages, although possibly at varying extensions. Therefore, it may be inferred that while some changes reflect general activation-induced remodelling of cellular phospholipids, others are specific to the polarization stimulus employed.

Altogether, the significant variations herein observed for several PL molecular species might arise from a wide array of adaptive mechanisms adopted by macrophages in response to polarization stimuli. The different changes between the PL profile of M1 and M2 macrophages might be associated with the different functions that differentially polarized macrophages acquire.

III.2. Macrophage responses to flavonoids

III.2.1. Cell viability

To determine the maximal flavonoids concentrations that could be used without significantly decreasing cell viability, THP-1 macrophages were treated with each flavonoid for 24h, at concentrations ranging from 0 to 200 µM.

The results obtained for quercetin are shown in **Figure 29**. Cell viability did not decrease at concentrations up to 60 µM. However, at 80 µM and above, there were significant decreases in macrophage viability. Therefore, the quercetin concentration chosen for subsequent assays was 60 µM.

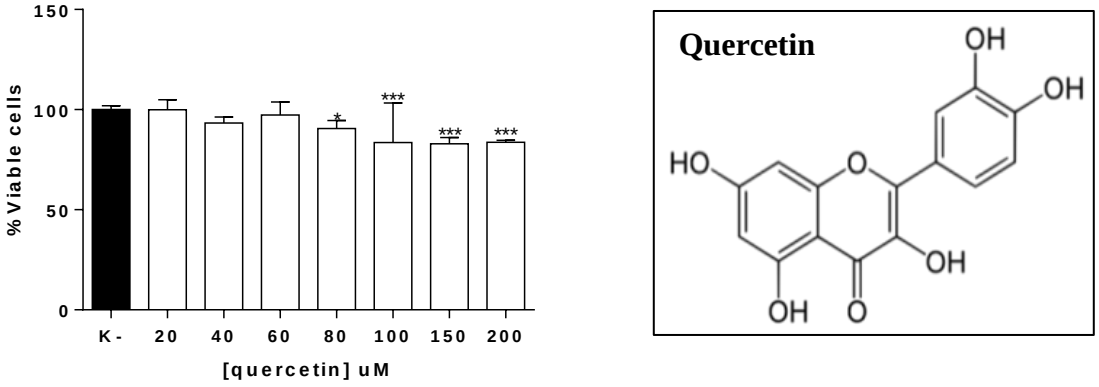

Figure 29 - Cell viability assessed by the Alamar Blue reduction assay. THP-1 macrophages were incubated with 0-200 µM of quercetin for 24 hours. *p<0.05, **p<0.01, ***p<0.001, ****p<0.0001, compared to control group (K^-). Error bars represented as mean±SD (n=5).

Figure 30 shows the viability results for naringin exposure. None of the concentrations tested (up to 200 µM) significantly affected cell viability, meaning that naringin was not toxic to cells during the 24h incubation period. Thus, the 200 µM concentration was selected for subsequent experiments.

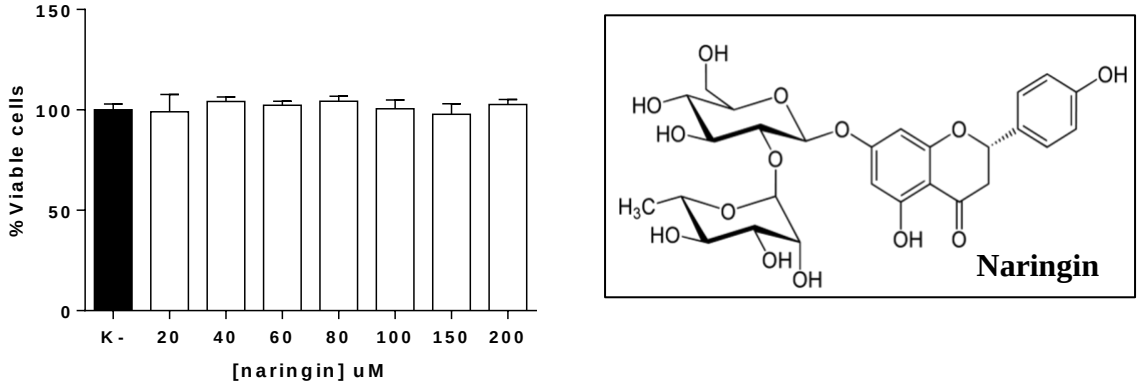

Figure 30 - Cell viability assessed by the Alamar Blue reduction assay. THP-1 macrophages were incubated with 0-200 µM of naringin for 24 hours. *p<0.05, **p<0.01, ***p<0.001, ****p<0.0001, compared to control group (K^-). Error bars represented as mean±SD (n=5).

Upon exposure to naringenin, cell viability decreased significantly at 150 and 200 µM flavonoid concentration, while the % viable cells remained high at lower concentrations (**Figure 31**). Accordingly, a concentration of 100 µM naringenin was used in the following assays.

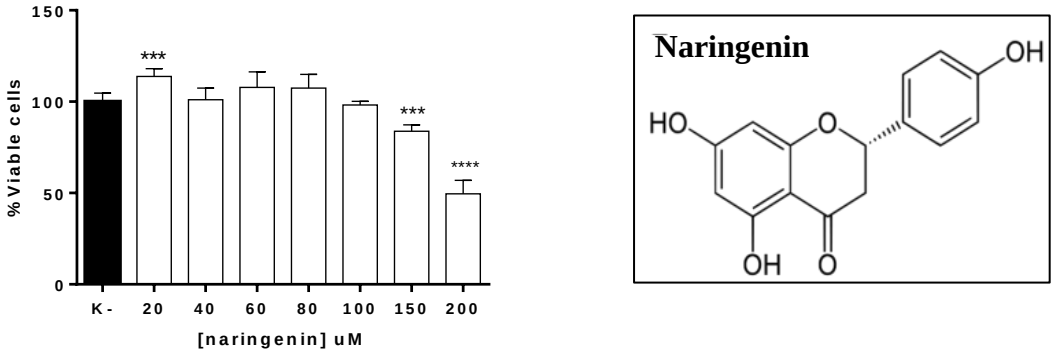

Figure 31 - Cell viability assessed by the Alamar Blue reduction assay. THP-1 macrophages were incubated with 0-200 µM of naringenin for 24 hours. *p<0.05, **p<0.01, ***p<0.001, ****p<0.0001, compared to control group (K^-). Error bars represented as mean±SD (n=5).

III.2.2. Production of pro- and anti-inflammatory cytokines

To evaluate the immunomodulatory activity of flavonoids, we measured their effect on the production of cytokines by resting (M0) and pre-polarized M1 macrophages. The results are shown in **Figure 32**. The pro-inflammatory mediator TNF-α decreased in M1 pre-polarized macrophages with all flavonoid treatments, although not reaching statistical significance in the case of quercetin. Also, treatment of M0 macrophages with naringin and naringenin led to very low TNF-α in these cells. The levels of IL-1β, another major pro-inflammatory cytokine, showed a similar variation pattern, characterized by a non-significant but consistent decrease in the culture medium of all flavonoid-treated pre-polarized macrophages. The inflammatory cytokine IL-6 also decreased in all treated M1 macrophages, whereas CXCL10 remained very high after M1 polarization and showed non-significant decreasing trends in M0 cells incubated with quercetin and naringenin. As for the anti-inflammatory cytokines evaluated, IL-1RA and CCL17, only the latter showed a significant up-regulation upon treatment of M1-polarized macrophages with naringenin.

The results described above generally agree with the existing literature, corroborating the anti-inflammatory action of these flavonoids. Pre-treatment with quercetin was reported to attenuate the production of TNF-α, IL-1β and IL-6 upon LPS stimulation [105]. Moreover, it could reduce basal levels of NF-κB activation, a downstream outcome of TLR4 induction, which regulates the transcription of TNF-α, IL-1β, COX-2, IL-6 and IL12p40 [165]. Naringin (at 100 and 200 μM) was also previously seen to decrease TNF-α, IL-6, COX-2 and iNOS levels in M1 macrophages [112,166], with similar results having been described for naringenin [104]. However, our results additionally showed that naringenin could up-regulate the production of an anti-inflammatory mediator, CCL17, which argues in favour of its potential role in the resolution of inflammation.

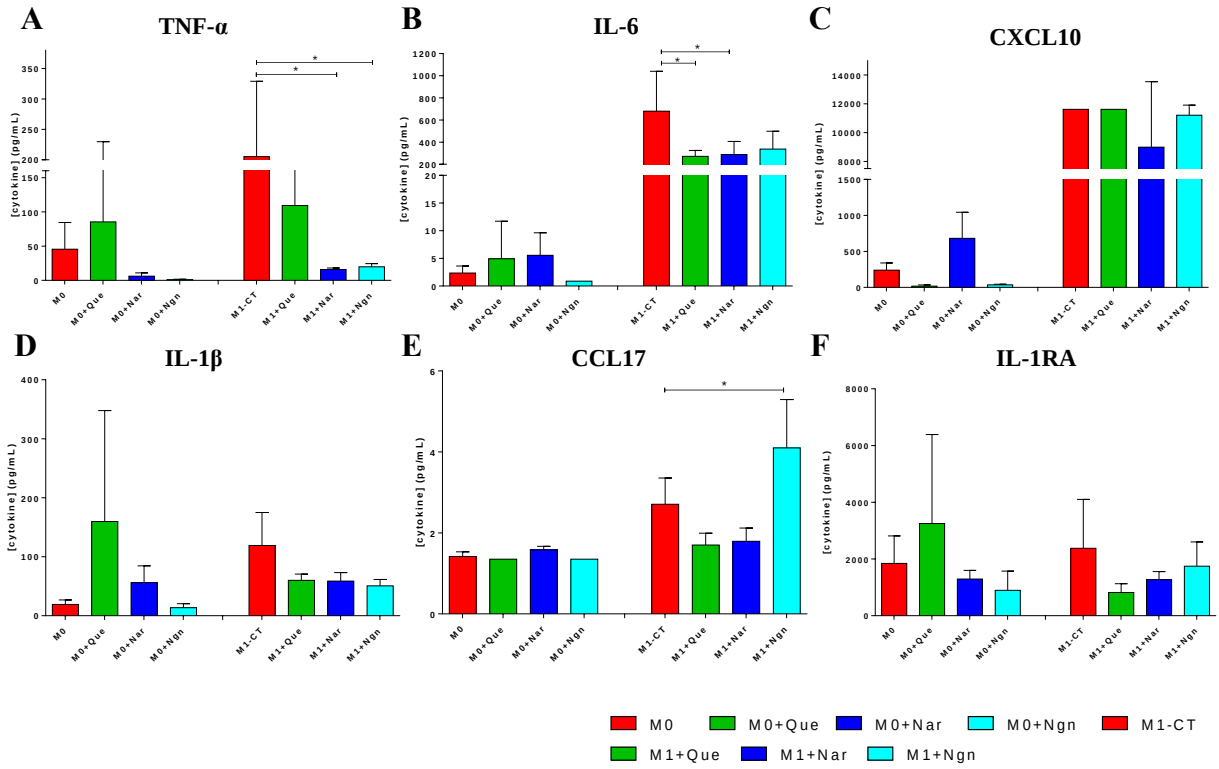

Figure 32 – Changes in the profile of different cytokines quantified in the culture medium of M0 and M1 pre-polarized macrophages after exposure to quercetin, naringin and naringenin. M0 macrophages incubated with each flavonoid for 48h. M1 pre-polarized macrophages incubated with each flavonoid for 24h (after 24h incubation with LPS/IFN-γ). (**A**) TNF-α; (**B**) IL-6; (**C**)CXCL10; (**D**) IL-1β; (**E**) CCL17; (**F**) IL-1RA. *, Statistical significance ($p<0.05$). Error bars represented as mean±SD (n=3).

III.2.3. Quercetin-induced changes in macrophage phospholipidome

In the first instance, overall changes in the different PL classes were inspected (**Figure 33A**). A 24/48h incubation with quercetin (60 µM) caused increases in total levels of PC in both M0 and pre-polarized M1 macrophages. On the other hand, total PE and SM decreased upon quercetin exposure. The total length of FA in PLs also changed with quercetin treatment (**Figure 33B**). Species containing 38 carbons significantly increased in treated M0 and pre-polarized M1 macrophages. An increase was also seen for 36 carbon-containing species in treated M0 macrophages, while shorter 34-carbon containing PL decreased.

The up-regulation of PL containing 36 and 38 carbons suggests an increase in C18 and C20 FAs. As already mentioned, C18 results from elongation of C16 FA species and C18 levels were indeed increased upon quercetin treatment (**Figure 33C**). This alteration may arise from an increase in ELOVL6 activity [167], thus leading to the preferential generation of C18/C18 or C18/C20 instead of the C16/C18 generally observed in PL-34. An increase in C20 might result from an increased consumption and turnover of arachidonic acid (AA). AA is a very long chain FA with an important role in modulating inflammation [77]. AA is used to produce eicosanoids with pro- and anti-inflammatory properties. As quercetin displays anti-inflammatory activity, it can be postulated that generation of anti-inflammatory eicosanoids can arise from flavonoid stimulation. Indeed, we observed that PL species containing AA increased in both M0 and M1 macrophages exposed to quercetin, compared to control group, which corroborates our hypothesis (**Figure 33D**).

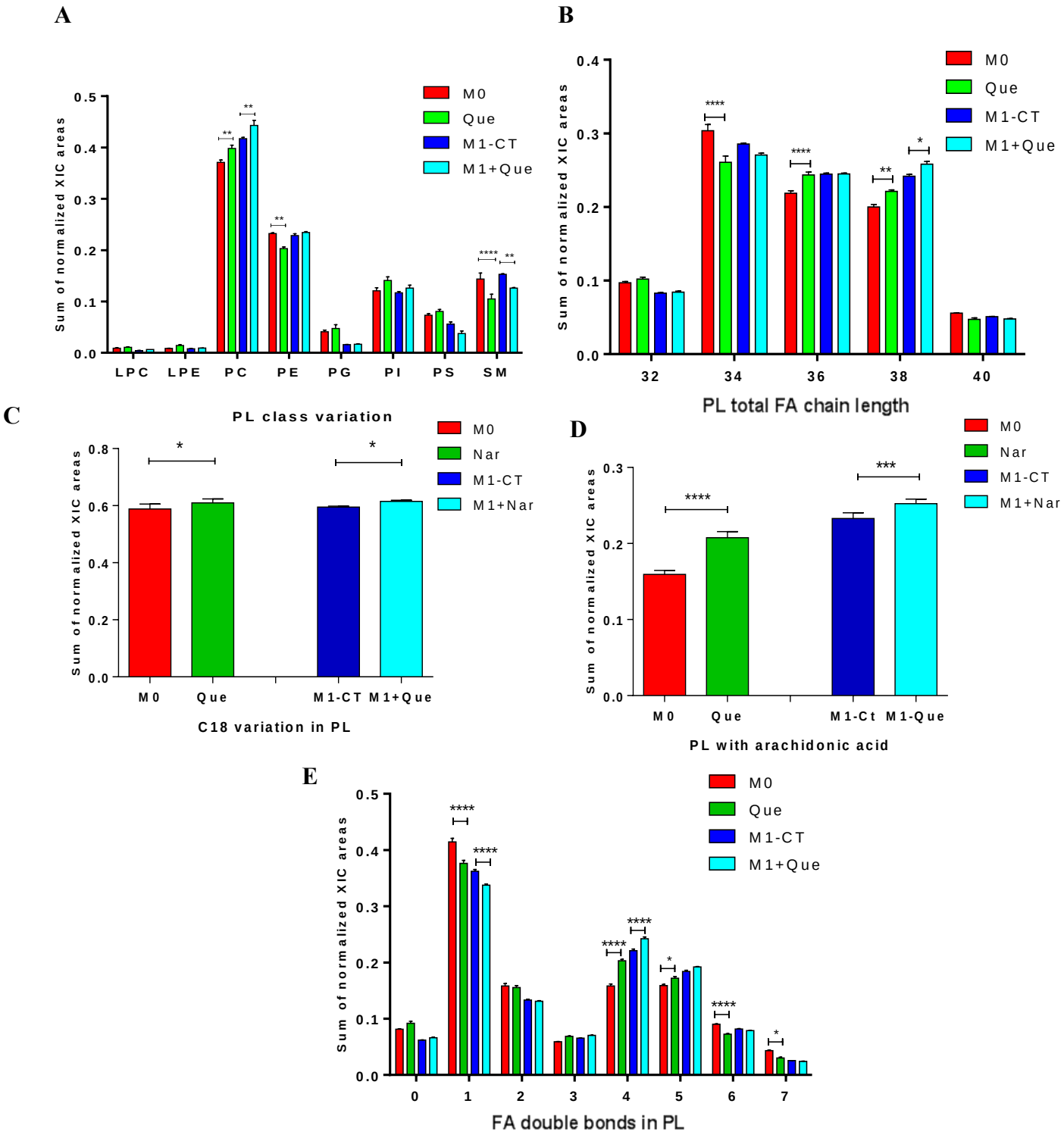

Figure 33 - Changes in PL class and structure observed in M0 macrophages treated with quercetin (60 µM) for 48h, and in pre-polarized M1 macrophages (24h, LPS+IFN-γ) subjected to 24h incubation with quercetin (60 µM). The different graphs represent total amounts of (**A**) different PL classes, (**B**) PL-composing FA differing in total number of carbons, (**C**) C18 FA-containing PL species, (**D**) AA-containing PL species, (**E**) PL-composing FA differing in the number of double bonds. *, **, ****, Statistical significance ($p<0.05$, $p<0.01$, $p<0.0001$). Error bars represented as mean±S (n=5).

To further assess quercetin effects on the macrophage lipidome, PCA and PLS-DA were applied to data matrices built from LC-MS data. The four groups are well separated in the resulting PCA scores scatter plot (**Figure 34A**). PC1 clearly distinguishes cellular subsets according to their primary polarization states (M0 and M1), while PC2 reflects flavonoid treatment. Indeed, quercetin-treated macrophages are located in positive PC2 and their respective controls in negative PC2. Interestingly, the separation along this axis between M0 cells and their quercetin-treated counterparts seems much larger than that between quercetin-treated M1 macrophages and M1 controls (corresponding, respectively, to cells stimulated with LPS/IFN for 24h and then exposed to the flavonoid or left to rest in new medium, for another 24h). The distinction between untreated and quercetin-treated cells was further verified through PLS-DA, which produced robust discriminations (**Figure 34B,C**). The corresponding VIP scores plots (**Figure 34D,E**) then revealed the lipid species displaying more important contributions for the multivariate models.

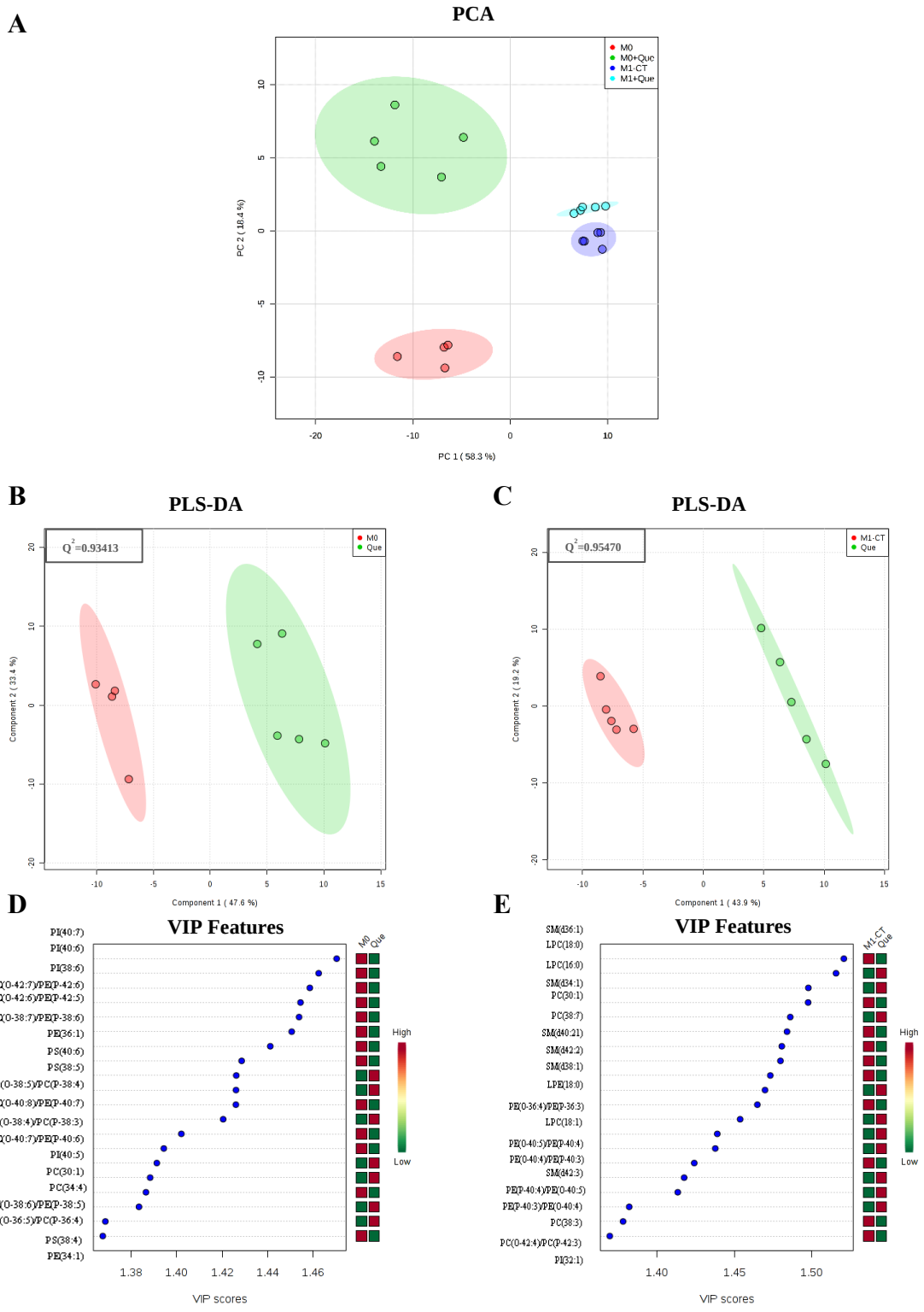

Figure 34 - Multivariate analysis of LC-MS data collected for M0 and M1 pre-polarized macrophages exposed to quercetin (60 µM). (**A**) PCA scores scatter plot; (**B**),(**C**) PLS-DA scores scatter plot obtained for pairwise comparisons between quercetin-treated M0 and M1 cells and their respective controls; (**D**), (**E**) Twenty PL species with higher VIP values i.e. higher importance to PLS-DA discrimination.

Univariate analysis of variations in individual lipid species corroborated the results of multivariate analysis. The volcano plots in **Figure 35A,B** show the variables with higher magnitude of variation (|ES|>0.8) in quercetin-treated M0 or M1 macrophages, relatively to respective controls. Then, for a clearer visualization of the most prominent changes, the top-20 varying species in each condition (M0+Quercetin; M1+Quercetin) were displayed in the form of a heatmap, organized by PL classes (**Figure 35C**).

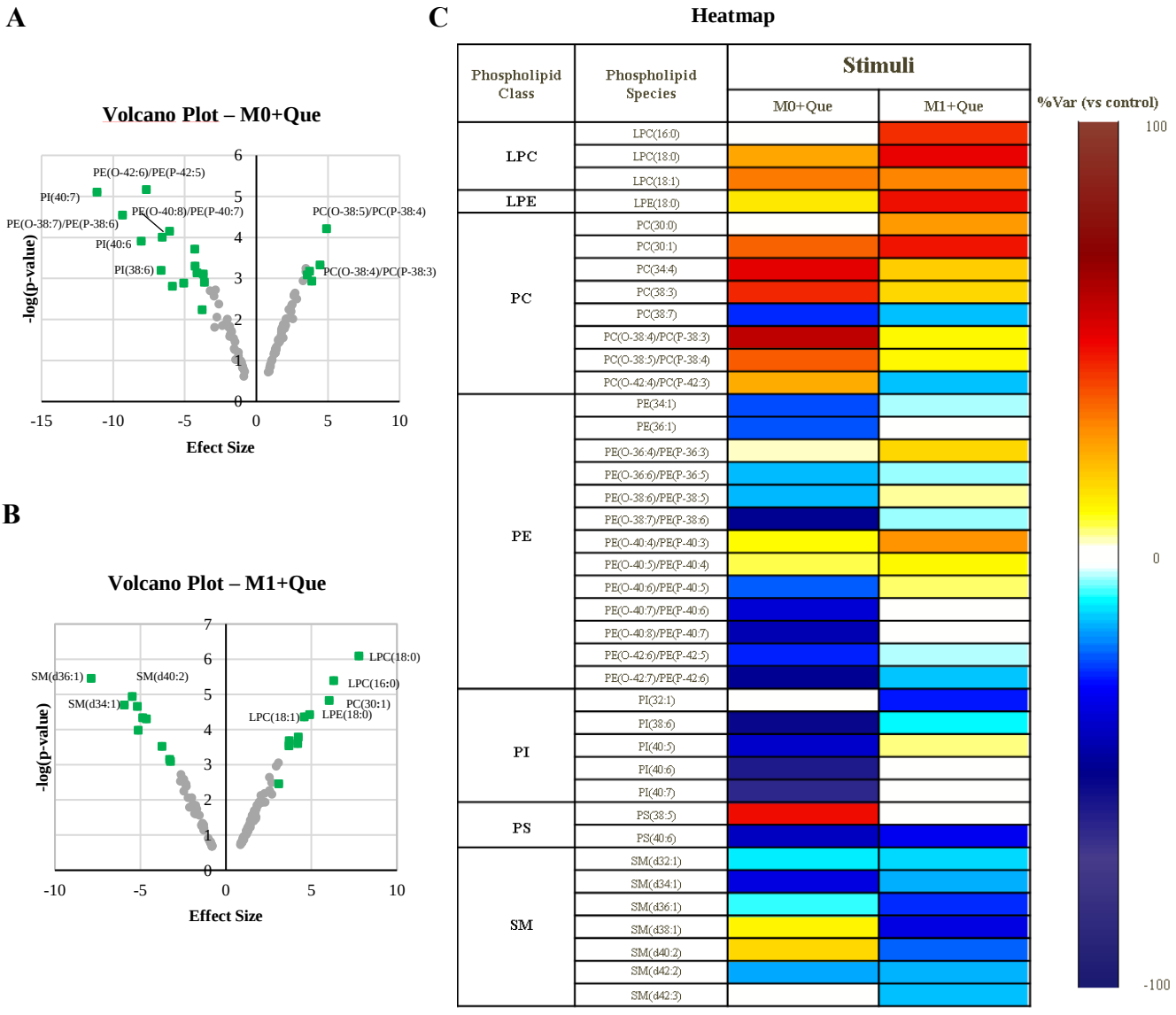

Figure 35 - (**A**) and (**B**) Volcano Plots representing the PL species with large magnitude (|ES|>0.8) in M0 and M1pre-polarized macrophages, relatively to respective controls. The 20 species with the highest |ES| are highlighted in green squares.(**C**) Heatmap representing the top-20 varying species in quercetin treated M0 macrophages (M0+Que) and quercetin-treated pre—polarized cells (M1+Que), color coded according according to the percentage of variation relatively to controls.

A first observation is that most top-20 species varied in the same direction in response to quercetin, independently of macrophage initial polarization state. There were however a few exceptions, namely in 3 plasmalogens (PC(O-42:4)/PC(P-42:3), PE(O-38:6)/PE(P-38:5) and PE(O-40:6)/PE(P-40:5)), PI(40:5), 2 SM species (d38:1 and d40:2). Considering all PL species with |ES|>0.8, the degree of similarity between M0 and M1 responses to quercetin was 74%, while only 26% of alterations differed (**Figure 36A**).

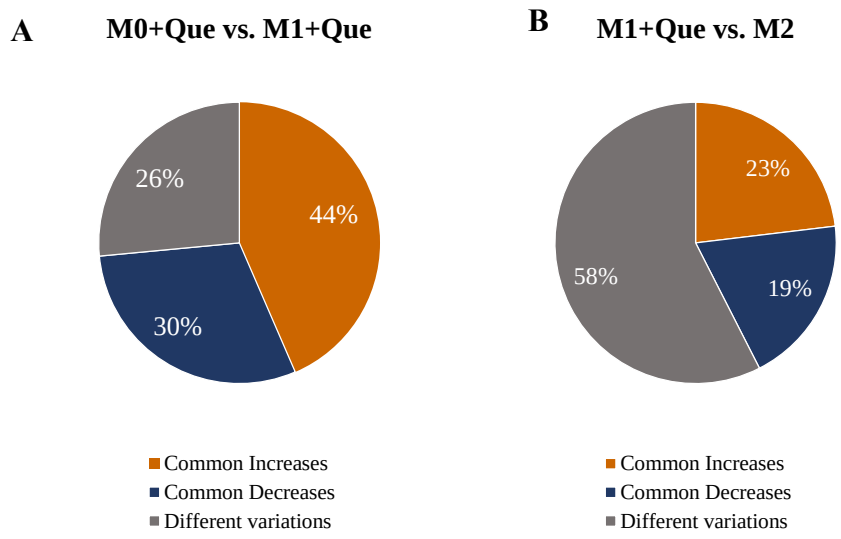

Figure 36 – Pie charts representing the % of common increases, common decreases and discrepant variations between PL data subsets collected for different exposure conditions.

Secondly, the variations within each class should be noted. LPC, LPE and PC species mostly increased with quercetin treatment, except for PC(38:7), which showed lower levels in treated cells. On the other hand, PE species decreased, while plasmanyl/plasmenyl PEs showed species-dependent alterations. PI, PS and SM species were also predominantly decreased, although increases were noted for PS(38:5), SM(d38:1) and SM(d40:2) in treated M0 macrophages.

As we are especially interested in revealing the PL changes putatively related to quercetin's anti-inflammatory activity, we have then focused on the changes that were common to quercetin-treatment of pre-polarized M1 macrophages and M2 polarization. The

degree of similarity between these conditions is displayed in **Figure 36B**. Out of the 42% species varying in the same direction in M1+Quercetin and M2 macrophages, we selected those that did not overlap with changes found in M1 polarization. We ended up of a list of 18 PL species, whose levels are displayed in boxplots (**Figure 37**). Those showing increased levels relative to controls were PC(34:1), 4 choline plasmalogens, PE(O-40:6)/PE(P-40:5) and 2 PI species (38:4 and 40:4). On the other hand, PL species decreasing in both M2 and quercetin-treated M1 macrophages were: PC(32:0), PE(O-36:6)/PE(P-36:5), PG(38:7), 3 PI species (32:1, 34:2, 38:6) and 4 PSs (34:1, 36:1, 36:4, 38:3).

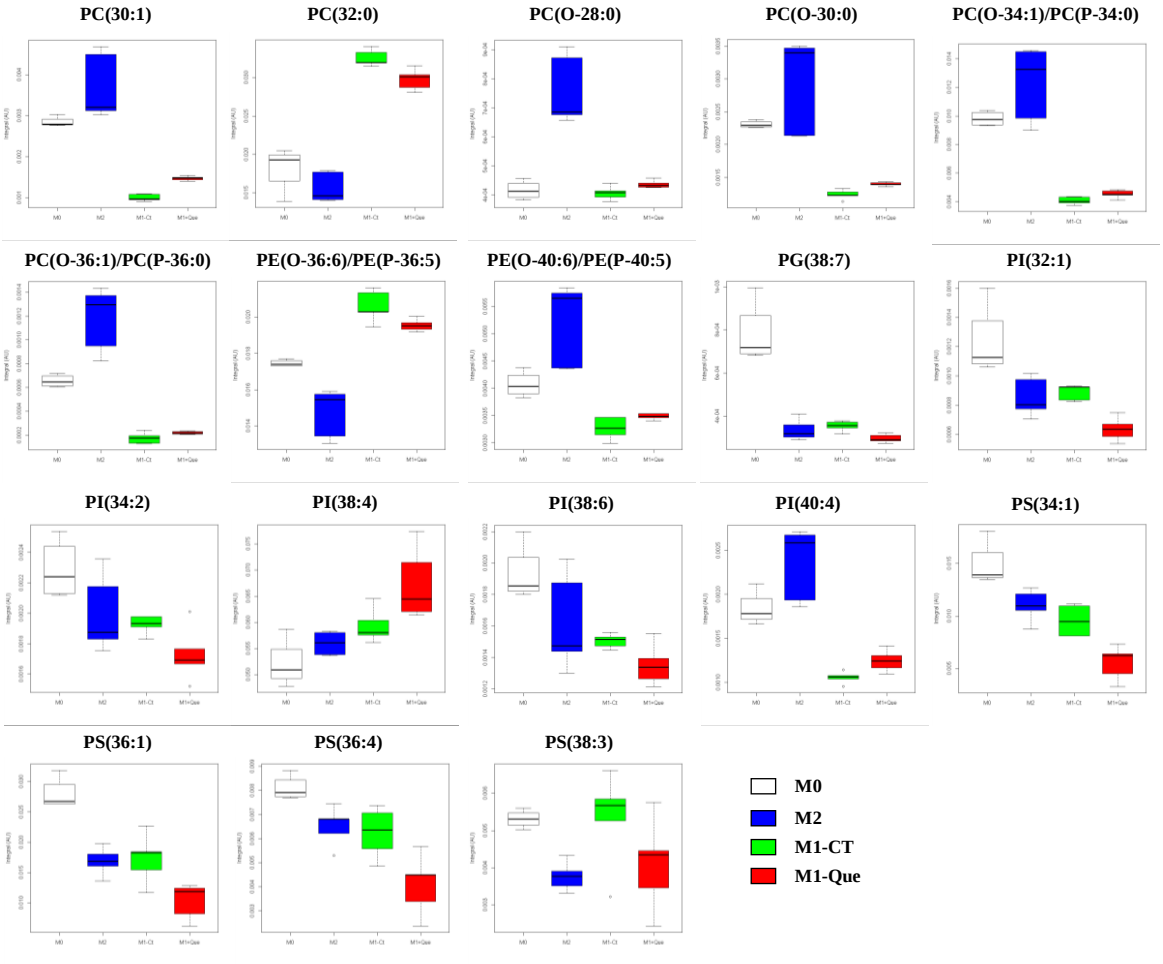

Figure 37 – Boxplots showing the levels of selected PL species in M0 macrophages, M2 macrophages, M1 pre-polarized macrophages (24h LPS/IFN + 24h fresh medium) and quercetin-treated M1 cells (24h LPS/IFN + 24h quercetin 60 uM). The species represented were selected based on the same direction of variation in flavonoid-treated and M2 macrophages, and the absence of overlap with changes characteristic of M1 polarization.

Although it is not possible to attribute individual PL variations to specific biological functions, some general observations can be inferred from the results described above. Several choline and ethanolamine plasmalogens were amongst the species commonly affected by quercetin and M2 polarization. These molecules are known to regulate the stability of lipid raft microdomains involved in cell signalling and cell communication [157], suggesting these processes to be involved in flavonoid-mediated lipid remodelling. Alterations in PI species may also reflect their role in signalling, specifically relating to PI3K activity and PI turnover. Notably, quercetin attenuated the production of some pro-inflammatory cytokines (IL-6 and TNF-α), which are under the regulation of the PI3K pathway. The decrease in some PS species is in line with the observed reduction in total PS levels observed in both M2 and quercetin treated M1 macrophages. Again, these lipids are important in cell signalling and inflammation [145]. They were reported to reduce TNF-α, IL-6, IL-8 and VEGF, as well, as PGE_2 production, in fibroblast-like synoviocytes from rheumatoid arthritis patients. In macrophages they might present a similar role; however, to the extent of our knowledge, the role of PS in macrophages is yet to be explored. Membrane fluidity was also likely affected by quercetin treatment, as suggested by changes in PC and SM species. Interestingly, however, SM variations were important within the response to quercetin but not within M2 polarization, likely reflecting membrane remodelling not related to anti-inflammatory activity.

III.2.4. Naringin-induced changes in macrophage phospholipidome

Analysis of overall changes in PL classes (**Figure 38A**) reveals that naringin (200 μM) caused a few significant changes. Only the total PC level increased significantly upon 48h incubation of M0 macrophages with naringin. Other noticeable but not statistically significant changes comprised: i) an increase in total PS in macrophages incubated for 24h with LPS/IFN-γ (M1 pre-polarized) followed by 24h exposure to the flavonoid (M1+Nar), ii) decreasing trends for PEs and SMs in both M0 and M1 macrophages treated with naringin.

Total carbon length was also affected by naringin (**Figure 38B**). PL species with 32 and 34 FA carbons showed a trend to decrease, whereas PL species with longer FA chains (36 and 38 carbons) displayed an increasing trend (although not reaching statistical significance). The increase in PL species containing 36 and 38 carbons, together with the decrease in species containing 34 carbons, suggests an increased production of C18 and, possibly, C20, as well as a preference to group C18 with C18 or C20 in the same PL. However, when we compared the levels of PL species containing C18 (**Figure 38C**), we did not observe any significant changes, suggesting that naringin did not increase C18 production but rather promoted redistribution of C18. Nonetheless, naringin increased the levels of species containing arachidonic acid (AA) (**Figure 34D**). Increased PL species containing AA suggests an increased production of C20 FA, which can explain the tendency to increase species containing 38 carbons. AA is involved in inflammation by acting as precursor to produce eicosanoids, which may have both pro- and anti-inflammatory activity. Thus, we postulate that the increase in AA might reflect an increased AA turnover and production of eicosanoids, an hypothesis that requires further verification in future studies.

Additionally, naringin affected the unsaturation degree of PL species (**Figure 34E**). Similarly to quercetin, naringin induced a decrease in MUFA and an increase in PUFA containing 4 or 5 double bonds. This effect was especially prominent in M0 macrophages.

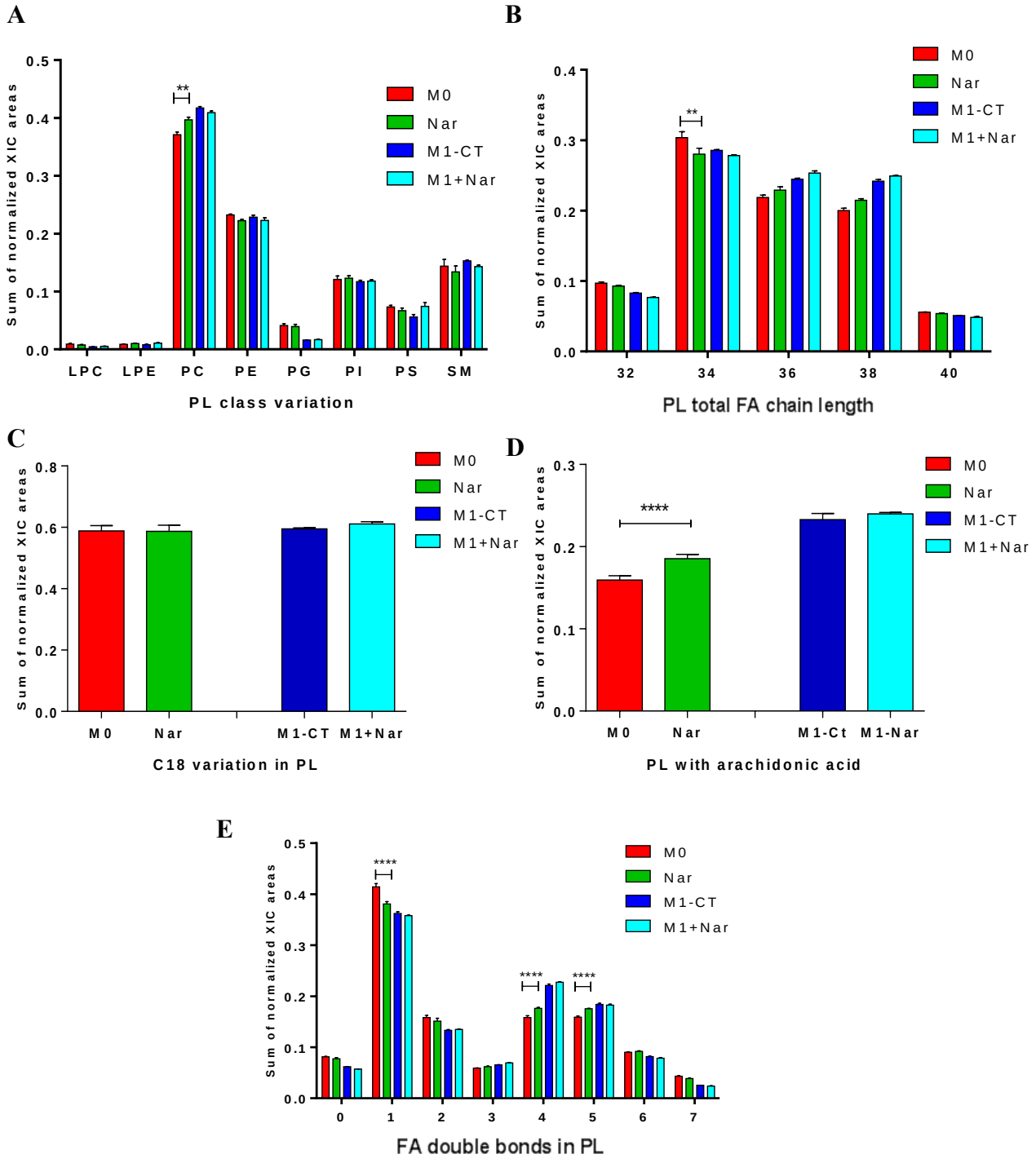

Figure 38 - Changes in PL class and structure observed in M0 macrophages treated with naringin (200 µM) for 48h, and in pre-polarized M1 macrophages (24h, LPS+IFN-γ) subjected to 24h incubation with naringin (200 µM). The different graphs represent total amounts of (**A**) different PL classes, (**B**) PL-composing FA differing in total number of carbons, (**C**) C18 FA-containing PL species, (**D**) AA-containing PL species, (**E**) PL-composing FA differing in the number of double bonds. *, **, ****, Statistical significance ($p<0.05$, $p<0.01$, $p<0.0001$). Error bars represented as mean±S (n=5).

Following a similar strategy to that presented for quercetin, multivariate analysis was applied to the LC-MS data collected for the PL species identified across the 4 groups (naringin-treated M0 and pre-polarized M1 cells, together with their respective controls). The resulting PCA scores scatter plot is presented in **Figure 39A**. Although the groups compared were not perfectly separated, this plot clearly shows clustering trends according to macrophage polarization state and flavonoid treatment. Then, pairwise PLS-DA modelling resulted in robust discrimination between naringin treated macrophages and control groups (**Figure 39B,C**), allowing for the most important variables for such discrimination to be highlighted (**Figure 39D,E**).

Further information on varying species was then obtained from PL quantification data and univariate statistical comparisons. The PL species with greater magnitude of variation ($|ES| > 0.8$) were represented in volcano plots (**Figure 40A,B**), and the top-20 altered species in each case were listed together in a heatmap, color-coded according to the percentage of variation relatively to controls (**Figure 40C**). Nine species varied upon naringin treatment in opposite directions depending on macrophage initial polarization state, while several other variations were noted in one of the conditions but not the other. Indeed, considering all varying species, only 44% were common between treated M0 macrophages (M0+Nar) and treated pre-polarized cells (M1+Nar) (**Figure 41A**).

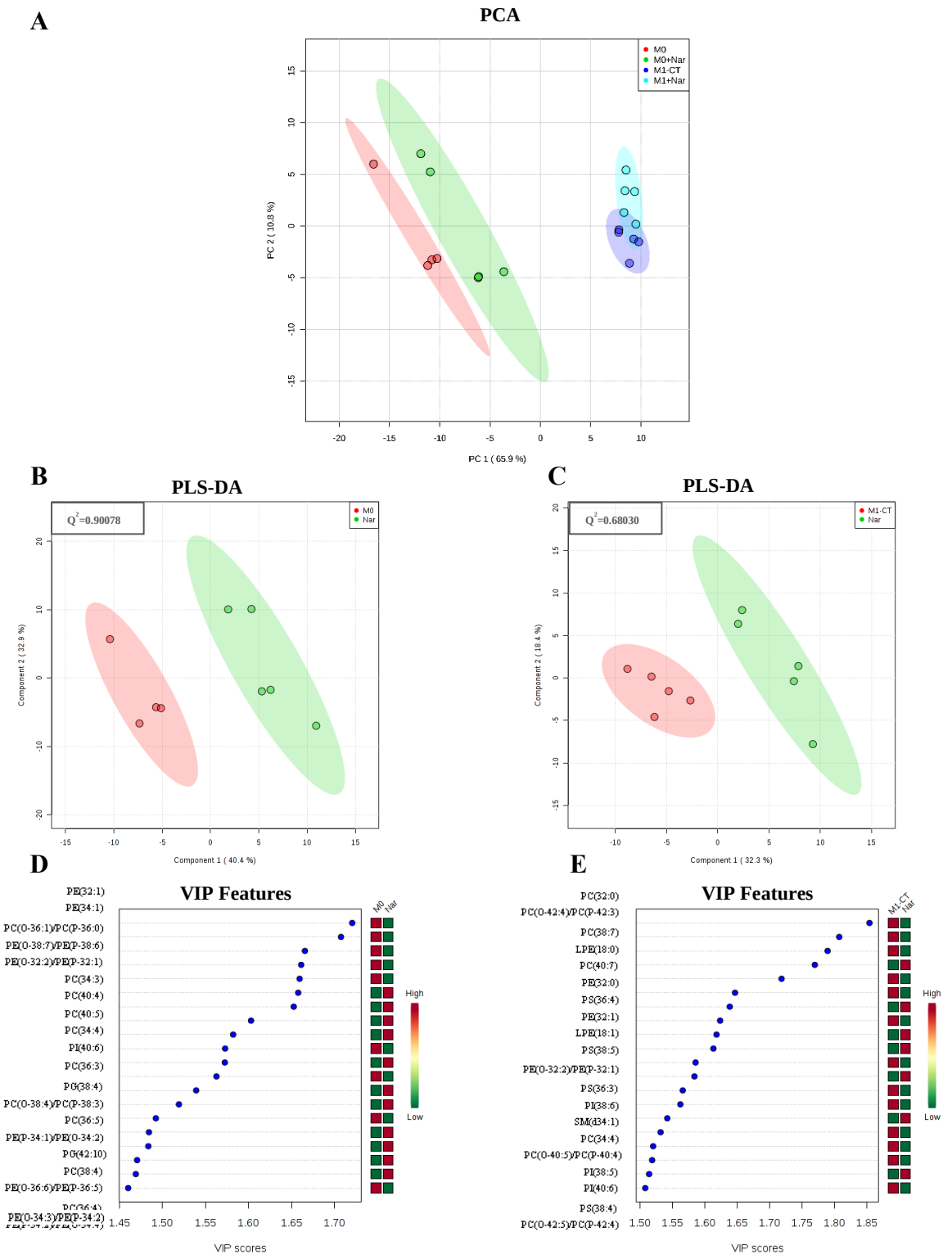

Figure 39 - Multivariate analysis of LC-MS data collected for M0 and M1 pre-polarized macrophages exposed to naringin (200 µM). (**A**) PCA scores scatter plot; (**B**),(**C**) PLS-DA scores scatter plot obtained for pairwise comparisons between naringin-treated M0 and M1 cells and their respective controls; (**D**), (**E**) Twenty PL species with higher VIP values i.e. higher importance to PLS-DA discrimination.

Considering the most prominent variations within each PL class (**Figure 40C**), naringin effects may be summarized as: i) decreased/increased LPE species in M0/M1 macrophages, respectively; ii) increased levels of several PC species in treated M0 macrophages, while the opposite trend is seen in treated M1 macrophages; iii) consistent decreases in several PE species, in both M0 and M1 macrophages; iv) decreasing trends for a few PG, PI and SM species, except for PG(42:10); v) consistent increases in PS species, especially upon treatment of pre-polarised macrophages.

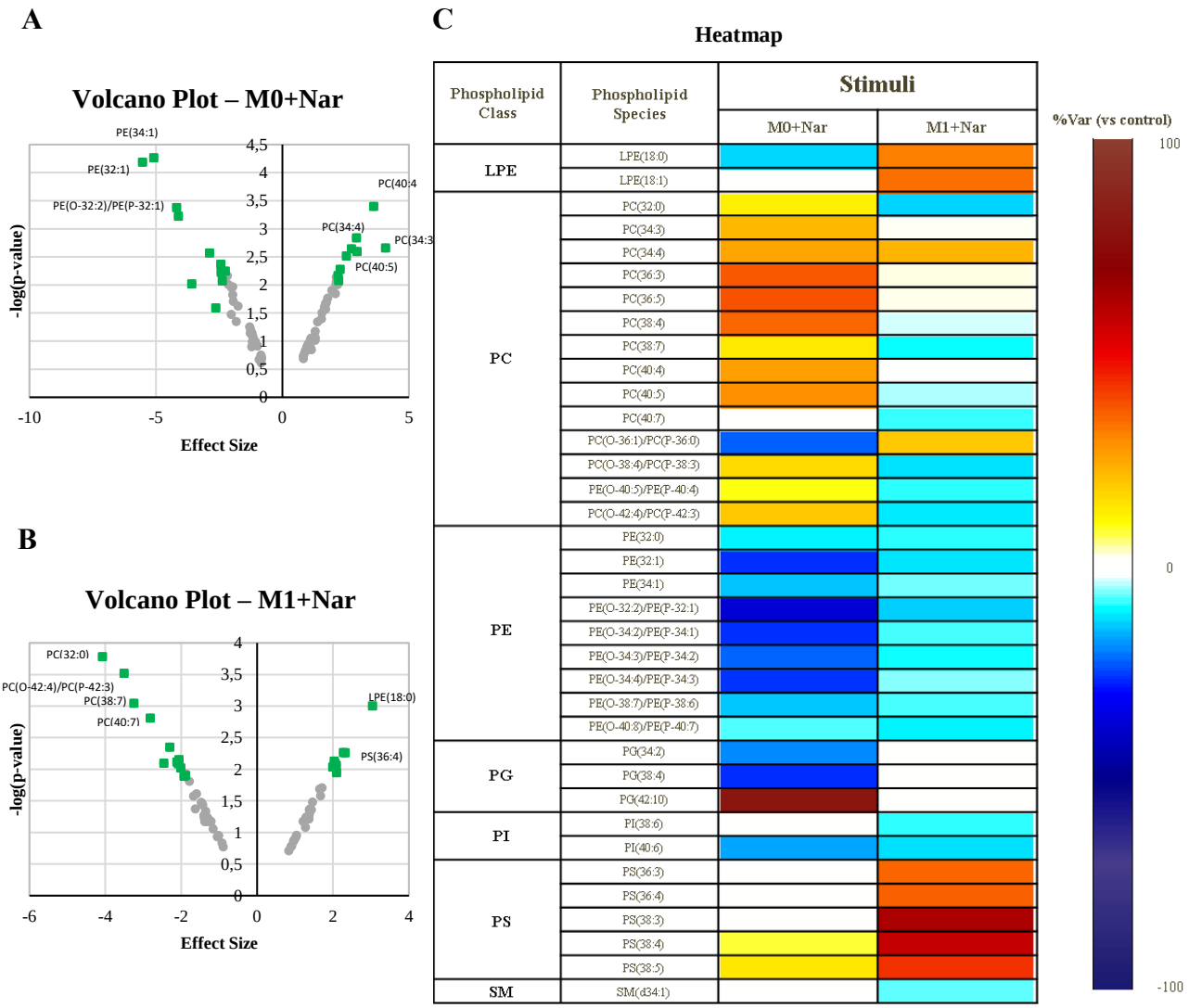

Figure 40 - (**A**) and (**B**) Volcano Plots representing the PL species with large magnitude (|ES|>0.8) in M0 and M1pre-polarized macrophages, relatively to respective controls. The 20 species with the highest |ES| are highlighted in green squares.(**C**) Heatmap representing the top-20 varying species in naringin treated M0 macrophages (M0+Nar) and naringin-treated pre—polarized cells (M1+Nar), color coded according according to the percentage of variation relatively to controls.

Comparing PL variations in naringin-treated pre-polarized M1 macrophages with those induced upon M2 polarization, we found only 18% similarity (**Figure 41B**). This indicates that, in spite of naringin's anti-inflammatory activity (assessed by the ability to attenuate pro-inflammatory cytokines), the modulation of cellular PLs by this flavonoid greatly differed from PL remodelling induced by IL-4/IL-13 (M2) stimulation. Indeed, after excluding the changes shared with M1 polarization, only 3 species were found to represent possible M2-like lipid markers. These were PC (32:0), PE(O-36:6)/PE(P-36:5) and PI(38:6), which decreased in M2 vs. M0 macrophages, as well as in naringin-treated M1 cells vs. M1 controls (**Figure 42**).

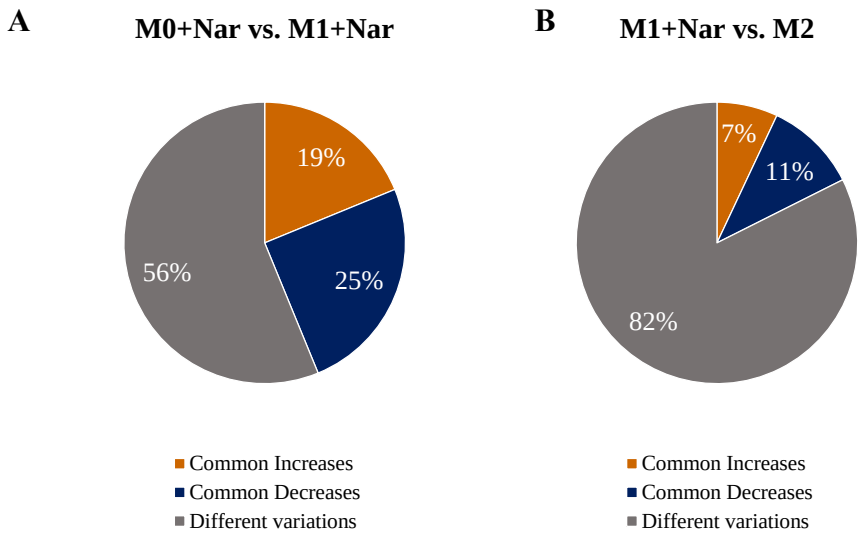

Figure 41 - Pie charts representing the % of common increases, common decreases and discrepant variations between PL data subsets collected for different exposure conditions.

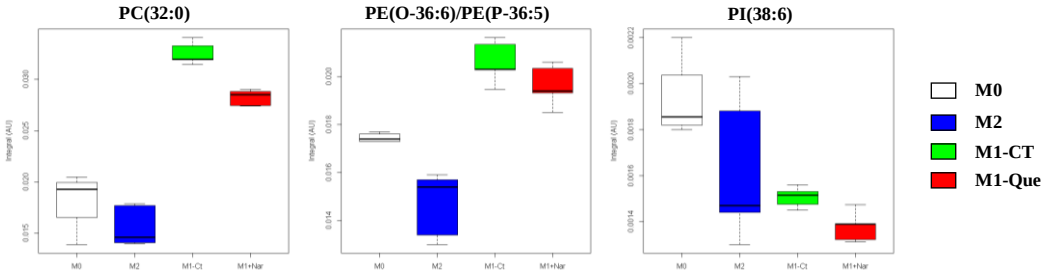

Figure 42 - Boxplots showing the levels of selected PL species in M0 macrophages, M2 macrophages, M1 pre-polarized macrophages (24h LPS/IFN + 24h fresh medium) and naringin-treated M1 cells (24h LPS/IFN + 24h naringin 200 uM). The species represented were selected based on the same direction of variation in flavonoid-treated and M2 macrophages, and the absence of overlap with changes characteristic of M1 polarization.

III.2.5. Naringenin-induced changes in macrophage phospholipidome

Following the trend observed for the other flavonoids, macrophage exposure to naringenin caused a significant increase in total PC levels (**Figure 43A**). On the other hand, total PE showed a significant decrease in treated M0 macrophages, while displaying the opposite trend in pre-polarized M1 macrophages. The apparent changes in other PL classes did not reach statistical significance. In regard to PL total FA chain length, there were no statistically significant changes, although species containing 34 or 36 carbons tended to decrease and those containing 38 carbons tended to increase, especially in treated M0 macrophages (**Figure 43B**). Analysis of PL containing C18 FAs and arachidonic acid (AA) further shows their increased levels in naringin-treated M0 macrophages (**Figure 43C,D**). As for FA unsaturation degree, the only significant change was a decrease in saturated species in naringenin-treated M0 macrophages (**Figure 43E**).

The multivariate analysis results obtained for naringenin-treated macrophages and their respective controls are shown in Figure 40. The PCA scores scatter plot (**Figure 44A**) shows that PC1 separates samples according to their initial polarization state, whereas the effect of naringenin is noted along PC2. PLS-DA scores plots show very good discrimination (Q^2>0.9) between naringenin-treated macrophages, either in the M0 or M1 state, and their respective controls (**Figure 44B,C**). The PL species with higher importance for this discriminant ability are highlighted in **Figure 44D,E** and were confirmed through quantitative analysis of variations (**Figure 45**). Among the top-20 varying species in naringenin-treated M0 or M1 pre-polarized cells, PC and PE species are clearly dominant (**Figure 45C**), suggesting major remodelling of cell membranes. Regarding the influence of macrophages initial polarization state towards the response to naringenin, 5 of the most relevant variations followed opposite directions. Overall, 57% of naringenin-related changes were commonly produced in M0 and M1 macrophages (**Figure 46A**).

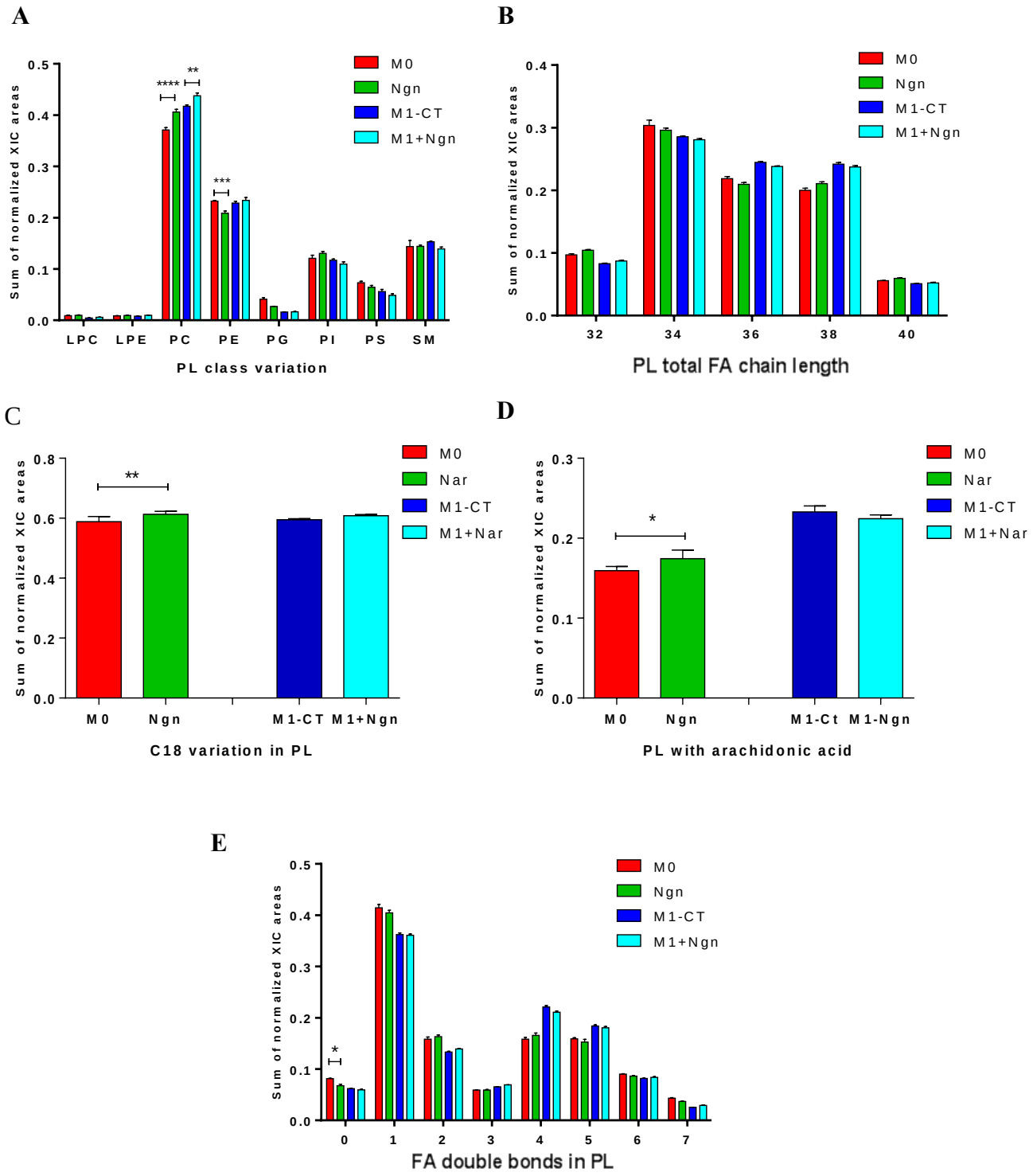

Figure 43 - Changes in PL class and structure observed in M0 macrophages treated with naringenin (100 µM) for 48h, and in pre-polarized M1 macrophages (24h, LPS+IFN-γ) subjected to 24h incubation with naringenin (100 µM). The different graphs represent total amounts of (**A**) different PL classes, (**B**) PL-composing FA differing in total number of carbons, (**C**) C18 FA-containing PL species, (**D**) AA-containing PL species, (**E**) PL-composing FA differing in the number of double bonds. *, **, ****, Statistical significance ($p<0.05$, $p<0.01$, $p<0.0001$). Error bars represented as mean±S (n=5).

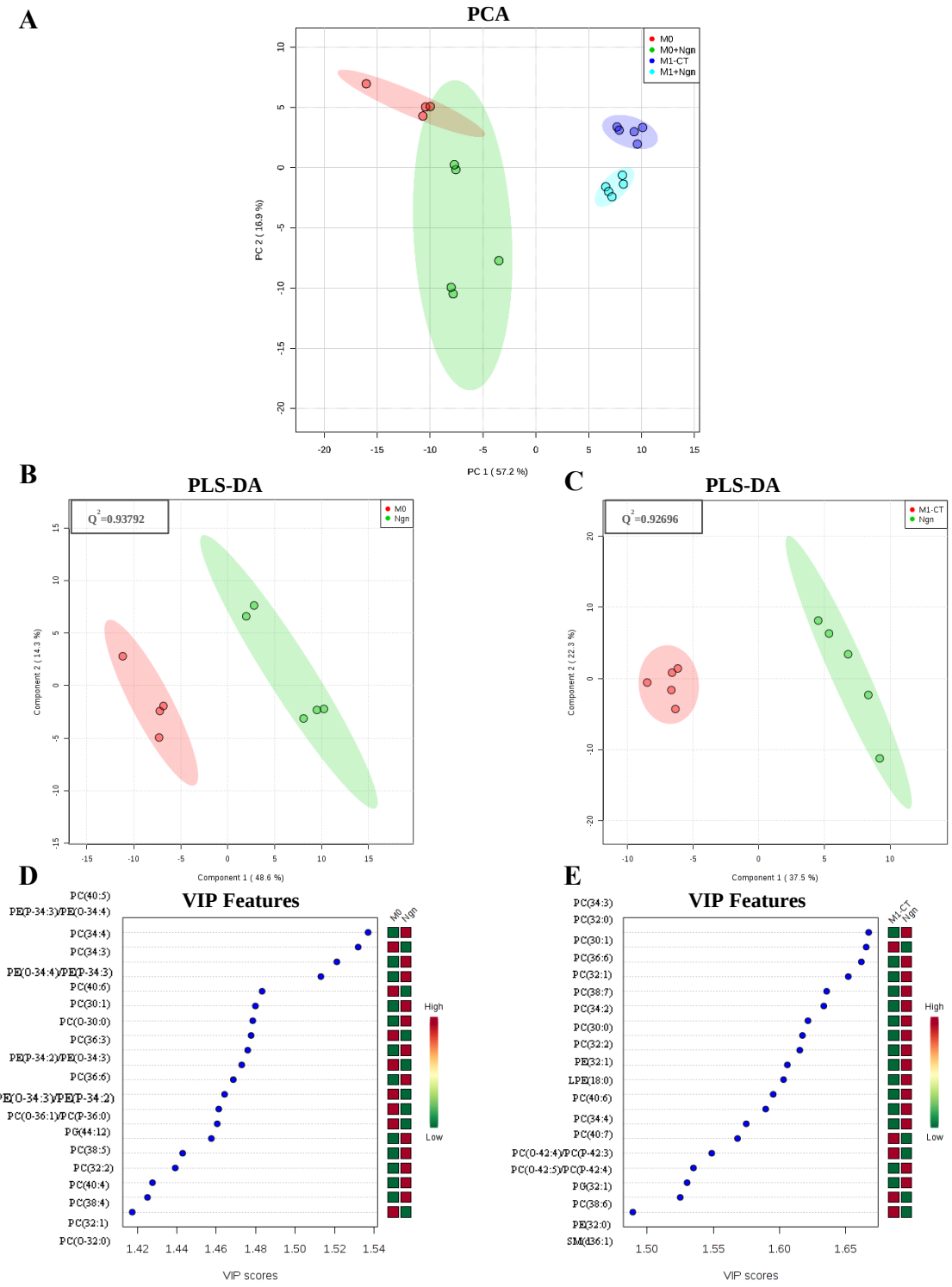

Figure 44 - Multivariate analysis of M0 and M1-like macrophages exposed to naringenin. (**A**) PCA scores for M0 and M1-like macrophages exposed to naringenin, and their respective controls. (**B**) PLS-DA scores for M0 macrophages exposed to naringenin for 48h, with a Q^2 of 0.90078. (**D**) PLS-DA scores for M1 macrophages exposed to naringenin with a Q^2 of 0.68030. (**E**) VIP scores from the 20 PL species with the highest VIP value in exposed M0 macrophages. (**F**) VIP scores from the 20 PL species with the highest VIP value in exposed M1-like macrophages. In VIP scores plot, red represents an increase, while green represents a decrease.

The degree of similarity between the impact of naringenin on M1 pre-polarized macrophages and that of canonical M2 polarization was 30% (**Figure 46B**). Taking a closer look at those variations and excluding the ones showing the same direction upon pro-inflammatory M1 stimulation, 13 species were highlighted (**Figure 47**). Those showing increased levels relative to controls were: PC(30:1), 2 ethanolamine plasmalogens (PE(O-36:5)/PE(P-36:4), PE(O-36:6)/PE(P-36:5)) and 2 PI (40:4, 40:6). On the other hand, PL species decreasing in both M2 and naringenin-treated M1 macrophages were: PC(32:0), 2 ethanolamine plasmalogens (PE(O-40:7)/PE(P-40:6), PE(O-42:7)/PE(P-42:6)), 2 PG (38:4, 42:10) and 3 PS (43:1, 36:1, 36:2). Again, these changes suggest cellular modifications at the level of membrane properties, signalling lipids and lipid raft microdomains.

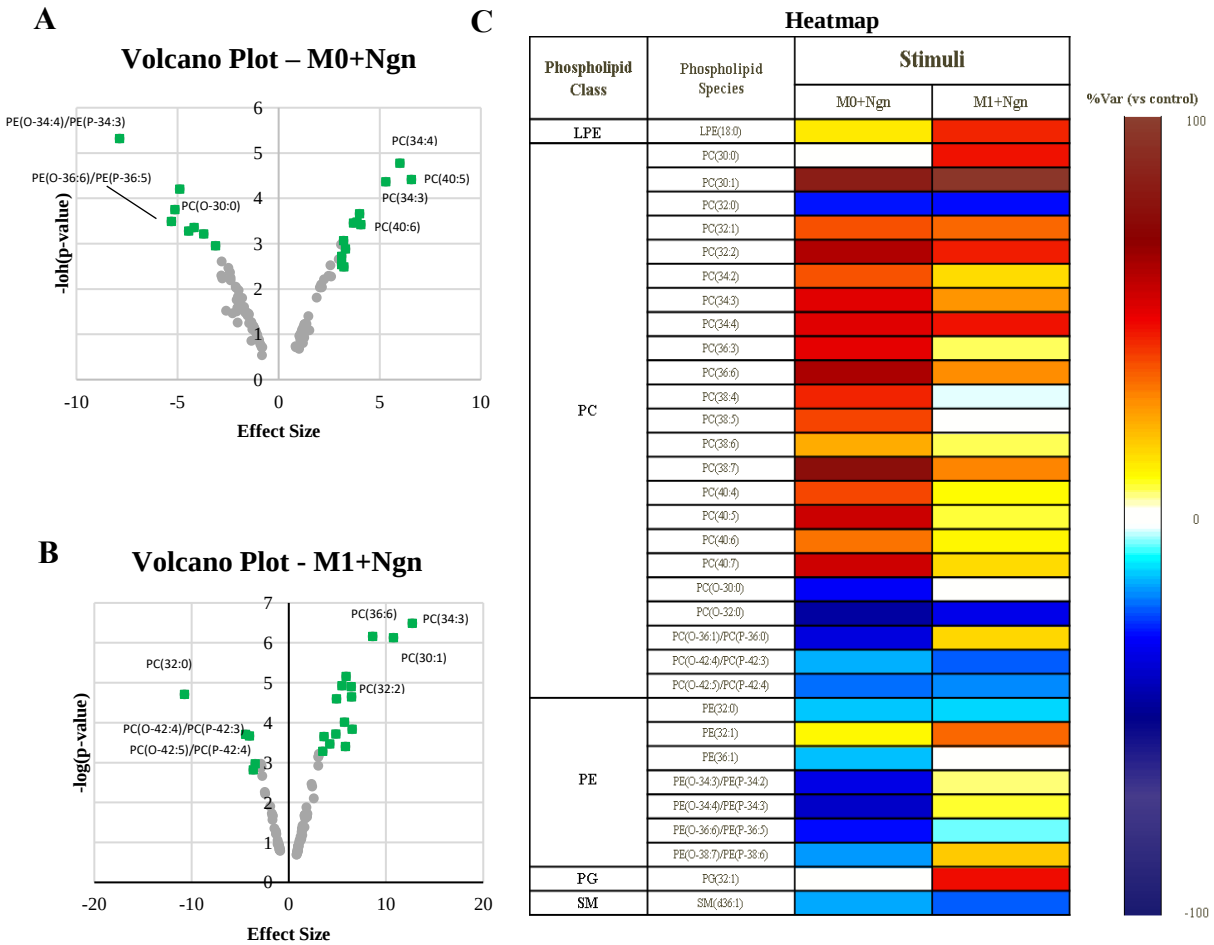

Figure 45 - (**A**) and (**B**) Volcano Plots representing the PL species with large magnitude (|ES|>0.8) in M0 and M1pre-polarized macrophages, relatively to respective controls. The 20 species with the highest |ES| are highlighted in green squares.(**C**) Heatmap representing the top-20 varying species in naringenin treated M0 macrophages (M0+Ngn) and naringenin-treated pre—polarized cells (M1+Ngn), color coded according to the percentage of variation relatively to controls.

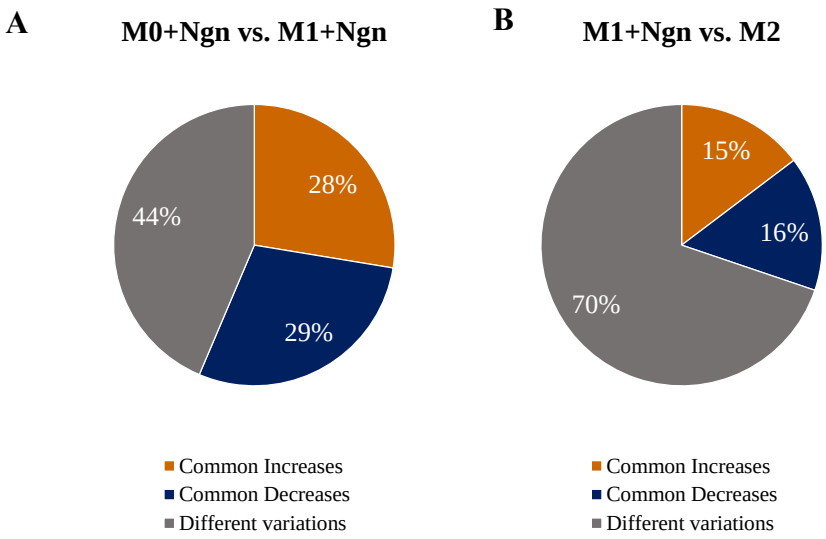

Figure 46 - Pie charts representing the % of common increases, common decreases and discrepant variations between PL data subsets collected for different exposure conditions.

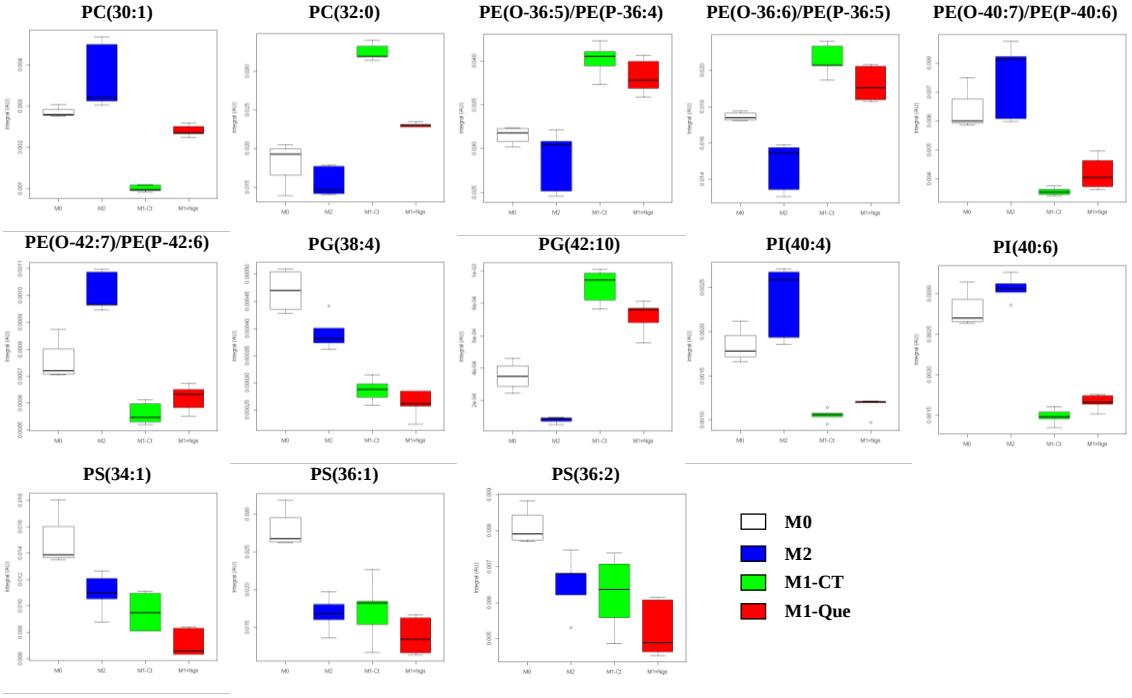

Figure 47 - Boxplots showing the levels of selected PL species in M0 macrophages, M2 macrophages, M1 pre-polarized macrophages (24h LPS/IFN + 24h fresh medium) and naringenin-treated M1 cells (24h LPS/IFN + 24h naringenin 100 uM). The species represented were selected based on the same direction of variation in flavonoid-treated and M2 macrophages, and the absence of overlap with changes characteristic of M1 polarization.

III.2.6. Comparison of the lipidomic changes induced by the three flavonoids

As described in the previous sections, the three flavonoids tested (quercetin, naringin and naringenin) had an extensive impact on the phospholipidome of human THP-1 derived macrophages. This section is now aimed at comparing the main alterations induced by these compounds upon 24h treatment of pre-polarized M1 macrophages. **Figure 48** shows a heatmap summarizing the species with highest magnitude of variation (top-20 varying species in each exposure condition).

Interestingly, several features common to the three flavonoids could be highlighted: the top-varying LPC, LPE and PG species increased with all three flavonoids, while some choline plasmalogens and several SM species decreased, although less markedly in naringin-treated cells.

On the other hand, the modulation of other PL species was clearly flavonoid-dependent. This was the case of most diacyl PC. In particular, it is interesting to note that, within this class, PC with 30, 32 or 34 FA carbons varied similarly for quercetin and naringenin exposures, while the variation in PC with 38 or 40 FA carbons and 6/7 unsaturations was shared by quercetin and naringin. Moreover, two diacyl PC species varied similarly in all treatments: PC(32:0) decreased while PC(34:4) increased, both variations being more prominent in naringenin-treated cells. Regarding PE species (diacyl and ethanolamine plasmalogens), the variations were not only flavonoid-dependent, as no general trend could be noted within the class (some species increased and others decreased). There is still to notice the modulation of PI species (decreased with quercetin and naringin, increased with naringenin), and of PS species (decreased with quercetin, increased with naringin and not varying in naringenin-treated cells).

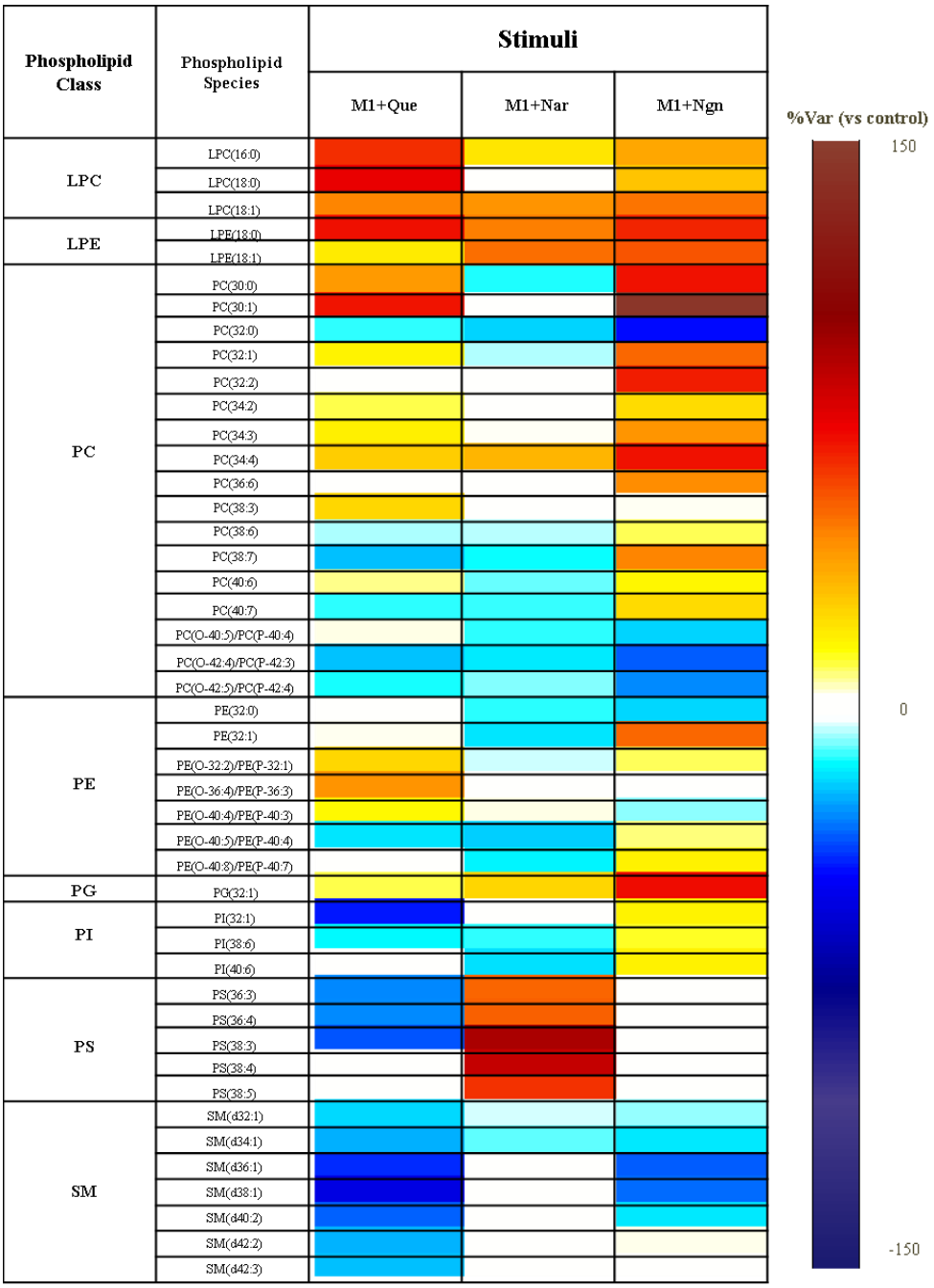

Figure 48 – Heatmap representing the top-20 varying species in quercetin, naringin and naringenin pre—polarized cells (M1+Que, M1+Nar and M1+Ngn, respectively), color coded according to the percentage of variation relatively to control.

By extending the comparison to all species showing large magnitude of variation (|ES|> 0.8), we could additionally get a more general view on the degree of similarity between flavonoids (**Figure 49**). Quercetin and naringenin produced the most similar impact (58% common variations), while in the other pairwise comparisons (quercetin vs. naringin, naringin vs. naringenin) the degree of similarity was around 40%.

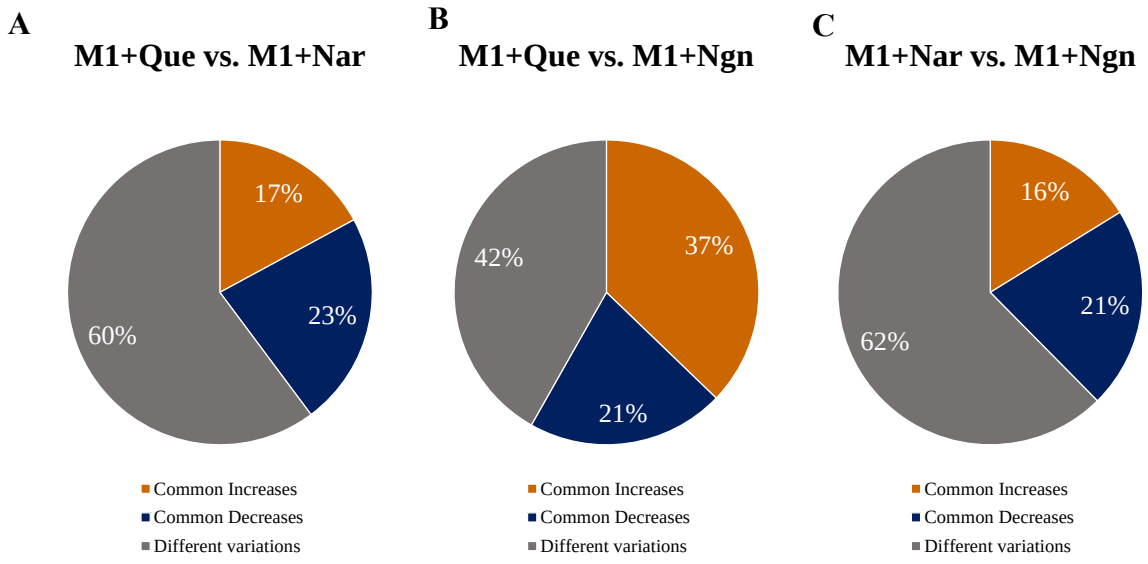

Figure 49 – Pie charts representing the % of common increases, common decreases and discrepant variations between PL data subsets collected for different exposure conditions.

Finally, we have looked for species that varied commonly between all M1 flavonoid-treated macrophages and M2-polarized (anti-inflammatory) macrophages, while showing opposite or no variation upon M1 (pro-inflammatory) polarization. Interestingly, only two species (with |ES| > 0.8) obeyed these criteria: PC(32:0) and PE(O-36:6)/PE(P-36:5). Their boxplot representations are shown in **Figure 50**. In both cases, their levels decreased in M2 macrophages (compared to M0), increased upon M1 polarization (M1-CT vs. M0) and then decreased upon flavonoid treatments, suggesting a relation to anti-inflammatory activity.

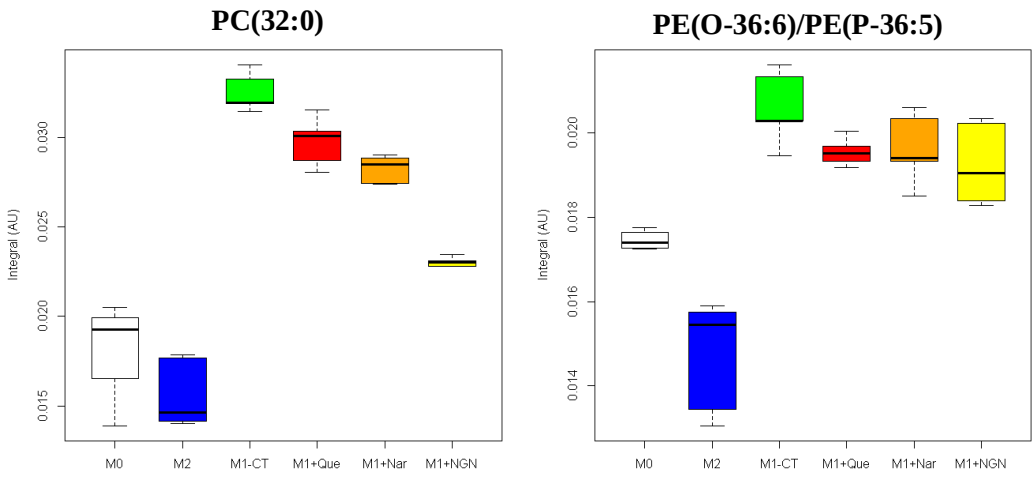

Figure 50 – PL species that varied commonly between flavonoid-treated M1 pre-polarized macrophages and M2-polarized (anti-inflammatory) macrophages, while showing opposite or no variation upon M1 (pro-inflammatory) polarization.

IV. Conclusions and Future Work

The HILIC-LC-MS approach applied to human THP-1 derived macrophage lipid extracts enabled the identification and relative quantification of 147 phospholipid (PL) species belonging to 8 different classes: phosphatidylcholines (PC), including diacyl and alkyl-acyl PC, phosphatidylethanolamines (PE), including diacyl and alkyl-acyl PE, lyso-phosphatidylcholines (LPC), lyso-phosphatidylethanolamines (LPE), phosphatidylglycerols (PG), phosphatidylinositols (PI), phosphatidylserines (PS), and sphingomyelins (SM). Then, multivariate and univariate analysis of LC-MS data enabled the changes in the levels of these species to be characterized under different conditions, namely under M1 and M2 canonical polarization, and upon treatment with three flavonoids (quercetin, naringin and naringenin). Although these compounds have well-known anti-inflammatory activity, to our knowledge, their effects on macrophage lipidome had never been reported, and were here presented and discussed for the first time.

As expected, the three flavonoids were found to attenuate the production of important pro-inflammatory cytokines by M1 macrophages, at 24h incubation time and specific concentrations (maximal doses not decreasing cell viability). Moreover, naringenin increased the levels of an anti-inflammatory mediator (CCL-17), suggesting its pro-resolving activity.

Regarding lipidomic results, all flavonoids were seen to have a pronounced impact on the macrophage phospholipidome, causing large magnitude variations in 47-77% of all identified PL species. The top-20 varying species were highlighted in each case and found to belong predominantly to: i) PC, PE, PI and SM in the case of quercetin, ii) PC, PE and PS in the case of naringin, iii) PC and PE in the case of naringenin. These alterations suggested flavonoid-induced modulation of cell membrane composition and fluidity (mainly affecting PC, PE and SM), interference with cell signalling pathways (mainly involving PI, PS and plasmalogens), and/or antioxidant activity (possibly related to plasmalogens).

Notably, the observed effects were dependent on macrophage initial polarization state, at different extents depending on the flavonoid considered. In particular, the degrees of similarity between the responses of uncommitted M0 macrophages and M1 pre-polarized macrophages to each flavonoid were 74% for quercetin, 44% for naringin and 57% for naringenin. This result was not unexpected given that macrophage activation has been shown

by us and others to deeply affect cellular lipids. Hence, it is likely that subsequent flavonoid effects depend on the initial cellular composition. On the other hand, the fact that many variations were independent of the initial polarization state underscored strong flavonoid specific effects, indicating flavonoid action to be effective even after a pro-inflammatory stimulus.

Then, focusing on PL species that varied commonly between flavonoid-treated M1 pre-polarized macrophages and M2-polarized (anti-inflammatory) macrophages (while showing opposite or no variation upon M1 polarization), a subset of potential markers of anti-inflammatory activity was highlighted for each flavonoid: 18 species in the case of quercetin, 3 in the case of naringin and 13 in the case of naringenin. It should be noted, however, that although canonical M2 polarization may serve as reference to assess changes related to anti-inflammatory activity, this may be viewed as a simplistic and limited approach, as other flavonoid-induced changes, not found in M2 macrophages, may also be linked to attenuation and/or resolution of macrophage-mediated inflammatory responses.

Furthermore, by comparing the most prominent effects of the three flavonoids on M1 pre-polarized macrophages, it was possible to conclude that flavonoid-mediated lipid remodelling was generally characterized by increases in LPC, LPE and PG species, accompanied by decreases in choline plasmalogens and SM species, whereas the modulation of other PL species was clearly flavonoid-dependent. Overall, quercetin and naringenin shared the greatest similarity. Finally, two species emerged as potential anti-inflammatory lipid markers of flavonoid activity: PC(32:0) and PE(O-36:6)/PE(P-36:5), both decreased in response to either M2 polarization and flavonoid treatment. Their anti-inflammatory activity and relevance to macrophage biology (e.g. membrane fluidity, production of cytokines, phagocytosis) should be explored in future studies.

One of the limitations of this study was that flavonoid effects were not evaluated at different concentrations and exposure times. Given that macrophages are highly plastic cells, it would be useful to perform time course experiments at different flavonoid doses. Future studies should also include the targeted analysis of eicosanoids (especially relevant in the

context of inflammation), and assessment of key proteins involved in lipid metabolism, to help clarifying the biochemical mechanisms underlying the changes observed in this work.

Overall, we expect that these results may open new research avenues towards a greater understanding of the interplay between flavonoid-induced PL modulation and the pro-/anti-inflammatory activity of macrophages.

V. References

1. Ferrero-Miliani L, Nielsen OH, Andersen PS, Girardin SE. Chronic inflammation: Importance of NOD2 and NALP3 in interleukin-1β generation. Clin Exp Immunol. 2007;147(2):227–35.

2. Prasad S, Aggarwal BB. Chronic Diseases Caused by Chronic Inflammation Require Chronic Treatment: Anti-inflammatory Role of Dietary Spices. J Clin Cell Immunol. 2014;05(04):1–11.

3. Brown BN, Londono R, Tottey S, Zhang L, Kukla KA, Wolf MT, Daly KA, Reing JE, Badylak SF. Macrophage phenotype as a predictor of constructive remodeling following the implantation of biologically derived surgical mesh materials. Acta Biomater. 2012;8(3):978–87.

4. van Furth R, Cohn ZA, Hirsch JG, Humphrey JH, Spector WG, Langevoort HL. The mononuclear phagocyte system : a new classification of macrophages , monocytes , and their percursor cells. Bull World Heal Organ. 1970;46(6):845–52.

5. Murray PJ, Wynn TA. Protective and pathogenic functions of macrophage subsets. Nat Rev Immunol. 2011;11(11):723–37.

6. Stremmel C, Schuchert R, Wagner F, Thaler R, Weinberger T, Pick R, Mass E, Ishikawa-Ankerhold HC, Margraf A, Hutter S, Vagnozzi R, Klapproth S, Frampton J, Yona S, Scheiermann C, Molkentin JD, Jeschke U, Moser M, Sperandio M, Massberg S, Geissmann F, Schulz C. Yolk sac macrophage progenitors traffic to the embryo during defined stages of development. Nat Commun. 2018;9(75):1–14.

7. Hashimoto D, Chow A, Noizat C, Teo P, Beth M, Leboeuf M, Becker CD, See P, Price J, Lucas D, Greter M, Mortha A, Boyer SW, Camilla E. Tissue resident macrophages self-maintain locally throughout adult life with minimal contribution from circulating monocytes. Immunity. 2013;38(4):792–804.

8. Wahl SM, Hunt D a, Wakefield LM, McCartney-Francis N, Wahl LM, Roberts a B, Sporn MB. Transforming growth factor type beta induces monocyte chemotaxis and growth factor production. Proc Natl Acad Sci U S A. 1987;84(16):5788–92.

9. Sokol RJ, Hudson G, James NT, Frost IJ, Wales J. Human macrophage development: a morphometric study. J Anat. 1987;151:27–35.

10. McCullough KC, Basta S, Knötig S, Gerber H, Schaffner R, Kim YB, Saalmüller A, Summerfield A. Intermediate stages in monocyte-macrophage differentiation modulate phenotype and susceptibility to virus infection. Immunology. 1999;98(2):203–12.

11. Kradin L, Schneeberger E. Flow-Cytometric and Ultrastructural Analysis of Alveolar Macrophage Matu ration. 1986;417(4):407–17.

12. Spiller KL, Wrona EA, Romero-Torres S, Pallotta I, Graney PL, Witherel CE, Panicker LM, Feldman RA, Urbanska AM, Santambrogio L, Vunjak-Novakovic G, Freytes DO. Differential gene expression in human, murine, and cell line-derived macrophages upon polarization. Exp Cell Res. 2016;347(1):1–13.

13. Zhang X, Mosser D. Macrophage activation by endogenous danger signals. J Pathol. 2008;214(2):161–78.

14. Curren Smith EW. Macrophage Polarization and Its Role in Cancer. J Clin Cell Immunol. 2015;6(4):4–11.

15. Liu Y-C, Zou X-B, Chai Y-F, Yao Y-M. Macrophage Polarization in Inflammatory Diseases. Int J Biol Sci. 2014;10(5):520–9.

16. Badylak SF, Valentin JE, Ravindra AK, McCabe GP, Stewart-Akers AM. Macrophage Phenotype as a Determinant of Biologic Scaffold Remodeling. Tissue Eng Part A. 2008;14(11):1835–42.

17. Drapier J, Petit J. Development of antitumor mouse activity in LPS-stimulated granuloma macrophages.

Inflammation. 1986;10(2):195–204.

18. Wang N, Liang H, Zen K. Molecular mechanisms that influence the macrophage M1-M2 polarization balance. Front Immunol. 2014;5(11):1–9.

19. Bauernfeind F, Bartok E, Rieger A, Franchi L, Núñez G, Hornung V. Reactive oxygen species inhibitors block priming, but not activation of the NLRP3 inflammasome. J Immunol. 2011;187(2):613–7.

20. Van Bruggen R, Köker MY, Jansen M, Van Houdt M, Roos D, Kuijpers TW, Van Den Berg TK. Human NLRP3 inflammasome activation is Nox1-4 independent. Blood. 2010;115(26):5398–400.

21. van de Veerdonk FL, Smeekens SP, Joosten LAB, Kullberg BJ, Dinarello CA, van der Meer JWM, Netea MG. Reactive oxygen species-independent activation of the IL-1 inflammasome in cells from patients with chronic granulomatous disease. Proc Natl Acad Sci. 2010;107(7):3030–3.

22. Schenk M, Fabri M, Krutzik SR, Lee DJ, Vu DM, Sieling PA, Montoya D, Liu PT, Modlin RL. Interleukin-1β triggers the differentiation of macrophages with enhanced capacity to present mycobacterial antigen to T cells. Immunology. 2014;141(2):174–80.

23. Jo E-K, Kim JK, Shin D-M, Sasakawa C. Molecular mechanisms regulating NLRP3 inflammasome activation. Cell Mol Immunol. 2016;13(2):148–59.

24. Genin M, Clement F, Fattaccioli A, Raes M, Michiels C. M1 and M2 macrophages derived from THP-1 cells differentially modulate the response of cancer cells to etoposide. BMC Cancer. 2015;15(1):577.

25. Chanput W, Mes JJ, Savelkoul HFJ, Wichers HJ. Characterization of polarized THP-1 macrophages and polarizing ability of LPS and food compounds. Food Funct. 2013;4(2):266–76.

26. Littlefield MJ, Teboul I, Voloshyna I, Reiss AB, Reiss AB, Hospital W, Plaza S. Polarization of Human THP-1 Macrophages: Link between Adenosine Receptors, Inflammation and Lipid Accumulation. Int J Immunol Immunother. 2014;1(1):1–8.

27. Xuan W, Qu Q, Zheng B, Xiong S, Fan G-H. The chemotaxis of M1 and M2 macrophages is regulated by different chemokines. J Leukoc Biol. 2015;97(1):61–9.

28. Zizz G, Hilliard BA, Monestier M, Cohen PL. Efficient clearance of early apoptotic cells by human macrophages requires “M2c” polarization and MerTK induction. J Imunol. 2012;189(7):3508–20.

29. Chinetti-Gbaguidi G, Colin S, Staels B. Macrophage subsets in atherosclerosis. Nat Rev Cardiol. 2015;12(1):10–7.

30. Wang Q, Ni H, Lan L, Wei X, Xiang R, Wang Y. Fra-1 protooncogene regulates IL-6 expression in macrophages and promotes the generation of M2d macrophages. Cell Res. 2010;20(6):701–12.

31. Vats D, Mukundan L, Odegaard JI, Zhang L, Smith KL, Morel CR, Greaves DR, Murray PJ, Chawla A. Oxidative metabolism and PGC-1β attenuate macrophage-mediated inflammation. Cell Metab. 2006;4(1):13–24.

32. Martinez FO, Helming L, Milde R, Varin A, Melgert BN, Draijer C, Thomas B, Fabbri M, Crawshaw A, Ho LP, Hacken NHT, Jiménez VC, Kootstra NA, Hamann J, Greaves DR, Locati M, Mantovani A, Gordon S. Genetic programs expressed in resting and IL-4 alternatively activated mouse and human macrophages: Similarities and differences. Blood. 2013;121(9):57–70.

33. Sinha P, Clements VK, Ostrand-Rosenberg S. Reduction of Myeloid-Derived Suppressor Cells and Induction of M1 Macrophages Facilitate the Rejection of Established Metastatic Disease. J Immunol. 2005;174(2):636–45.

34. Fahy E, Subramaniam S, Brown HA, Glass CK, Merrill AH, Murphy RC, Raetz CRH, Russell DW, Seyama Y, Shaw W, Shimizu T, Spener F, van Meer G, VanNieuwenhze MS, White SH, Witztum JL,

Dennis EA. A comprehensive classification system for lipids. J Lipid Res. 2005;46(5):839–62.

35. de Paula Rogerio A, Sorgi CA rtério, Sadikot R, Carlo T. The role of lipids mediators in inflammation and resolution. Biomed Res Int. 2015;2015(605959):1–2.

36. Schulz H. Beta oxidation of fatty acids. Biochim Biophys Acta (BBA)/Lipids Lipid Metab. 1991;1081(2):109–20.

37. Moon JS, Lee S, Park MA, Siempos II, Haslip M, Lee PJ, Yun M, Kim CK, Howrylak J, Ryter SW, Nakahira K, Choi AMK. UCP2-induced fatty acid synthase promotes NLRP3 inflammasome activation during sepsis. J Clin Invest. 2015;125(2):665–80.

38. Wei X, Song H, Yin L, Rizzo Jr MG, Sidhu R, Covey DF, Ory DS, Semenkovich CF. Fatty acid synthesis configures the plasma membrane for inflammation in diabetes. Nature. 2016;539(7628):294–8.

39. Makowski L, Brittingham§ KC, Reynolds JM, Suttles J, Hotamisligil GS. The Fatty Acid-binding Protein, aP2, Coordinates Macrophage Cholesterol Trafficking and Inflammatory Activity: Macrophage Expression Of aP2 Impacts Peroxisome Proliferator activated receptor γ and IκB Kinase Activities. J Biol Chem. 2005;280(13):12888–95.

40. Lammers B, Chandak PG, Aflaki E, Van Puijvelde GHM, Radovic B, Hildebrand RB, Meurs I, Out R, Kuiper J, Van Berkel TJC, Kolb D, Haemmerle G, Zechner R, Levak-Frank S, Van Eck M, Kratky D. Macrophage Adipose Triglyceride Lipase Deficiency Attenuates Atherosclerotic Lesion Development in Low-Density Lipoprotein Receptor Knockout Mice. Arterioscler Thromb. 2011;31(1):67–73.

41. Boström P, Magnusson B, Svensson PA, Wiklund O, Borén J, Carlsson LMS, Ståhlman M, Olofsson SO, Hultén LM. Hypoxia converts human macrophages into triglyceride-loaded foam cells. Arterioscler Thromb Vasc Biol. 2006;26(8):1871–6.

42. Haschemi A, Kosma P, Gille L, Evans CR, Burant CF, Starkl P, Knapp B, Haas R, Schmid JA, Jandl C, Amir S, Lubec G, Park J, Esterbauer H, Bilban M, Brizuela L, Pospisilik JA, Otterbein LE, Wagner O. The sedoheptulose kinase CARKL directs macrophage polarization through control of glucose metabolism. Cell Metab. 2012;15(6):813–26.

43. Jha AK, Huang SCC, Sergushichev A, Lampropoulou V, Ivanova Y, Loginicheva E, Chmielewski K, Stewart KM, Ashall J, Everts B, Pearce EJ, Driggers EM, Artyomov MN. Network integration of parallel metabolic and transcriptional data reveals metabolic modules that regulate macrophage polarization. Immunity. 2015;42(3):419–30.

44. Infantino V, Convertini P, Cucci L, Panaro MA, Di Noia MA, Calvello R, Palmieri F, Iacobazzi V. The mitochondrial citrate carrier: a new player in inflammation. Biochem J. 2011;438(3):433–6.

45. Infantino V, Iacobazzi V, Palmieri F, Menga A. ATP-citrate lyase is essential for macrophage inflammatory response. Biochem Biophys Res Commun. 2013;440(1):105–11.

46. Na TY, Lee HJ, Oh HJ, Huh S, Lee IK, Lee MO. Positive cross-talk between hypoxia inducible factor-1α and liver X receptor α induces formation of triglyceride-loaded foam cells. Vol. 31, Arteriosclerosis, Thrombosis, and Vascular Biology. 2011. 2949-2956 p.

47. Cao H, Gerhold K, Mayers JR, Wiest MM, Steve M, Hotamisligil GS. Identification of a Lipokine, a Lipid Hormone Linking Adipose Tissue to Systemic Metabolism. Cell. 2009;134(6):933–44.

48. Wang Y, Kurdi-Haidar B, Oram JF. LXR-mediated activation of macrophage stearoyl-CoA desaturase generates unsaturated fatty acids that destabilize ABCA1. J Lipid Res. 2004;45(5):972–80.

49. Sun Y, Hao M, Luo Y, Liang CP, Silver DL, Cheng C, Maxfield FR, Tall AR. Stearoyl-CoA desaturase inhibits ATP-binding cassette transporter A1-mediated cholesterol efflux and modulates membrane domain structure. J Biol Chem. 2003;278(8):5813–20.

50. Rousselle A, Qadri F, Leukel L, Yilmaz R, Fontaine J, Sihn G, Bader M, Ahluwalia A, Duchene J. CXCL5 limits macrophage foam cell formation in atherosclerosis. J Clin Invest. 2013;123(3):1343–7.

51. Saito R, Matsuzaka T, Karasawa T, Sekiya M, Okada N, Igarashi M, Matsumori R, Ishii K, Nakagawa Y, Iwasaki H, Kobayashi K, Yatoh S, Takahashi A, Sone H, Suzuki H, Yahagi N, Yamada N, Shimano H. Macrophage Elovl6 deficiency ameliorates foam cell formation and reduces atherosclerosis in low-density lipoprotein receptor-deficient mice. Arterioscler Thromb Vasc Biol. 2011;31(9):1973–9.

52. Ecker J, Liebisch G, Englmaier M, Grandl M, Robenek H, Schmitz G. Induction of fatty acid synthesis is a key requirement for phagocytic differentiation of human monocytes. Proc Natl Acad Sci. 2010;107(17):7817–22.

53. Gimeno RE. Fatty acid transport proteins. Curr Opin Lipidol. 2007;18(3):271–6.

54. Huang SC-C, Everts B, Ivanova Y, O'Sullivan D, Nascimento M, M. Smith A, Beatty W, Love-Gregory L, Wing Y. L, O'Neill C, Yan C, Du H, A. Abumrad N, F. Urban Jr. J, N. Artyomov M, L. Pearce E, J. Pearce E. Cell-intrinsic lysosomal lipolysis is essential for macrophage alternative activation. Nat Immunol. 2014;15(9):846–55.

55. Malandrino MI, Fucho R, Weber M, Calderon-Dominguez M, Mir JF, Valcarcel L, Escoté X, Gómez-Serrano M, Peral B, Salvadó L, Fernández-Veledo S, Casals N, Vázquez-Carrera M, Villarroya F, Vendrell JJ, Serra D, Herrero L. Enhanced fatty acid oxidation in adipocytes and macrophages reduces lipid-induced triglyceride accumulation and inflammation. Am J Physiol - Endocrinol Metab. 2015;308(9):756–69.

56. Goldberg EL, Dixit VD. Carnitine acetyltransferase (CRAT) expression in macrophages is dispensable for nutrient stress sensing and inflammation. Mol Metab. 2017;6(2):219–25.

57. Namgaladze D, Brüne B. Fatty acid oxidation is dispensable for human macrophage IL-4-induced polarization. Biochim Biophys Acta - Mol Cell Biol Lipids. 2014;1841(9):1329–35.

58. Johnson AR, Qin Y, Cozzo AJ, Freemerman AJ, Huang MJ, Zhao L, Sampey BP, Milner JJ, Beck MA, Damania B, Rashid N, Galanko JA, Lee DP, Edin ML, Zeldin DC, Fueger PT, Dietz B, Stahl A, Wu Y, Mohlke KL, Makowski L. Metabolic reprogramming through fatty acid transport protein 1 (FATP1) regulates macrophage inflammatory potential and adipose inflammation. Mol Metab. 2016;5(7):506–26.

59. Szanto A, Balint BL, Nagy ZS, Barta E, Dezso B, Pap A, Szeles L, Poliska S, Oros M, Evans RM, Barak Y, Schwabe J, Nagy L. STAT6 transcription factor is a facilitator of the nuclear receptor PPARγ-regulated gene expression in macrophages and dendritic cells. Immunity. 2010;33(5):699–712.

60. Van den Bossche J, Baardman J, Otto NA, van der Velden S, Neele AE, van den Berg SM, Luque-Martin R, Chen HJ, Boshuizen MCS, Ahmed M, Hoeksema MA, de Vos AF, de Winther MPJ. Mitochondrial Dysfunction Prevents Repolarization of Inflammatory Macrophages. Cell Rep. 2016;17(3):684–96.

61. Tan Z, Xie N, Cui H, Moellering DR, Abraham E, Thannickal VJ, Liu G. Pyruvate dehydrogenase kinase 1 participates in macrophage polarization via regulating glucose metabolism. J Immunol. 2015;194(12):6082–9.

62. Van Veldhoven PP. Biochemistry and genetics of inherited disorders of peroxisomal fatty acid metabolism. J Lipid Res. 2010;51(10):2863–95.

63. Geric I, Tyurina YY, Krysko O, Krysko D V, De Schryver E, Kagan VE, Van Veldhoven PP, Baes M, Verheijden S. Lipid homeostasis and inflammatory activation are disturbed in classically activated macrophages with peroxisomal β-oxidation deficiency. Immunology. 2017;1–35.

64. Van Tits LJH, Stienstra R, van Lent PL, Netea MG, Joosten LAB, Stalenhoef AFH. Oxidized LDL enhances pro-inflammatory responses of alternatively activated M2 macrophages: A crucial role for Krüppel-like factor 2. Atherosclerosis. 2011;214(2):345–9.

65. Boß M, Kemmerer M, Brüne B, Namgaladze D. FABP4 inhibition suppresses PPARγ activity and VLDL-induced foam cell formation in IL-4-polarized human macrophages. Atherosclerosis. 2015;240(2):424–30.

66. Coleman RA, Lee DP. Enzymes of triacylglycerol synthesis and their regulation. Prog Lipid Res. 2004;43(2):134–76.

67. Dinasarapu AR, Gupta S, Maurya MR, Fahy E, Min J, Sud M, Gersten MJ, Glass CK, Subramaniam S. A combined omics study on activated macrophages - Enhanced role of STATs in apoptosis, immunity and lipid metabolism. Bioinformatics. 2013;29(21):2735–43.

68. Li J, Wang X, Zhang T, Wang C, Huang Z, Luo X, Deng Y. A review on phospholipids and their main applications in drug delivery systems. Asian J Pharm Sci. 2014;10(2):81–98.

69. Naraba H, Murakami M, Matsumoto H, Shimbara S, Ueno A, Kudo I, Oh-ishi S. Segregated coupling of phospholipases A2, cyclooxygenases, and terminal prostanoid synthases in different phases of prostanoid biosynthesis in rat peritoneal macrophages. JImmunol. 1998;160(6):2974–82.

70. Dieter P, Kolada A, Kamionka S, Schadow A, Kaszkin M. Lipopolysaccharide-induced release of arachidonic acid and prostaglandins in liver macrophages: Regulation by Group IV cytosolic phospholipase A2, but not by Group V and Group IIA secretory phospholipase A2. Cell Signal. 2002;14(3):199–204.

71. Ruipérez V, Astudillo AM, Balboa M a, Balsinde J. Coordinate regulation of TLR-mediated arachidonic acid mobilization in macrophages by group IVA and group V phospholipase A2s. J Immunol. 2009;182(6):3877–83.

72. Rubio JM, Rodriguez JP, Gil-de-Gomez L, Guijas C, Balboa M a., Balsinde J. Group V Secreted Phospholipase A2 Is Upregulated by IL-4 in Human Macrophages and Mediates Phagocytosis via Hydrolysis of Ethanolamine Phospholipids. J Immunol. 2015;194(7):3327–39.

73. Dennis EA, Deems RA, Harkewicz R, Quehenberger O, Brown HA, Milne SB, Myers DS, Glass CK, Hardiman G, Reichart D, Merrill AH, Sullards MC, Wang E, Murphy RC, Raetz CRH, Garrett TA, Guan Z, Ryan AC, Russell DW, McDonald JG, Thompson BM, Shaw WA, Sud M, Zhao Y, Gupta S, Maurya MR, Fahy E, Subramaniama S. A mouse macrophage lipidome. J Biol Chem. 2010;285(51):39976–85.

74. Pruett ST, Bushnev A, Hagedorn K, Adiga M, Haynes CA, Sullards MC, Liotta DC, Merrill AH. Thematic Review Series: Sphingolipids. Biodiversity of sphingoid bases ("sphingosines") and related amino alcohols. J Lipid Res. 2008;49(8):1621–39.

75. Nixon GF. Sphingolipids in inflammation: Pathological implications and potential therapeutic targets. Br J Pharmacol. 2009;158(4):982–93.

76. Sims K, Haynes CA, Kelly S, Allegood JC, Wang E, Momin A, Leipelt M, Reichart D, Glass CK, Cameron Sullards M, Merrill AH. Kdo2-lipid A, a TLR4-specific agonist, induces de Novo sphingolipid biosynthesis in RAW264.7 macrophages, which is essential for induction of autophagy. J Biol Chem. 2010;285(49):38568–79.

77. Harizi H, Corcuff JB, Gualde N. Arachidonic-acid-derived eicosanoids: roles in biology and immunopathology. Trends Mol Med. 2008;14(10):461–9.

78. Tarique AA, Logan J, Thomas E, Holt PG, Sly PD, Fantino E. Phenotypic,functional,and plasticity features of classical and alternatively activated human macrophages. Am J Respir Cell Mol Biol. 2015;53(5):676–88.

79. Shay AE, Diwakar BT, Guan BJ, Narayan V, Urban JF, Prabhu KS. IL-4 up-regulates cyclooxygenase-1 expression in macrophages. J Biol Chem. 2017;292(35):14544–55.

80. Simons K, Ikonen E. How Cells Handle Cholesterol. Science (80-). 2000;290(12):1721–6.

81. Kunjathoor V V., Febbraio M, Podrez EA, Moore KJ, Andersson L, Koehn S, Rhee JS, Silverstein R, Hoff HF, Freeman MW. Scavenger receptors class A-I/II and CD36 are the principal receptors responsible for the uptake of modified low density lipoprotein leading to lipid loading in macrophages. J Biol Chem. 2002;277(51):49982–8.

82. Ishiyama J, Taguchi R, Yamamoto A, Murakami K. Palmitic acid enhances lectin-like oxidized LDL receptor (LOX-1) expression and promotes uptake of oxidized LDL in macrophage cells. Atherosclerosis. 2010;209(1):118–24.

83. Mills EL, O'Neill LA. Reprogramming mitochondrial metabolism in macrophages as an anti-inflammatory signal. Eur J Immunol. 2016;46(1):13–21.

84. Schneider JG, Yang Z, Chakravarthy M V., Lodhi IJ, Wei X, Turk J, Semenkovich CF. Macrophage fatty-acid synthase deficiency decreases diet-induced atherosclerosis. J Biol Chem. 2010;285(30):23398–409.

85. Im S, Yousef L, Blaschitz C, Liu JZ, Edwards RA, Young SG, Raffatellu M, Osborne TF. Linking Lipid Metabolism to the Innate Immune Response in Macrophages through Sterol Regulatory Element Binding Protein -1a. Cell Metab. 2012;13(5):540–9.

86. Jeon SM. Regulation and function of AMPK in physiology and diseases. Exp Mol Med. 2016;48(7):245–58.

87. Kelly B, O'Neill LA. Metabolic reprogramming in macrophages and dendritic cells in innate immunity. Cell Res. 2015;25(7):771–84.

88. Sag D, Carling D, Stout RD, Suttles J. Adenosine 5'-monophosphate-activated protein kinase promotes macrophage polarization to an anti-inflammatory functional phenotype. J Immunol. 2008;181(12):8633–41.

89. Lee WJ, Kim M, Park HS, Kim HS, Jeon MJ, Oh KS, Koh EH, Won JC, Kim MS, Oh GT, Yoon M, Lee KU, Park JY. AMPK activation increases fatty acid oxidation in skeletal muscle by activating PPARα and PGC-1. Biochem Biophys Res Commun. 2006;340(1):291–5.

90. Galic S, Fullerton M, Schertzer J. Hematopoietic AMPK-β1 reduces mouse adipose tissue macrophage inflammation and insulin resistance in obesity. J Clin Invest. 2011;121(12):4903–15.

91. Zhou G, Myers R, Li Y, Chen Y, Shen X, Fenyk-melody J, Wu M, Ventre J, Doebber T, Fujii N, Musi N, Hirshman MF, Goodyear LJ, Moller DE. Role of AMP-Activated Protein Kinase in Mechanism of Metformin Action Role of AMP-activated protein kinase in mechanism of metformin action. J Clin Invest. 2001;108(8):1167–74.

92. Kelly B, Tannahill GM, Murphy MP, O'Neill LAJ. Metformin inhibits the production of reactive oxygen species from NADH: Ubiquinone oxidoreductase to limit induction of interleukin-1β (IL-1β) and boosts interleukin-10 (IL-10) in lipopolysaccharide (LPS)-activated macrophages. J Biol Chem. 2015;290(33):20348–59.

93. Kim J, Kwak HJ, Cha JY, Jeong YS, Rhee SD, Kim KR, Cheon HG. Metformin suppresses lipopolysaccharide (LPS)-induced inflammatory response in murine macrophages via Activating Transcription Factor-3 (ATF-3) induction. J Biol Chem. 2014;289(33):23246–55.

94. Chan KL, Pillon NJ, Sivaloganathan DM, Costford SR, Liu Z, Théret M, Chazaud B, Klip A. Palmitoleate reverses high fat-induced proinflammatory macrophage polarization via AMP-activated protein kinase (AMPK). J Biol Chem. 2015;290(27):16979–88.

95. Seleem D, Pardi V, Murata RM. Review of flavonoids: A diverse group of natural compounds with anti-

Candida albicans activity in vitro. Arch Oral Biol. 2017;76:76–83.

96. Wang T yang, Li Q, Bi K shun. Bioactive flavonoids in medicinal plants: Structure, activity and biological fate. Asian J Pharm Sci. 2017;13(1):12–23.

97. Saqib U, Sarkar S, Suk K, Mohammad O, Braig MS, Savai R. Phytochemicals as modulators of M1-M2 macrophages in inflammation. J Manuf Sci Eng Trans ASME. 2018;9(25):17937–50.

98. Hirai S, Kim YI, Goto T, Kang MS, Yoshimura M, Obata A, Yu R, Kawada T. Inhibitory effect of naringenin chalcone on inflammatory changes in the interaction between adipocytes and macrophages. Life Sci. 2007;81(16):1272–9.

99. Bodet C, La VD, Epifano F, Grenier D. Naringenin has anti-inflammatory properties in macrophage and ex vivo human whole-blood models. J Periodontal Res. 2008;43(4):400–7.

100. Chao CL, Weng CS, Chang NC, Lin JS, Kao S Te, Ho FM. Naringenin more effectively inhibits inducible nitric oxide synthase and cyclooxygenase-2 expression in macrophages than in microglia. Nutr Res. 2010;30(12):858–64.

101. Hämäläinen M, Nieminen R, Asmawi MZ, Vuorela P, Vapaatalo H, Moilanen E. Effects of flavonoids on prostaglandin E2 production and on COX-2 and mPGES-1 expressions in activated macrophages. Planta Med. 2011;77(13):1504–11.

102. Yilma AN, Singh SR, Morici L, Dennis VA. Flavonoid naringenin: A potential immunomodulator for Chlamydia trachomatis inflammation. Mediators Inflamm. 2013;2013(4):1–13.

103. Pinho-Ribeiro FA, Zarpelon AC, Mizokami SS, Borghi SM, Bordignon J, Silva RL, Cunha TM, Alves-Filho JC, Cunha FQ, Casagrande R, Verri WA. The citrus flavonone naringenin reduces lipopolysaccharide-induced inflammatory pain and leukocyte recruitment by inhibiting NF-κB activation. J Nutr Biochem. 2016;33:8–14.

104. Jin L, Zeng W, Zhang F, Zhang C, Liang W. Naringenin Ameliorates Acute Inflammation by Regulating Intracellular Cytokine Degradation. J Immunol. 2017;199(10):3466–77.

105. Endale M, Park SC, Kim S, Kim SH, Yang Y, Cho JY, Rhee MH. Quercetin disrupts tyrosine-phosphorylated phosphatidylinositol 3-kinase and myeloid differentiation factor-88 association, and inhibits MAPK/AP-1 and IKK/NF-κB-induced inflammatory mediators production in RAW 264.7 cells. Immunobiology. 2013;218(12):1452–67.

106. Overman A, Chuang CC, McIntosh M. Quercetin attenuates inflammation in human macrophages and adipocytes exposed to macrophage-conditioned media. Int J Obes. 2011;35(9):1165–72.

107. Lara-Guzman OJ, Tabares-Guevara JH, Leon-Varela YM, Alvarez RM, Roldan M, Sierra JA, Londono-Londono JA, Ramirez-Pineda JR. Proatherogenic Macrophage Activities Are Targeted by the Flavonoid Quercetin. J Pharmacol Exp Ther. 2012;343(2):296–306.

108. Lu H, Wu L, Liu L, Ruan Q, Zhang X, Hong W, Wu S, Jin G, Bai Y. Quercetin ameliorates kidney injury and fibrosis by modulating M1/M2 macrophage polarization. Biochem Pharmacol. 2018;154(3):203–12.

109. Li X, Jin Q, Yao Q, Xu B, Li L, Zhang S, Tu C. The flavonoid quercetin ameliorates liver inflammation and fibrosis by regulating hepatic macrophages activation and polarization in mice. Front Pharmacol. 2018;9(2):1–14.

110. Kanno SI, Shouji A, Tomizawa A, Hiura T, Osanai Y, Ujibe M, Obara Y, Nakahata N, Ishikawa M. Inhibitory effect of naringin on lipopolysaccharide (LPS)-induced endotoxin shock in mice and nitric oxide production in RAW 264.7 macrophages. Life Sci. 2006;78(7):673–81.

111. Liu Y, Su WW, Wang S, Li PB. Naringin inhibits chemokine production in an LPS-induced RAW 264.7

macrophage cell line. Mol Med Rep. 2012;6(6):1343–50.

112. Gil M, Kim YK, Hong SB, Lee KJ. Naringin decreases TNF-α and HMGB1 release from LPS-stimulated macrophages and improves survival in a CLP-induced sepsis mice. PLoS One. 2016;11(10):1–16.

113. Singh NA, Mandal AKA, Khan ZA. Potential neuroprotective properties of epigallocatechin-3-gallate (EGCG). Nutr J. 2016;15(1):1–17.

114. Zhong Y, Chiou YS, Pan MH, Shahidi F. Anti-inflammatory activity of lipophilic epigallocatechin gallate (EGCG) derivatives in LPS-stimulated murine macrophages. Food Chem. 2012;134(2):742–8.

115. Zhang W yu, Liu H qing, Xie K qiang, Yin L lin, Li Y, Kwik-Uribe CL, Zhu X zu. Procyanidin dimer B2 [epicatechin-(4β-8)-epicatechin] suppresses the expression of cyclooxygenase-2 in endotoxin-treated monocytic cells. Biochem Biophys Res Commun. 2006;345(1):508–15.

116. Hou DX, Masuzaki S, Hashimoto F, Uto T, Tanigawa S, Fujii M, Sakata Y. Green tea proanthocyanidins inhibit cyclooxygenase-2 expression in LPS-activated mouse macrophages: Molecular mechanisms and structure-activity relationship. Arch Biochem Biophys. 2007;460(1):67–74.

117. Abe Y, Hashimoto S, Horie T. Curcumin inhibition of inflammatory cytokine production by human peripheral blood monocytes and alveolar macrophages. Pharmacol Res. 1999;39(1):41–7.

118. Chen D, Nie M, Fan MW, Bian Z. Anti-inflammatory activity of curcumin in macrophages stimulated by lipopolysaccharides from Porphyromonas gingivalis. Pharmacology. 2008;82(4):264–9.

119. Yadav R, Jee B, Awasthi SK. Curcumin Suppresses the Production of Pro-inflammatory Cytokine Interleukin-18 in Lipopolysaccharide Stimulated Murine Macrophage-Like Cells. Indian J Clin Biochem. 2015;30(1):109–12.

120. Saenz J, Santa-María C, Reyes-Quiroz ME, Geniz I, Jiménez J, Sobrino F, Alba G. Grapefruit Flavonoid Naringenin Regulates the Expression of LXRα in THP-1 Macrophages by Modulating AMP-Activated Protein Kinase. Mol Pharm. 2018;15(5):1735–45.

121. Li S, Cao H, Shen D, Jia Q, Chen C, Xing SL. Quercetin protects against ox-LDL-induced injury via regulation of ABCAl, LXR-α and PCSK9 in RAW264.7 macrophages. Mol Med Rep. 2018;18(1):799–806.

122. Jia Y, Hoang MH, Jun HJ, Lee JH, Lee SJ. Cyanidin, a natural flavonoid, is an agonistic ligand for liver X receptor alpha and beta and reduces cellular lipid accumulation in macrophages and hepatocytes. Bioorganic Med Chem Lett. 2013;23(14):4185–90.

123. Wang S, Zhang X, Liu M, Luan H, Ji Y, Guo P, Wu C. Chrysin inhibits foam cell formation through promoting cholesterol efflux from RAW264.7 macrophages. Pharm Biol. 2015;53(10):1481–7.

124. Dong J, Zhang X, Zhang L, Bian H-X, Xu N, Bao B, Liu J. Quercetin reduces obesity-associated ATM infiltration and inflammation in mice: a mechanism including AMPKα1/SIRT1. J Lipid Res. 2014;55(3):363–74.

125. Brügger B. Lipidomics: Analysis of the Lipid Composition of Cells and Subcellular Organelles by Electrospray Ionization Mass Spectrometry. Annu Rev Biochem. 2014;83(1):79–98.

126. Lydic TA, Goo Y-H. Lipidomics unveils the complexity of the lipidome in metabolic diseases. Clin Transl Med. 2018;7(4):1–13.

127. Folch J, Lees M, Sloane GH. A simple method for the isolation and purification of total lipids from animal tissues. J Biol Chem. 1953;226(3):497–509.

128. Dyer WJ, Bligh EG. A rapid method of total lipid extraction and purification. Can J of Bioch and Physiol. 1963;37(8):911–7.

129. Andreyev AY, Fahy E, Guan Z, Kelly S, Li X, McDonald JG, Milne S, Myers D, Park H, Ryan A, Thompson BM, Wang E, Zhao Y, Brown HA, Merrill AH, Raetz CRH, Russell DW, Subramaniam S, Dennis EA. Subcellular organelle lipidomics in TLR-4-activated macrophages. J Lipid Res. 2010;51(9):2785–97.

130. Lee JW, Mok HJ, Lee DY, Park SC, Kim GS, Lee SE, Lee YS, Kim KP, Kim HD. UPLC-QqQ/MS-Based Lipidomics Approach to Characterize Lipid Alterations in Inflammatory Macrophages. J Proteome Res. 2017;16(4):1460–9.

131. Montenegro-Burke JR, Sutton JA, Rogers LM, Milne GL, McLean JA, Aronoff DM. Lipid profiling of polarized human monocyte-derived macrophages. Prostaglandins Other Lipid Mediat. 2016;127:1–8.

132. Zhang C, Wang Y, Wang F, Wang Z, Lu Y, Xu Y, Wang K, Shen H, Yang P, Li S, Qin X, Yu H. Quantitative profiling of glycerophospholipids during mouse and human macrophage differentiation using targeted mass spectrometry. Sci Rep. 2017;7(1):1–13.

133. Wallner S, Orso E, Grandl M, Konovalova T, Liebisch G, Schmitz G. Phosphatidylcholine and phosphatidylethanolamine plasmalogens in lipid loaded human macrophages. PLoS One. 2018;13(10):1–21.

134. Huynh K, Pernes G, Mellett NA, Meikle PJ, Murphy AJ, Lancaster GI. Lipidomic profiling of murine macrophages treated with fatty acids of varying chain length and saturation status. Metabolites. 2018;8(29):1–17.

135. Kim Y, Gromovsky AD, Brown JM, Chung S. Gamma-tocotrienol attenuates the aberrant lipid mediator production in NLRP3 inflammasome-stimulated macrophages. J Nutr Biochem. 2018;58:169–77.

136. Chen Q, Wang N, Zhu M, Lu J, Zhong H, Xue X, Guo S, Li M, Wei X, Tao Y, Yin H. TiO2 nanoparticles cause mitochondrial dysfunction, activate inflammatory responses, and attenuate phagocytosis in macrophages: A proteomic and metabolomic insight. Redox Biol. 2018;15:266–76.

137. Zhao C, Tang Z, Yan J, Fang J, Wang H, Cai Z. Bisphenol S exposure modulate macrophage phenotype as defined by cytokines profiling, global metabolomics and lipidomics analysis. Sci Total Environ. 2017;592:357–65.

138. Peng H, Wu X, Zhao L, Feng Y. Dynamic analysis of phospholipid metabolism of mouse macrophages treated with common non-steroidal anti-inflammatory drugs. Mol Cell Biochem. 2016;411:161–71.

139. Negrão F, Abánades DR, Jaeeger CF, Rocha DFO, Belaz KRA, Giorgio S, Eberlin MN, Angolini CFF. Lipidomic alterations of: In vitro macrophage infection by L. infantum and L. amazonensis. Mol Biosyst. 2017;13(11):2401–6.

140. Bartlett EM, Lewis DH. Spectrophotometric determination of phosphate esters in the presence and absence of orthophosphate. Anal Biochem. 1970;36(1):159–67.

141. Pluskal T, Castillo S, Villar-Briones A, Orešič M. MZmine 2: Modular framework for processing, visualizing, and analyzing mass spectrometry-based molecular profile data. BMC Bioinformatics. 2010;11(395):1–11.

142. Xia J, Sinelnikov I V., Han B, Wishart DS. MetaboAnalyst 3.0-making metabolomics more meaningful. Nucleic Acids Res. 2015;43(1):251–7.

143. Forrester MA, Wassall HJ, Hall LS, Cao H, Wilson HM, Barker RN, Vickers MA. Similarities and differences in surface receptor expression by THP-1 monocytes and differentiated macrophages polarized using seven different conditioning regimens. Cell Immunol. 2018;332(7):58–76.

144. Antonios JK, Yao Z, Li C, Rao AJ, Goodman SB. Macrophage polarization in response to wear particles in vitro. Cell Mol Immunol. 2013;10(6):471–82.

145. Yeom M, Hahm DH, Sur BJ, Han JJ, Lee HJ, Yang HI, Kim KS. Phosphatidylserine inhibits inflammatory responses in interleukin-1β-stimulated fibroblast-like synoviocytes and alleviates carrageenan-induced arthritis in rat. Nutr Res. 2013;33(3):242–50.

146. Matsura T. Oxidized phosphatidylserine: Production and bioactivities. Yonago Acta Med. 2014;57(4):119–27.

147. Maulucci G, Cohen O, Daniel B, Sansone A, Petropoulou PI, Filou S, Spyridonidis A, Pani G, De Spirito M, Chatgilialoglu C, Ferreri C, Kypreos KE, Sasson S. Fatty acid-related modulations of membrane fluidity in cells: detection and implications. Free Radic Res. 2016;50:S40–50.

148. Xue B, Yang Z, Wang X, Shi H. Omega-3 Polyunsaturated Fatty Acids Antagonize Macrophage Inflammation via Activation of AMPK/SIRT1 Pathway. PLoS One. 2012;7(10):2–7.

149. Werz O, Gerstmeier J, Libreros S, De La Rosa X, Werner M, Norris PC, Chiang N, Serhan CN. Human macrophages differentially produce specific resolvin or leukotriene signals that depend on bacterial pathogenicity. Nat Commun. 2018;9(1):1–12.

150. Caughey GE, Cleland LG, Penglis PS, Gamble JR, James MJ. Roles of Cyclooxygenase (COX)-1 and COX-2 in Prostanoid Production by Human Endothelial Cells: Selective Up-Regulation of Prostacyclin Synthesis by COX-2. J Immunol. 2001;167(5):2831–8.

151. Berben L, Sereika SM, Engberg S. Effect size estimation: Methods and examples. Int J Nurs Stud. 2012;49(8):1039–47.

152. Kanno K, Wu MK, Scapa EF, Roderick SL, David E. Structure and Function of Phosphatidylcholine Transfer Protein (PC-TP)/StarD2. Structure. 2009;1771(6):654–62.

153. Fajardo VA, McMeekin L, Leblanc PJ. Influence of phospholipid species on membrane fluidity: A meta-analysis for a novel phospholipid fluidity index. J Membr Biol. 2011;244(2):97–103.

154. Chakravarthy M V., Lodhi IJ, Yin L, Malapaka RR V., Xu HE, Turk J, Semenkovich CF. Identification of a Physiologically Relevant Endogenous Ligand for PPARα in Liver. Cell. 2009;138(3):476–88.

155. Otoki Y, Kato S, Kimura F, Furukawa K, Yamashita S, Arai H, Miyazawa T, Nakagawa K. Accurate quantitation of choline and ethanolamine plasmalogen molecular species in human plasma by liquid chromatography–tandem mass spectrometry. J Pharm Biomed Anal J Pharm Biomed. 2017;134:77–85.

156. Nagan N, Zoeller RA. Plasmalogens: Biosynthesis and functions. Progress in Lipid Research. 2001. 40:199-229.

157. Koivuniemi A. The biophysical properties of plasmalogens originating from their unique molecular architecture. FEBS Lett. 2017;591(18):2700–13.

158. Rubio JM, Astudillo AM, Casas J, Balboa MA, Balsinde J. Regulation of phagocytosis in macrophages by membrane ethanolamine plasmalogens. Front Immunol. 2018;9(7):1–14.

159. Rog T, Koivuniemi A. The biophysical properties of ethanolamine plasmalogens revealed by atomistic molecular dynamics simulations. Biochim Biophys Acta - Biomembr. 2016;1858(1):97–103.

160. Pike LJ, Han X, Chung KN, Gross RW. Lipid rafts are enriched in arachidonic acid and plasmenylethanolamine and their composition is independent of caveolin-1 expression: A quantitative electrospray ionization/mass spectrometric analysis. Biochemistry. 2002;41(6):2075–88.

161. Reiss D, Beyer K, Engelmann B. Delayed oxidative degradation of polyunsaturated diacyl phospholipids in the presence of plasmalogen phospholipids in vitro. Biochem J. 1997;323:807–14.

162. Morand OH, Zoeller RA, Raetz CRH. Disappearance of plasmalogens from membranes of animal cells subjected to photosensitized oxidation. J Biol Chem. 1988;263(23):11597–606.

163. Gardocki ME, Jani N, Lopes JM. Phosphatidylinositol biosynthesis: Biochemistry and regulation. Biochim Biophys Acta - Mol Cell Biol Lipids. 2005;1735(2):89–100.

164. Vergadi E, Ieronymaki E, Lyroni K, Vaporidi K, Tsatsanis C. Akt Signaling Pathway in Macrophage Activation and M1/M2 Polarization. J Immunol. 2017;198(3):1006–14.

165. Shi J, Li Q, Sheng M, Zheng M, Yu M, Zhang L. The Role of TLR4 in M1 Macrophage-Induced Epithelial-Mesenchymal Transition of Peritoneal Mesothelial Cells. Cell Physiol Biochem. 2016;40(6):1538–48.

166. Kanno S, Tomizawa A, Hiura T, Osanai Y, Shouji A, Ujibe M, Ohtake T, Kimura K, Ishikawa M. Inhibitory Effects of Naringenin on Tumor Growth in Human Cancer Cell Lines and Sarcoma S-180-Implanted Mice. Biol Pharm Bull. 2005;28(3):527–30.

167. Shi HB, Wu M, Zhu JJ, Zhang CH, Yao DW, Luo J, Loor JJ. Fatty acid elongase 6 plays a role in the synthesis of long-chain fatty acids in goat mammary epithelial cells. J Dairy Sci. 2017;100(6):4987–95.